KFA

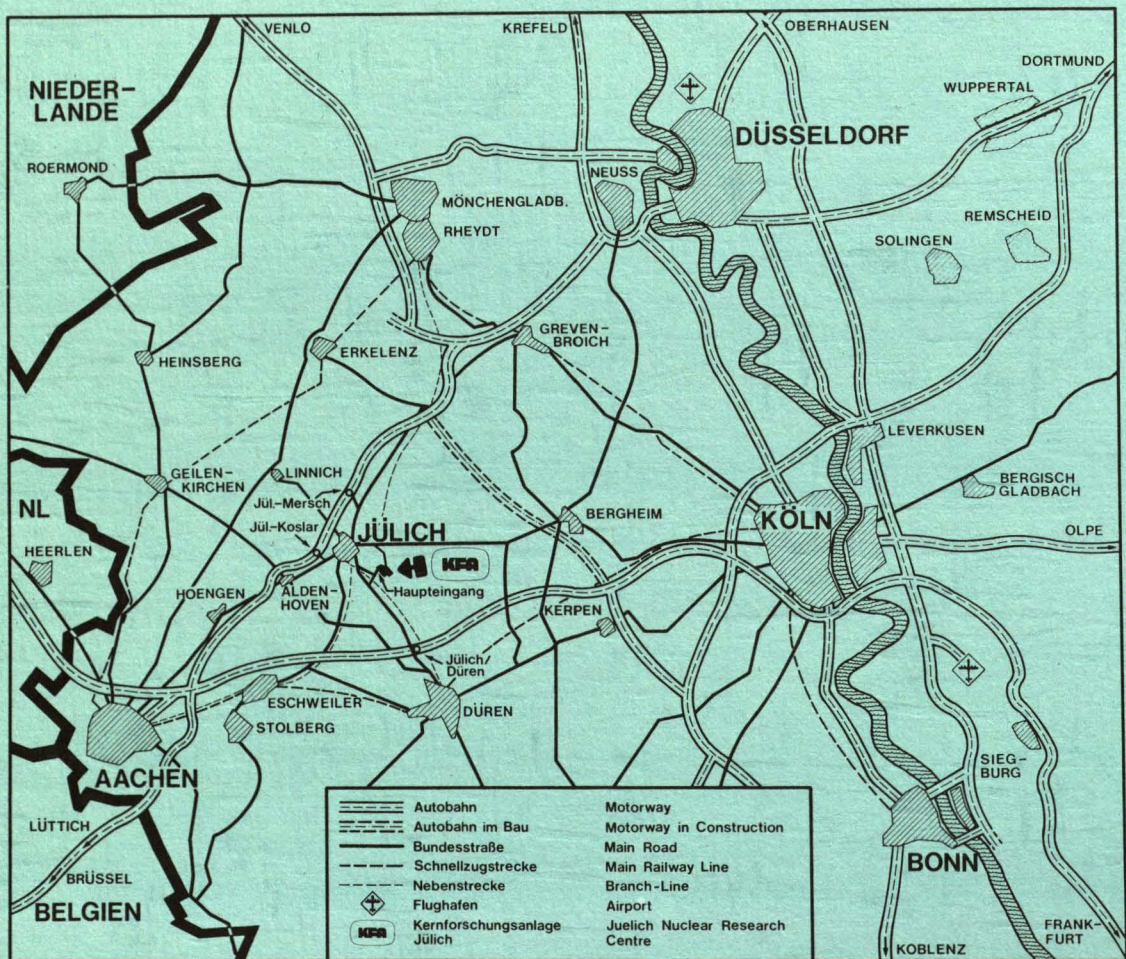# KERNFORSCHUNGSANLAGE JÜLICH GmbH

Institut für Chemische Technologie

A Study of Pulse Columns for Thorium Fuel Reprocessing

by

H. Fumoto

Map of the Jülich region showing Autobahn, Autobahn im Bau (Motorway in Construction), Bundesstraße (Main Road), Schnellzugstrecke (Main Railway Line), Nebenstrecke (Branch-Line), Flughafen (Airport), Kernforschungsanlage Jülich (KFA / Juelich Nuclear Research Centre).

Als Manuskript gedruckt

Berichte der Kernforschungsanlage Jülich – Nr. 1770

Institut für Chemische Technologie Jül – 1770

A Study of Pulse Columns for Thorium Fuel Reprocessing

by

H. Fumoto

Abstract

Pulse columns have been studied long and a great variety of
experimental investigations have been carried out, using them.
In this study, two 5 m pulse columns with the same cartridge
geometries are installed to investigate the performances.
First of all, the characteristic differences of the aqueous
continuous and the organic continuous columns were investigated
experimentally. Secondly, a ternary system of 30 % TBP in
dodecane-acetic acid-water was adopted for the mass-transfer
study. It was concluded that the overall mass-transfer
coefficient K_x was independent of whether the mass-transfer
is from the dispersed to the continuous phase or from the
continuous to the dispersed phase. Next, thorium nitrate was
extracted and reextracted using both modes of operation for
comparison. Both HETS and HTU were obtained. According to
the results for the extraction, the aqueous continuous column
gave much shorter HTU than the organic continuous column.
On the other hand, in reextraction the organic continuous
column gave shorter HTU. Finally, the Thorex-processes for
uranium and thorium co-extraction, co-stripping, and
partitioning were studied. As for the extraction process,
both acid feed solution and acid deficiend feed solution
were investigated for comparison. The concentration profiles
along the column height were obtained. The data were analysed
with McCABE-THIELE diagrams to evaluate HETS.

Zusammenfassung

Für Solventextraktions-Prozesse werden Pulskolonnen schon
lange benutzt, und eine Vielzahl von experimentellen Unter-
suchungen sind mit ihnen durchgeführt worden. In dieser Ar-
beit sind zwei 5 m lange Pulskolonnen mit der gleichen Sieb-
boden-Geometrie auf ihr Betriebsverhalten untersucht worden.
Zunächst sind die charakteristischen Unterschiede ermittelt
worden, die sich ergeben, wenn in der Kolonne entweder die
wäßrige oder die organische Phase kontinuierlich vorliegt.
Dann sind Stofftransport-Phänomene mit den ternären Systemen
- 30 % TBP in Dodekan - Essigsäure - Wasser - untersucht
worden. Aus den Versuchen kann geschlossen werden, daß der
Stofftransport-Koeffizient K_x nicht davon abhängig ist, ob
der Stofftransport von der dispersen zur kontinuierlichen
oder umgekehrt erfolgt. Weiterhin ist ein Vergleich beider
Verfahrensweisen (organisch bzw. wäßrig kontinuierlich) für
die Extraktion und Reextraktion von Thoriumnitrat durchge-
führt worden. Sowohl HETS- als auch HTU-Werte sind dabei er-
mittelt worden. Nach den Ergebnissen besitzt die wäßrig
kontinuierliche Kolonne bei der Extraktion wesentlich kürzere
HTU-Werte als die organisch kontinuierliche. Andererseits
zeigt die organisch kontinuierliche Kolonne kürzere HTU-Werte
bei der Reextraktion. Schließlich ist der THOREX-Prozeß für
die Ko-Extraktion, das Ko-Stripping und die Trennung von
Thorium und Uran untersucht worden. Der Extraktions-Prozeß
ist sowohl mit saurer als auch mit säureunterschüssiger
Speiselösung vergleichend durchgeführt worden. Die Konzen-
trationsprofile entlang der Kolonnenhöhe sind bestimmt worden.
Die experimentell ermittelten Werte sind dann durch McCABE-
THIELE-Diagramme interpretiert worden.

Table of contents

List of tables

List of figures

Acknowledgment

The author would like to thank sincerely:

1. Introduction

A nuclear fuel reprocessing plant separates and
purifies the fissile and fertile materials from the fission
products. The main separation procedure practically used
today is only the solvent extraction process. The dry process
using fluoride volatilization, has been studied extensively
because of its advantage of reducing the waste volume,
However, the dry process has many problems involving
fluorine corrosion problems. Therefore, the aqueous
process of solvent extraction would be adopted for the
nuclear fuel reprocessing plant for the time being. As for
plutonium-uranium fuel cycle, the Purex process was adopted
commonly for LWR fuel reprocessing. Diluted TBP is used as
extractant in almost all reprocessing plants.

In the head-end of reprocessing, the fuel elements are
prepared for the dissolution of the fuel by nitric acid.
Nowadays the head-end procedure provides the so-called
chop-leach method. The fuel rods are chopped into segment 2.5 to
12.5 cm long and then, the dissolution of the fuel can
take place. After dissolution, the concentrations of uranium
and nitric acid are adjusted for the first extraction cycle.
In the first decontamination cycle, uranium and plutonium
are extracted together. The heavy elements are separated
by re-extracting the plutonium after reduction of
$Pu^{4+} \rightarrow Pu^{3+}$ with $U(NO_3)_4$. Also the electrolytic reduction
is under development. After the partitioning, the plutonium
and the uranium are purified in the second cycles.

For the reprocessing of thorium-uranium fuel, the Thorex
process has been developed. Since the thorium-uranium
fuel cycle is not widely in use, there is not much
experience with the reprocessing of this fuel by the Thorex
process. There are two choices for the Thorex process flow
sheet; they are the single-cycle Thorex process and the
two-cycle Thorex process. In the single-cycle Thorex process,

thorium and uranium are co-extracted and partitioned in the
first cycle corresponding to the Purex process. In the two-
cycle Thorex process, uranium and thorium are co-extracted
and co-striped in the first cycle and partitioned in the second
cycle. First, 41 % diluted TBP was used for solvent but 30 %
TBP is used now. Though the aluminium nitrate-salted process
was used first, nitric acid is adopted as the salting agent
these days. In order to improve the decontamination factors,
acid deficient feed solution was developed for fuel of high
burn-up.

The solvent extraction process can be performed in three
different types of extraction equipment; pulse columns, mixer-
settlers, and centrifugal extractors. Among these three types
of extractors, mixer-settlers and pulse columns have been
long used in the actual Purex-reprocessing plants. They seem
to give about the same performances in the point of
mechanical maintenance. However, pulse columns have less
holdup and a shorter contact time than mixer-settlers, though
they need much more head room. Centrifugal extractors have
the shortest contact time, about a few seconds for one stage.
They are well suited for high burn-up fuel reprocessing like
FBR fuel reprocessing, preventing the solvent from radiation
damage. However, in comparison with pulse columns and mixer-
settlers, centrifugal extractors have the disadvantages of
difficult maintenance and less reliability for long term
operation.

Pulse columns have been studied for several decades in the
separation process of nuclear fuel reprocessing. However,
their behaviour has not yet been understood completely, since
it is very hard to analyse the complicated flowing effects
of the two phases. In this study, two 5 m high columns are
installed and studied for thorium fuel reprocessing. The
characteristic differences between the aqueous and the organic
continuous operation were examined first. The flow
characteristics of flooding, holdup and axial mixing were
investigated in both modes of operation. Secondly, the
mass-transfer behaviour was studied in experiments using acetic
acid for solute. The concentration profile along the column

height was obtained. In the next step, thorium nitrate was
extracted in both aqueous and organic continuous modes of
operation for comparison. Both HETS (Height Equivalent
Theoretical Stage) and HTU (Height of a Transfer Unit) were
evaluated. Then uranium and thorium were co-extracted, co-
stripped and partitioned for the study of thorium fuel
reprocessing. HETS was calculated in each cases. As for co-
extraction process, both acid feed solution (H^+ = 1.0 $\underline{M}$) and
acid deficient feed solution (H^+ = - 0.14 $\underline{M}$) were investigated
for comparison. Throughout the experiment, different profiles
of the HNO_3 concentration were obtained along the column height.

2.   Thorium fuel cycle

Thorium itself has a very small cross section for fission but
it can be used as a fertile material. Thorium is converted
into the fissile ^{233}U by the capture of a neutron[1].

$$^{232}Th(n,\gamma) \rightarrow ^{233}Th \xrightarrow[T=22.1 \text{ min}]{\beta^-} ^{233}Pa \xrightarrow[T=27.4 \text{ d}]{\beta^-} ^{233}U(T=1.6\times10^5 \text{ yr})$$
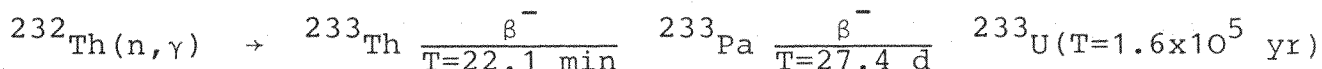
^{232}Th captures a neutron and is transformed into ^{233}Th, releasing
γ rays. ^{233}Th decays to ^{233}Pa by β^- emission and ^{233}Pa decays
again to ^{233}U by β^- emission. ^{233}Pa has a relatively long half-
life of about 27 days. In order to reduce the loss of ^{233}Pa,
the cooling time of the spent fuel must be decided, considering
the half-life, since protactinium cannot be extracted in the
Thorex process. ^{233}U releases the largest number of fast
neutrons on thermal fission compared with ^{235}U and ^{239}Pu.
Thorium-uranium fuel cycle has the advantage of producing
fewer actinide nuclides, which simplifies the waste management.
However, the presence of ^{232}U and ^{228}Th in the products causes
handling problems since their daughter nuclides have considerable
activities[2].

Thorium fuel has been studied and developed mainly for HTR fuel.
The HTR (High Temperature Reactor) is expected to be used not
only for electric power production but also for producing

industrial process heat at temperatures of up to nearly $1000^{O}C$. Since the utilization of the thorium fuel cycle in the HTR yields a high breeding ratio, the fuel reprocessing and the fuel recycling is necessary from the economic standpoint. However, for the performance of the Th/U fuel cycle, ^{235}U is necessary for the start and the make-up.

3.   Thorium fuel reprocessing

3.1   Head-end process

Coated particle fuel has been used for the HTR. The fuel elements are composed of 0.6 - 1.0 mm particle fuels and carbon as moderator. The fuel particle of UO_2 is coated by two or three layers of pyrocarbon and SiC[3]. These layers are very hard and stable, which adds some difficulties to the head-end process of the reprocessing plant. As for the dissolution process, grind-leach[4] and burn-leach methods were investigated before[5]. Off-gas treatment is also different from that of LWR fuel dissolution since the dissolution process is different. After the dissolution, the solution is adjusted for the following solvent extraction process.

3.2   Feed adjustment, particularly for acid deficient
feed solution

Though acid deficient feed solutions give good results for decontamination factors, they need a more complicated feed adjustment, using evaporator. Rainey and Moore[6] prepared the acid deficient solution by two different methods. One method is using steam strip to remove the nitric acid. The solution was evaporated to a boiling point of $135^{O}C$ first. Then steam strip was started to remove the remainder. The alternative feed adjustment method was to evaporate the solution to a boiling point of $165^{O}C$. The latter method does not need the steam stripping process, but it has the

disadvantage of increasing corrosion rate at the higher
temperature. In ICT in KFA Jülich GmbH, Germany, the acid
aeficient feed adjustment was carried out with formaldehyde
in laboratory-scale[7]. It was reported that this method
reduces the waste volume by about half, compared with former
method without using formaldehyde.

3.3   Separation process

The Interim 23 process[8] was developed for the recovery of
U-233 from irradiated thorium when recovery of thorium was not
required. This process was used for short cooled irradiated
thorium fuel to recover only uranium 233, using lower
concentration of diluted TBP (1.5 to 5 %) for solvent. In some
cases[9] di-sec-butylphenylphosphate was chosen as extractant
since the selectivity of di-sec-butylphenylphosphate for
uranium is higher than that of TBP.

The single-cycle Thorex process was designed to recover both
uranium and thorium from the irradiated fuel. Gresky et al[8]
developed the Thorex process No. 2 in 1952. In this process,
41 % TBP in Amsco was used for the solvent and aluminium
nitrate was chosen as the salting agent in the first co-
extraction process. Thorium and uranium were co-extracted
in the first extraction column and only thorium was stripped
at the second partitioning column. Then, in the third
stripping column, U-233 was stripped as product.

More severe requirements were imposed on the thorium fuel
reprocessing, when the fuel of high burn-up from power
reactors was to be processed. From this point of view, the
two-cycle Thorex process[10] was developed to reduce the
inventory charges of the fuel, shortening the cooling time.
The process consists of a co-extraction and co-strip in the
first cycle, followed by the equivalent of the single-cycle
Thorex process. In the first design, 41 % TBP in Amsco was
used for solvent. A third uranium cycle[10] was developed to
increase the fission product decontamination in the case of
high burn-up and short cooled spent fuel and also for the

decontamination of long stored U-233 from the decay products
of U-232. In this process, 5 to 10 % diluted TBP or 2.5 % di-
sec-butylphenylphosphonate was used for solvent.

Because, the HTR fuel elements have no cladding, there was not
much incentive to use aluminium nitrate as the salting agent.
Therefore nitric acid tended to be used for salting agent.
First the Acid Thorex process[11] was investigated in Savannah
River and Knolls Atomic Power Laboratories. It was called
KAPL Acid Thorex process and the solvent used was 30 % diluted
TBP. According to the results, the process had the defects of
lower ruthenium decontamination. In order to increase the
decontamination and to decrease the stage height for the
extraction column, the acid Thorex process using an acid
deficient feed[6] was developed in ORNL. Decontamination
factors obtained in the experiment were 1000, 5000, 10000, and
100,000 for ruthenium, zirconium-niobium, protoactinium, and
rare earths, respectively. The recovery of protoactinium was
studied to shorten the cooling time[12] in some institutes.

In the German JUPITER project, 5 various kinds of extraction
processes are to be investigated; they are

>   Single-cycle Thorex process
>   Two-cycle Thorex process
>   Interim process with acid feed solution
>   Interim process with acid deficient solution
>   Uranium purification cycle

In both single-cycle and two cycle Thorex processes, nitric
acid should be used for salting agent and acid deficient feed
solution should be used for the co-extraction process in the
partitioning cycle. 30 % TBP in dodecane has been chosen as
solvent in the Thorex process and 5 % TBP in dodecane has been
chosen in Interim and uranium purification processes.

Some flow sheets of the processes are shown in the Appendix.

4. Equipment for Extraction

4.1 Pulse column

A pulse column is a vertical countercurrent liquid-liquid
extraction device. With the help of the reciprocating motion
to the liquids, the extraction efficiencies are improved in
comparison to other extraction columns. The pulsing motion was
supplied mechanically first, but these days a so-called air
pulser is likely to be adopted, since it has better reliability.
Packed and plate type columns have been investigated with
pulsing. They were applied for a long time to the extraction
of radioactive materials to recover heavy metals. Nowadays
plate type columns are in use mainly. The reports handling
irradiated nuclear fuel with pulse columns were classified
first, but after the Atom-For-Peace conference at Geneve in
1955, they became declassified.

In 1960's pulse columns were extensively studied in the field
of chemical engineering. The characteristics of their flooding,
holdup, and axial mixing and evaluation of extraction
efficiencies were investigated. L.D. Smoot[15] gave the
following correlation for the flooding velocity

$$U_c + U_d = 8.04 \times 10^3 \; \frac{\Delta\rho^{0.63} \; d^{0.458}}{\gamma^{0.144} \; \psi_f^{0.207} \; \mu_d^{0.20}} \; (\frac{U_c}{U_d})^{0.0143} \qquad (3\text{-}1)$$

$$\psi_f = \frac{\pi^2 (1-\epsilon^2) \; (fa)^3}{2\epsilon^2 \; C_o^2 \; l} \qquad (3\text{-}2)$$

where C_o is the orifice coefficient. As for holdup G.A. Sehmel[16]
observed that the dispersed phase holdup was a minimum at the
transition frequency between mixer-settler and emulsion type
of operation. The following empirical correlation was given to
predict the transition frequency for water-Hexane, water-Benzene,
and water-Methyl Isobutyl Keton systems

$$f_H = 4.0 \; (0.832 \times 10^{-5} \; \mu_d \; \gamma \; \Delta\rho - \ln a - 5.237) \qquad (3\text{-}3)$$

R.L. Bell[17] shows the next correlation to estimate the holdup

$$\eta = \frac{V_{org}}{8.6} (F+(1.25 \times 10^{-5}+7.93 \times 10^{-7} V_{aq})) (23.6 \, af-G)) \quad (3-4)$$

where

F = 0.03 (n-hexane), 0.05 (MIBK)

G = 64 (n-hexane), 38 (MIBK)

Axial mixing cannot be avoided in pulse columns. As for the longitudinal eddy diffusion coefficient, M.W. Mar[18] gave the following correlation using a steady state technique

$$E = \frac{K \, l^{0.68} \, U_d^{0.30} \, f^{0.36} \, a^{0.07} \, d^{0.30} \, \gamma^{0.42}}{U_c^{0.45} \, t^{0.06}} \quad (3-5)$$

HTU and HETS (Height of a Transfer Unit and Height Equivalent Theoretical Stage) are the parameters for the efficiency of extraction columns. HETS can be defined as the height of the column equivalent to one theoretical extraction stage. HTU based on the aqueous phase can be calculated by equations (3-6) and (3-7) for a piston flow system[19]

$$HTU = \frac{h}{NTU} \quad (3-6)$$

$$NTU = \int_{x_i}^{x_o} \frac{dx}{x-x_e} \quad (3-7)$$

L.D. Smoot[15] gave the simplified HTU correlation as follows

$$(HTU)_{oc} = \frac{K \, \Delta\rho^{1.04} \, \gamma^{0.97} \, V_c^{0.539} \, D^{0.317} \, l^{0.683}}{V_o^{0.434} \, d^{0.434} \, \rho_d^{2.342} \, \mu_d^{3.27} \, D_v^{0.865} \, V_d^{0.636}} \quad (3-8)$$

J.D. Thornton[20] gave another method for the evaluation of HTU. However, it is too complicated for practical use.

Generally speaking, pulse columns have the advantages of relatively easy maintenance. The residence time in pulse columns is shorter than in mixer-settlers. Moreover, it is easier in pulse

columns to control the interface since there is only one inter-
face in pulse columns whereas in mixer-settlers are as many
interfaces as chambers. Since pulse columns have less holdup
than mixer-settlers, they can start up and shut down in shorter
time[21]. However, they have the disadvantage of requiring a
high head room.

As for thorium fuel reprocessing, pulse columns have long been
used. For examples, R.H. Rainey[6] developed the Acid Thorex
process with a pulse column and A.D. Ryon[9] investigated pulse
columns for the separation of uranium from thorium.

4.2   Mixer-settler

A mixer-settler is a countercurrent stagewise contacting device.
In every stage the mixing is accomplished mechanically by an
impeller with variable speed. Air-pulsed mixer-settlers were
also investigated[22]. The two immiscible phases are separated
by gravity.

Mixer-settlers are in use in some nuclear fuel reprocessing
plants. However, they are being replaced now by pulse columns
for LWR fuel reprocessing, since they have the disadvantage of
larger holdup. Concerning the thorium fuel cycle, A.T. Gresky[23]
examined the batch countercurrent extraction in a laboratory
scale to give the basic data for the stage extraction devices.
J. Klitgaard[24] investigated mixer-settlers for the Acid Thorex
process and evaluated the extraction efficiencies.

4.3   Centrifugal extractor

A centrifugal extractor is a countercurrent liquid-liquid
contacting device. The basical concept is the same as that of
mixer-settlers, consisting of stages in which both the mixing
and the separation of the two phases are carried out, but
accelerated by centrifugal forces. Though one unit consists of
one stage in the design of SRL[25], the Robatel contactor[26]
developed in France contains a lot of stages in one unit.

This type of extractor has the great advantage of a short contact time about a few seconds for a stage. The shorter contact time is very favorable to prevent the solvent from radiation damage, especially on handling the high burn-up fuel. However, centrifugal extractors have less mechanical reliability than other extractors since they use more than 1500 rpm to generate the centrifugal forces. And moreover, it must be noticed that a centrifugal extractor doesn't stand well against the impurities of the feed solutions since they have the narrow and complicated flowing pass of fluids and weirs to keep the interface in the device.

5. Description of the equipment employed here

Figure 5.1 shows the upper part of the experimental equipment and Fig. 5.2 shows the lower part.

The column geometries are the same for the aqueous continous and the organic continuous column. The height of the cartridge section is 5 m for each column. The inside diameter of the column is 38 mm. The diameter of the holes in the plate is 2 mm and their triangular pitch is 4 mm, which gives a free area of 22.6 %. The plate spacing is 29 mm. Figure 5.3 shows the sieve plate and spacer.

The columns and the pulse pumps are supplied by QVF Glastechnik GmbH, Germany. The pulse amplitude is fixed at 15 mm throughout the experiment. The frequency can be changed from 16 to 133 (cycle/min). The pulse is produced by teflon bellows and the shape is a sinusoidal curve.

Figure 5.4 shows the schematic diagram of this equipment.

For the organic continuous column, a proportionating pump is installed for the aqueous feed and a gear pump for the organic feed. Two gear pumps are installed to supply both phases for the aqueous continuous column. The flow rates of the gear pumps are measured by a rotameter. In order to calibrate the scale, graduated glass tubes are installed between the tanks and the pumps. The scaled tubes stand vertically and with the help of
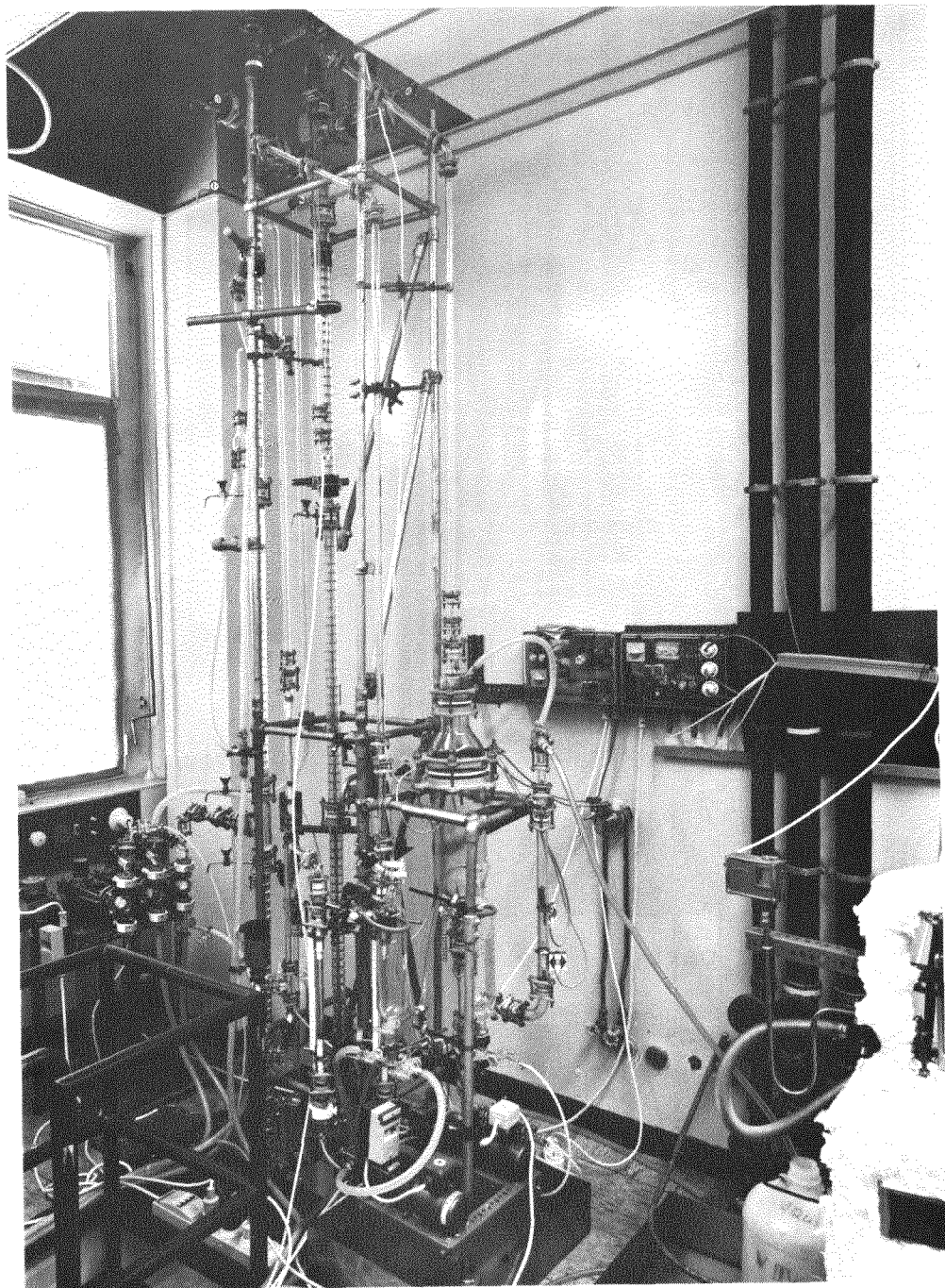
Fig. 5.1:   Upper part of the experimental equipment
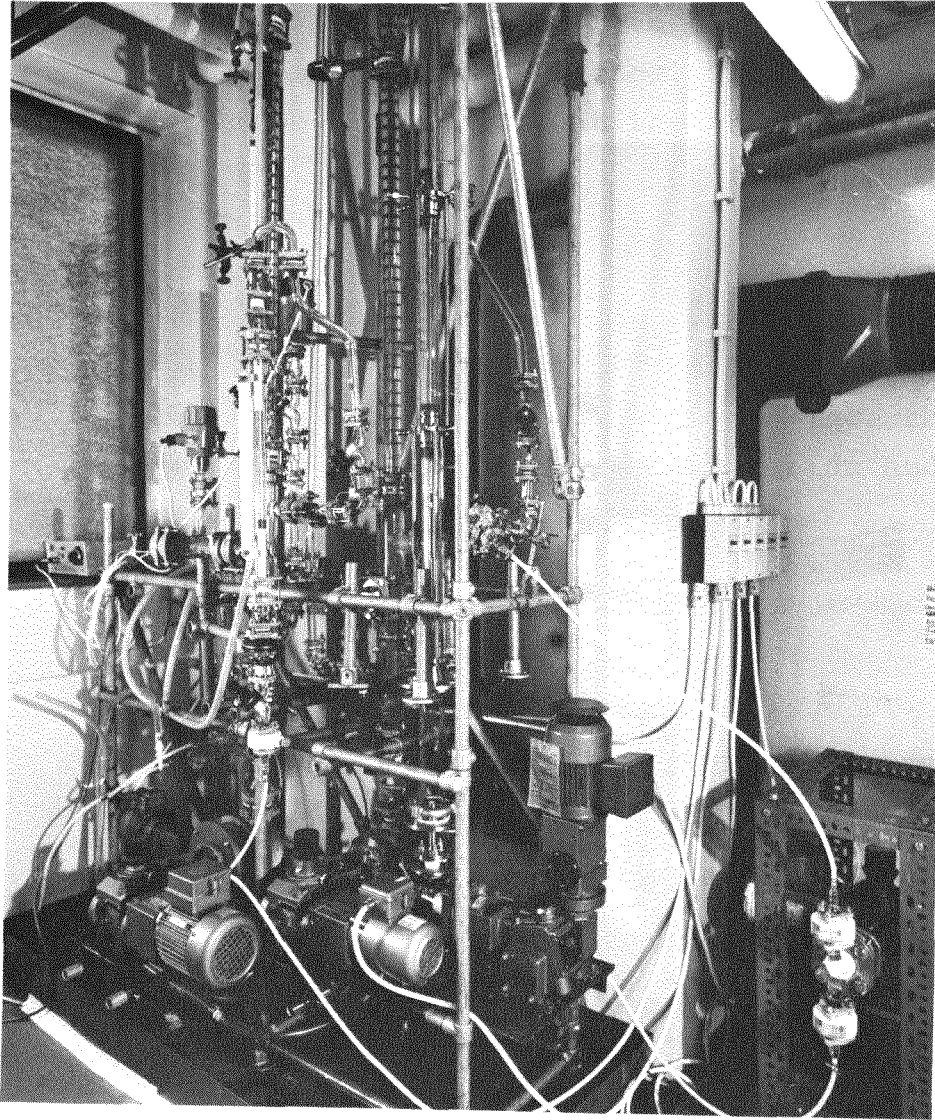
Fig. 5.2: Lower part of the experimental equipment
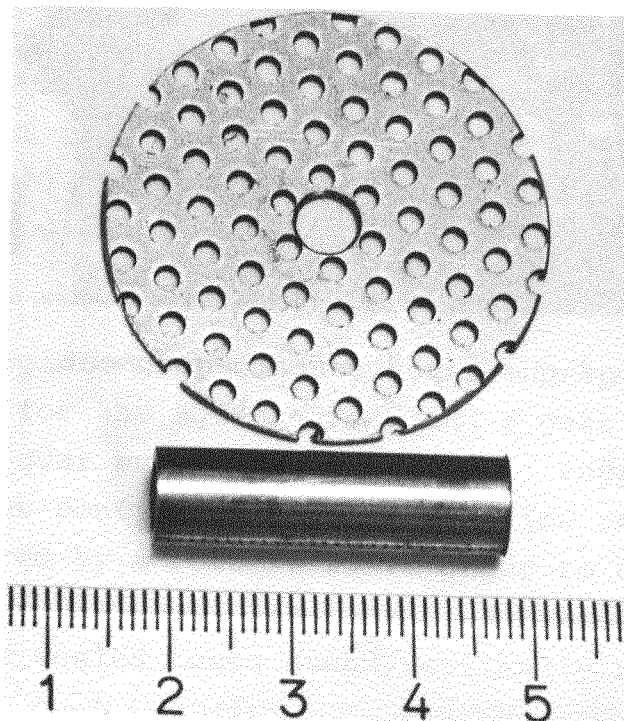
Fig. 5.3: Sieve-plate and spacer
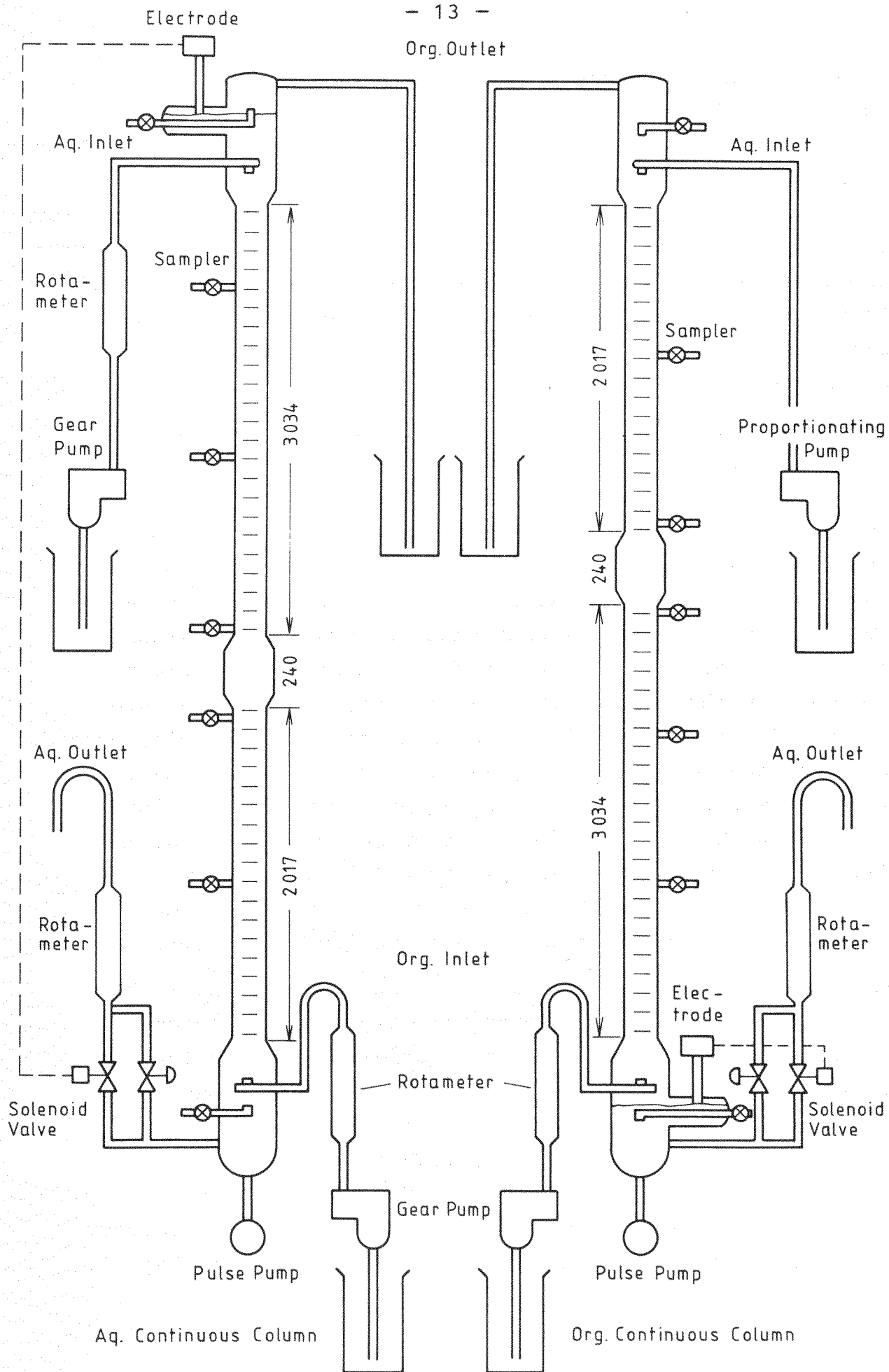
Fig. 5.4: Schematic diagram of equipment

a vacuum line, they are filled with liquid. Then, changing the valves, the liquid is pumped out. By timing the change of volume, the correct flow rate will be obtained. This procedure is also adopted to determine the flow rate through the proportionating pump. The interface in the columns is controlled by a Vegator 420 S supplied by QVF. This equipment determines the interface by measuring the electrical capacity. Responding to the signal from the electrode, the solenoid valve is switched on and off to open and close the by-pass in the aqueous phase outlet.

The pulse column is composed of 1 m long glass tubes and at every connection, samplers are installed. The sampling outlet is positioned in the middle of the cell. In the extraction experiment, the continuous phase was sampled for titration. When the sampling rate was very small, the continuous phase could be collected. Almost none of the dispersed phase was obtained for the aqueous continuous column. In the organic continuous column, however, penetration of water could not be avoided. In the case of the holdup study, both phases are collected together at higher sampling rate (valve fully opened). The sampling point of the collected dispersed phase is located 4 cm above the interface in the aqueous continuous column or 4 cm below the interface in the organic continuous column. That of the continuous phase is installed 5 cm below the dispersed phase inlet in the aqueous continuous column or 5 cm above the inlet in the organic continuous column.

Since this pulse column is of multi-purpose design, it has an additional inlet pipe in the middle, which is located 2 meters above the bottle of the cartridge section in the organic continuous column. In the aqueous continuous column, the additional inlet pipe is 3 meters above the bottle of the cartridge section. As a result, both columns have a 24 cm long section of no cartridges (see Fig. 6.1). In this study, the third inlet was used in the case of the Thorex process. The details of the experiment will be explained in chap. 8

6.   General flow characteristics of the pulse columns

To investigate flooding, holdup, and axial mixing characteristics,
the columns are operated, using distilled water for aqueous
phase and 30 % TBP in dodecane for organic. The aqueous to
organic flow rate ratio was chosen to be 1/3 as representative
for extraction and 1/1 for reextraction.

6.1   Flooding

First of all, the flooding characteristics were investigated,
changing the pulse frequency. The columns were operated for
30 minutes to observe whether the visual flooding occurs or
not. Fig. 6.1 shows the typical flooding in the middle of the
column at the no cartridge section.
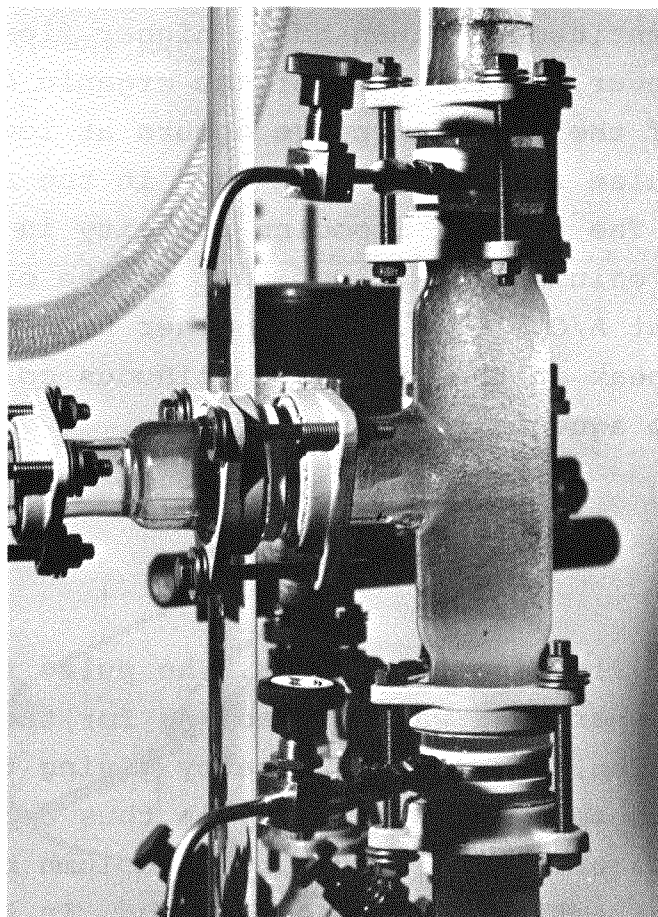
Fig. 6.1: Visual flooding at no cartridge section

The pulse amplitude was kept constant at 15 mm and the frequency was changed from 16 to 133 per minute. The A/O ratio was chosen to be 0.33 or 1.0 as explained before.

Figure 6.2 shows the flooding curve of the aqueous continuous column and Fig. 6.3 shows that of the organic continuous column. The correlation by L.D. Smoot et al.[15] is also shown in these figures. It will be seen that the results are reasonable compared with other experiments. However, in this experiment the dependency on A/O ratio is greater than that of the correlation, especially at lower frequency.

Figure 6.4 shows the difference of the flooding curves between the two modes of operation at A/O = 1/3 and Fig. 6.5 shows that at A/O = 1.0.

These figures show that, at A/O ratios around 0.33, the organic continuous column has higher capacity than the aqueous continuous column. On the other hand, at an A/O ratio of 1.0, the aqueous continuous column has a higher flooding velocity. And moreover, in the case of the organic continuous column, the peak of the flooding curve occurs at lower frequency (lower pulse intensity) than that in the aqueous continuous column. The peak of flooding velocity in the aqueous continuous column was 67 % of that in the organic continuous column at A/O = 0.33. On the other hand, at an A/O ratio of 1.0, the peak in the organic continuous column was 89 % of that in the aqueous continuous column.

6.2　Holdup

From the results of flooding experiment, the pulse frequency for the following experiment was decided. As for the mixer-settler type operation, the pulse frequency giving the highest flow velocity was chosen. This frequency is thus determined to be 32 per minute for the organic continuous column both in extraction and reextraction. On the other hand, in the aqueous continuous column, f = 32 gives the maximal capacity for extraction and f = 48 for reextraction. As for the higher frequency of the so-called emuslion region, f = 64 was chosen
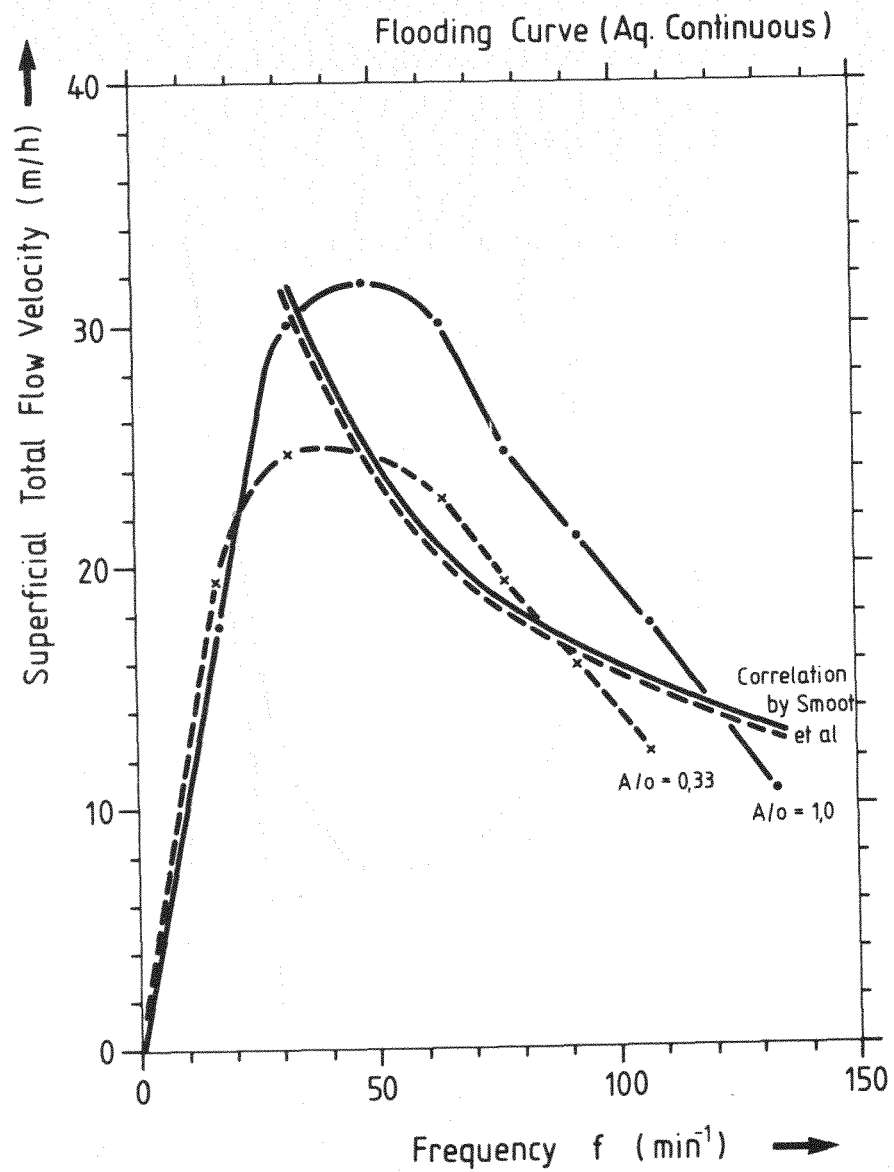
Fig. 6.2: Flooding curve of the aqueous continuous column
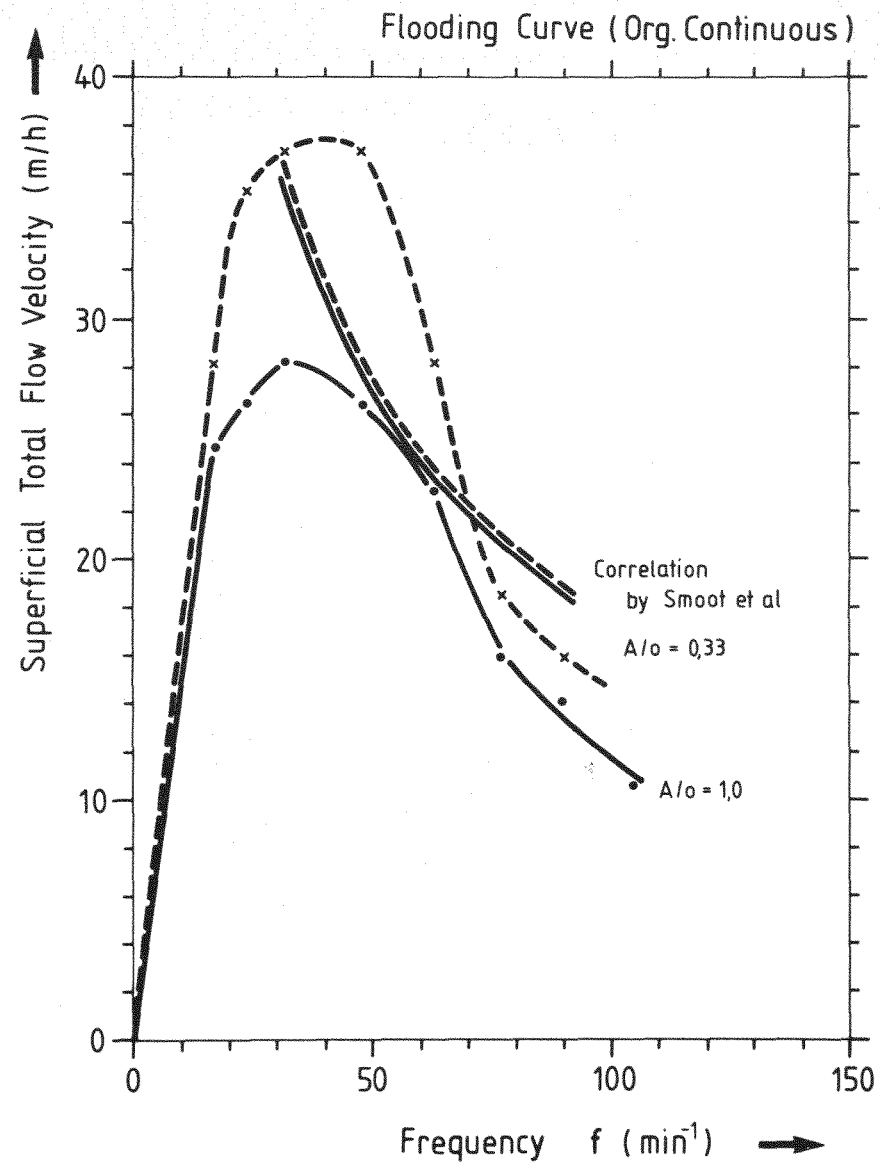
Fig. 6.3: Flooding curve of the organic continuous column
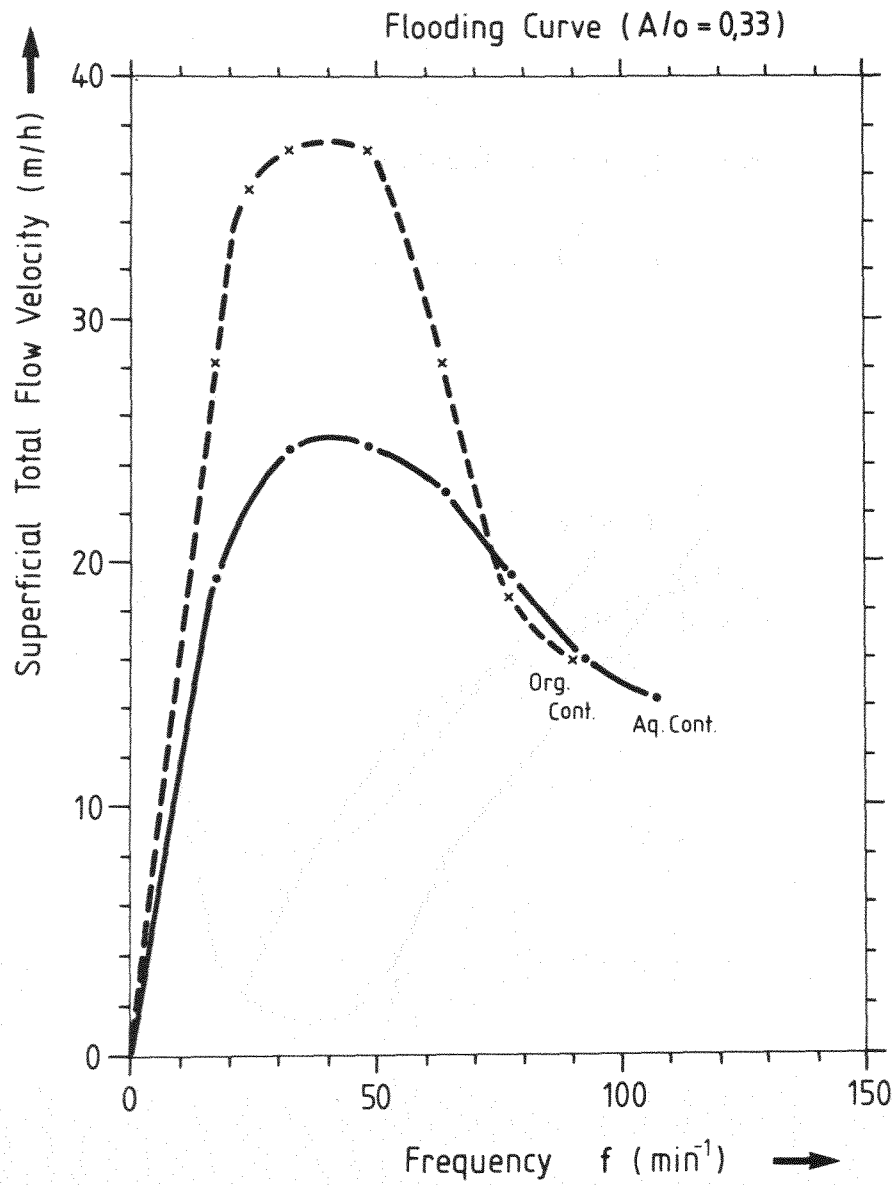
Fig. 6.4: Flooding curves at A/O = 0.33
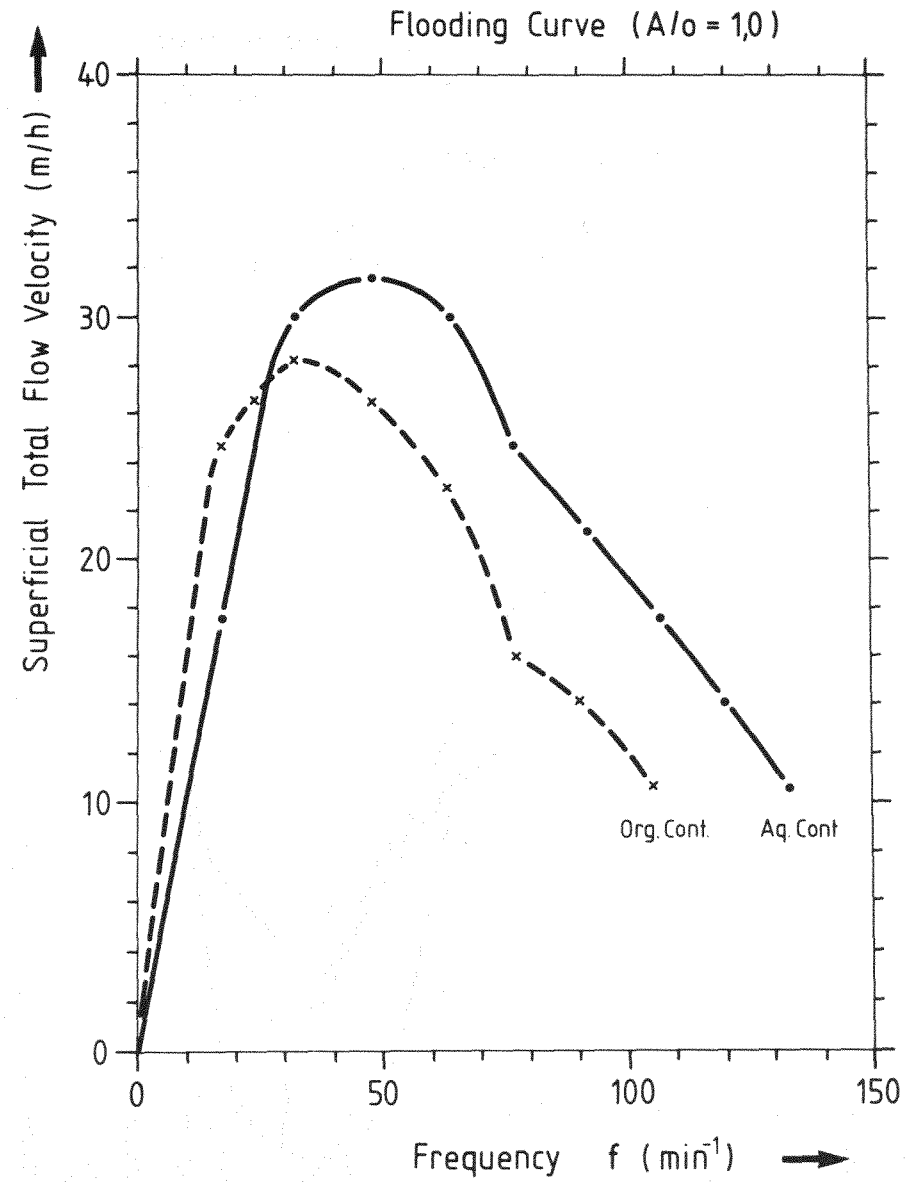
Fig. 6.5: Flooding curves at A/O = 1.0

for the organic continuous column and f = 77 for the aqueous
continuous column, so as to reduce the disadvantages of decreasing
the capacity. At each frequency, holdup dispersion along the
axis of the column was measured, while changing the throughputs
at the A/O ratio of 1/3 or 1/1.

In this experiment, the dispersed phase fraction was determined
by taking samples of 100 ml. The whole volume was measured in
a 100 ml cylinder and the dispersed phase was measured in a
10 ml cylinder. In this method, the obtained holdup might be
smaller than the real value, since the sample does not contain
the dead space which can be seen on the plate. However, from the
result it can be said that the value is fairly good. The flow
rates were chosen in the range from 60 % to 90 % of the flooding
flow rate.

Figures 6.6 to 6.13 show the holdup distribution along the column
height. The abscissa shows the distance from the dispersed phase
inlet.

At higher flow rates, holdup is increasing with the distance from
the inlet of the dispersed phase. R.L. Bell studied the integral
holdup and the axial distribution of holdup[27]. According to
the report, it was concluded that the holdup was uniform through-
out the column for columns having 23 cells or more. However,
contrary to the former report these experiments have shown that
the holdup tends to increase with distance from the dispersed
phase inlet especially at a higher flow rate. High holdup rates
improve the mass-transfer, because the contact time is longer.
Therefore, the column sections remote from the inlet of the
dispersed phase have a better extraction efficiency at the
operational flow rates.

The average holdup can be calculated by integrating the holdup
with respect to the column height. Since in some cases, the
graphical integration was equal within a few percent to the
average of 6 samples disregarding the value at the dispersed
phase inlet, the mean value was figured out by averaging the
6 values. Table 6-1 shows the holdup, flowrate, pulse frequency
and contact time.
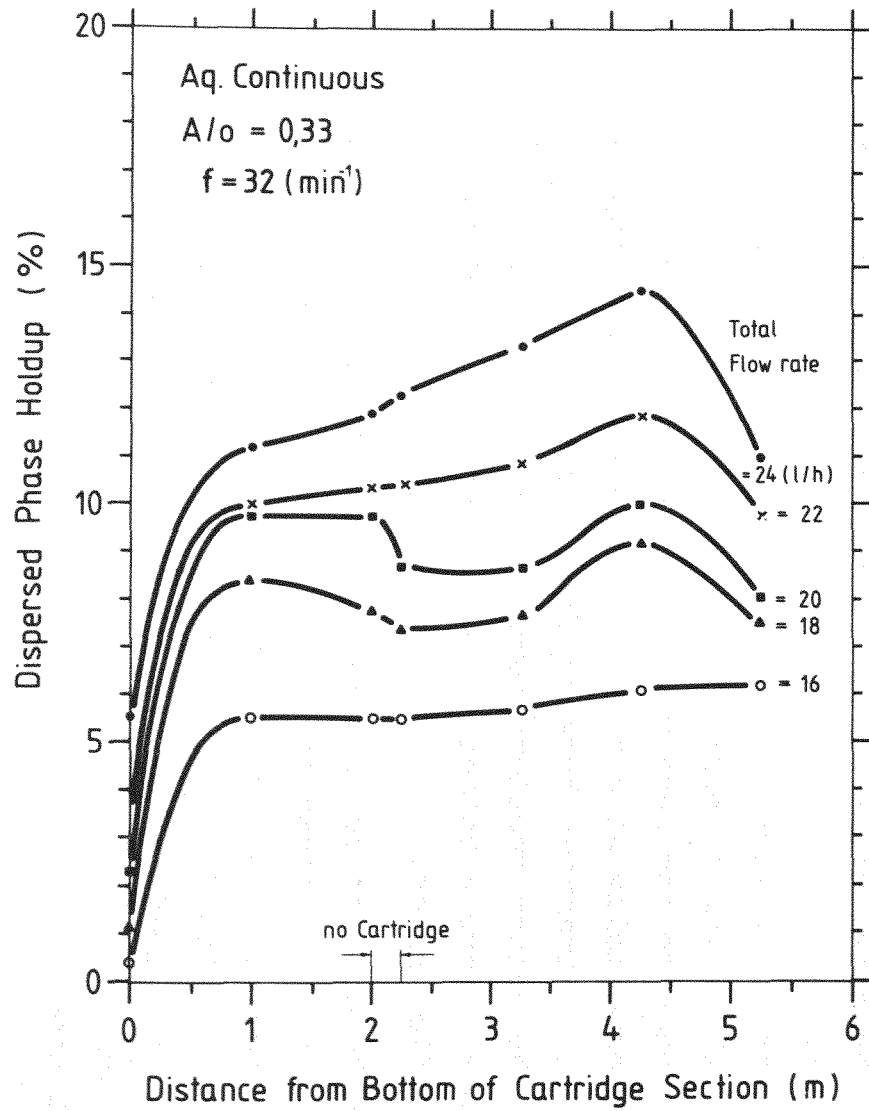
Fig. 6.6: Holdup distribution in the aqueous continuous column (A/O = 0.33, f = 32)
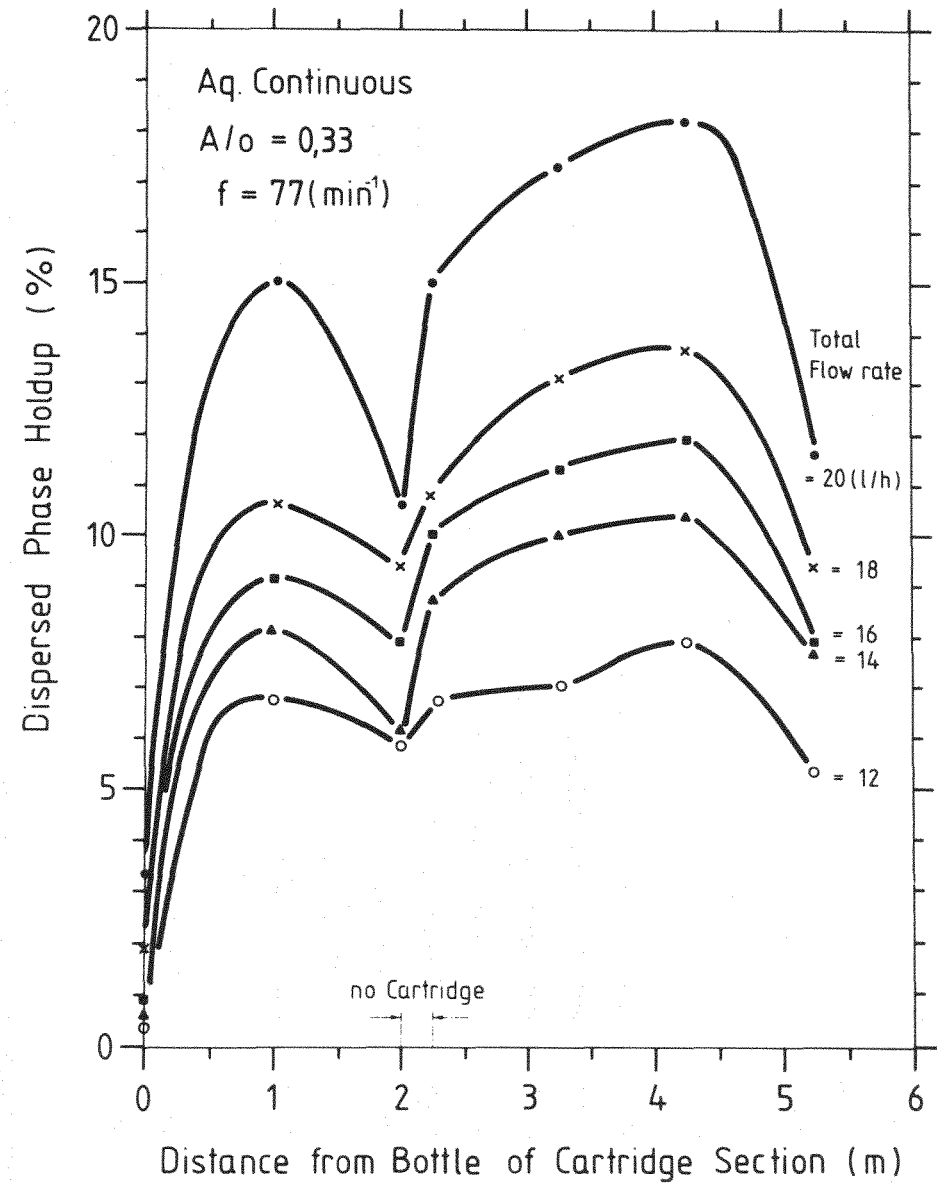
Fig. 6.7: Holdup distribution in the aqeuous continuous column (A/O = 0.33, f = 77)
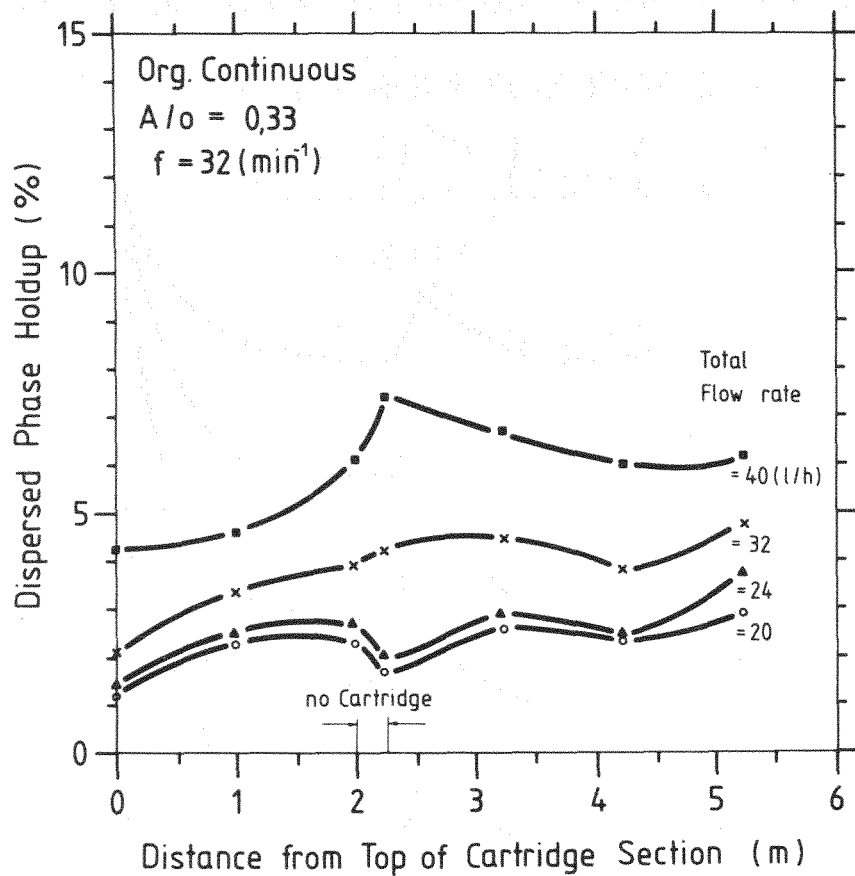
Fig. 6.8: Holdup distribution in the organic continuous column (A/O = O.33, f = 32)
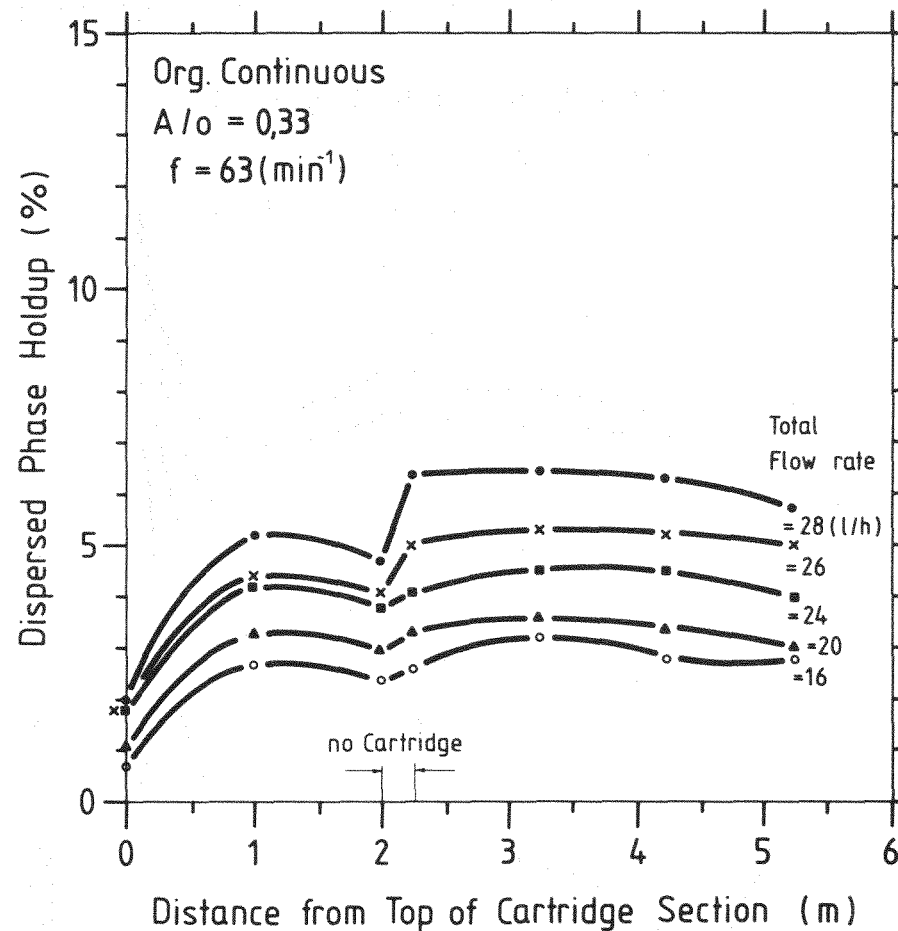
Fig. 6.9: Holdup distribution in the organic continuous column (A/O = O.33, f = 63)
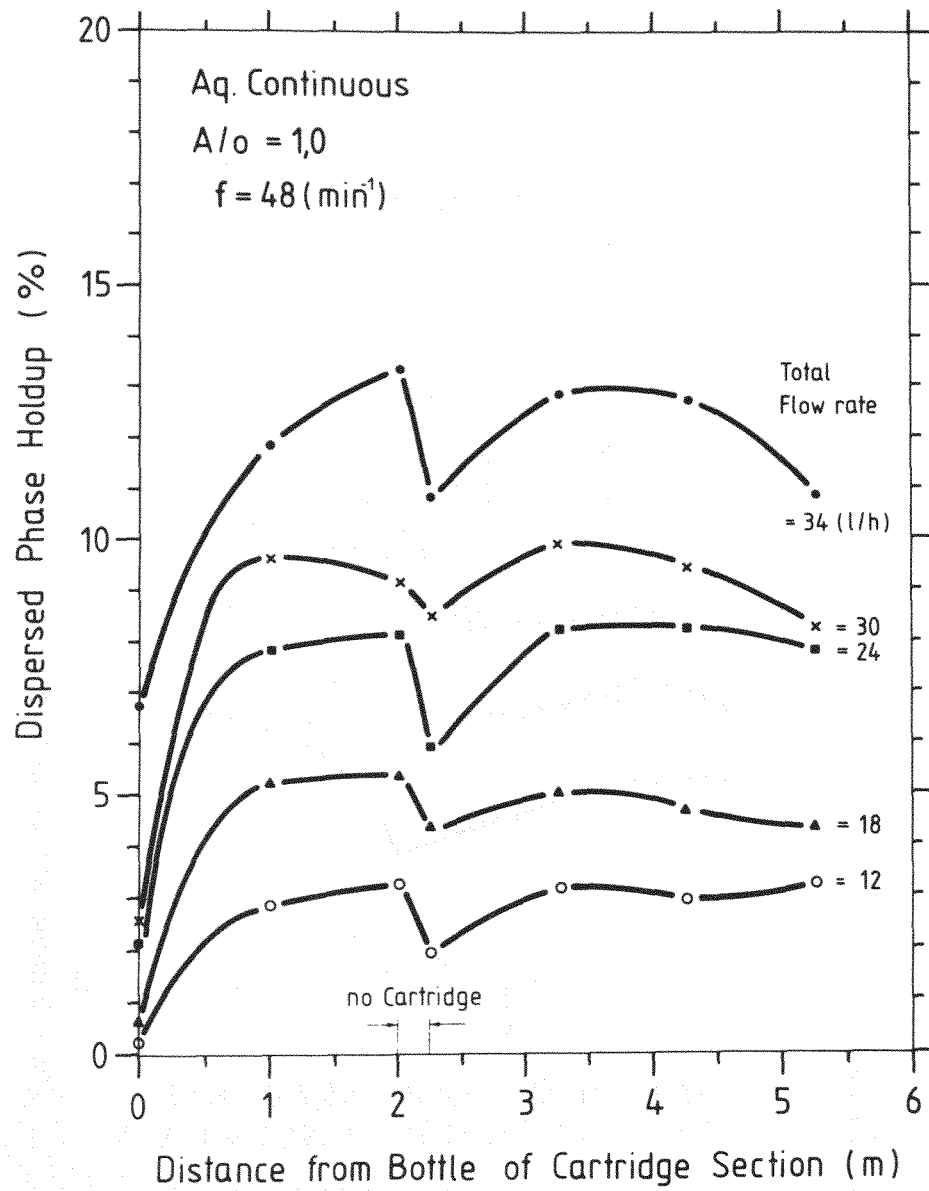
Fig. 6.10: Holdup distribution in the aqueous continuous column (A/O = 1.0, f = 48)
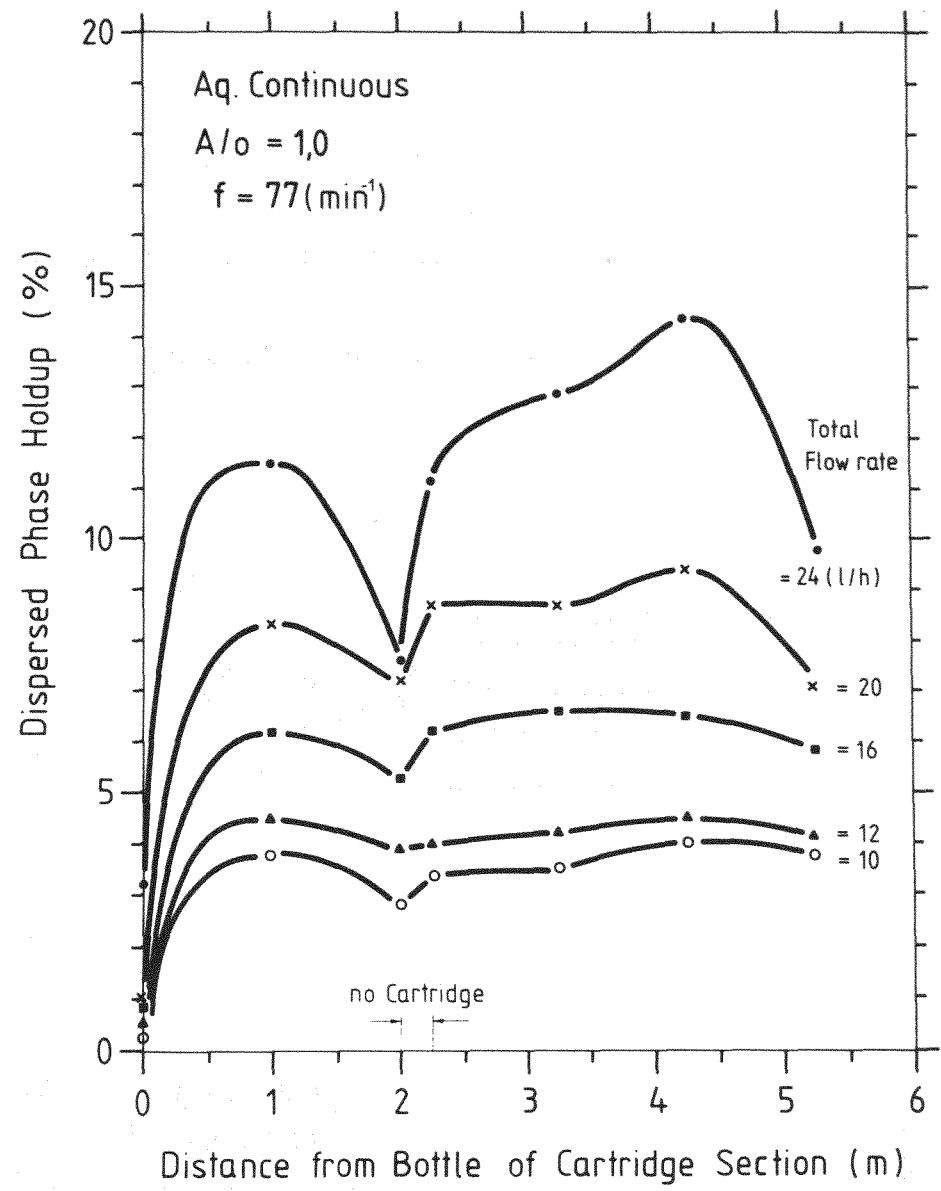
Fig. 6.11: Holdup distribution in the aqueous continuous column (A/O = 1.0, f = 77)
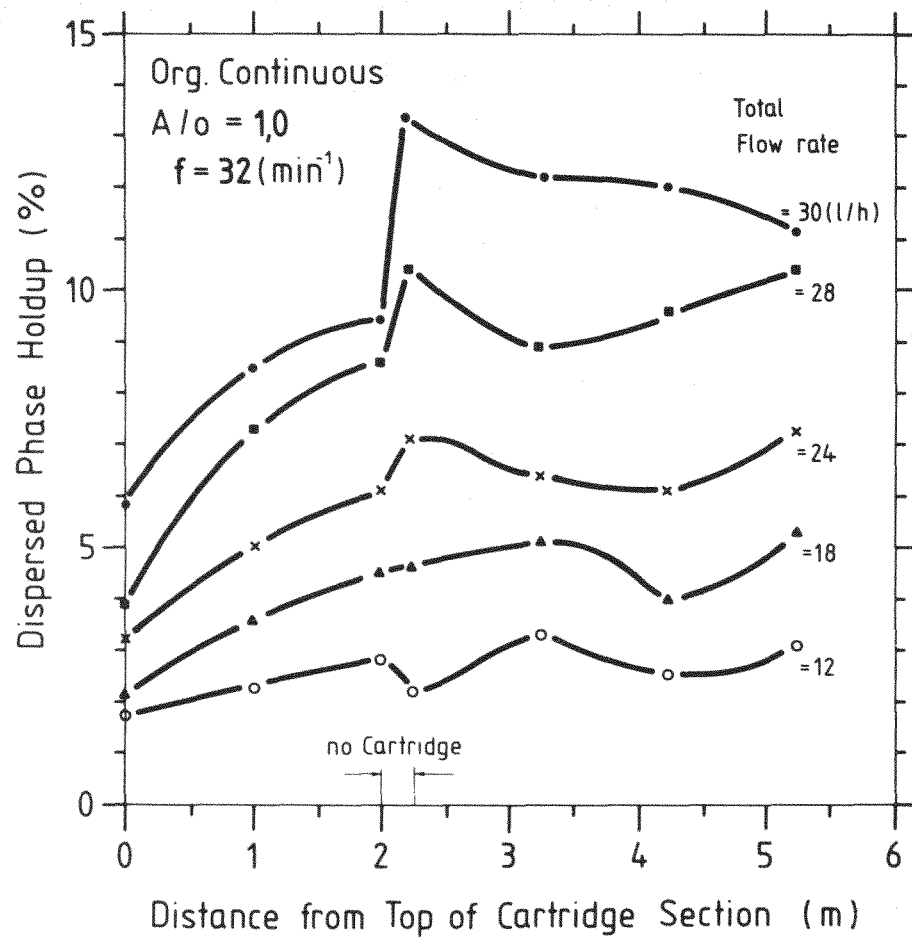
Fig. 6.12: Holdup distribution in the organic continuous column (A/O = 1.0, f = 32)
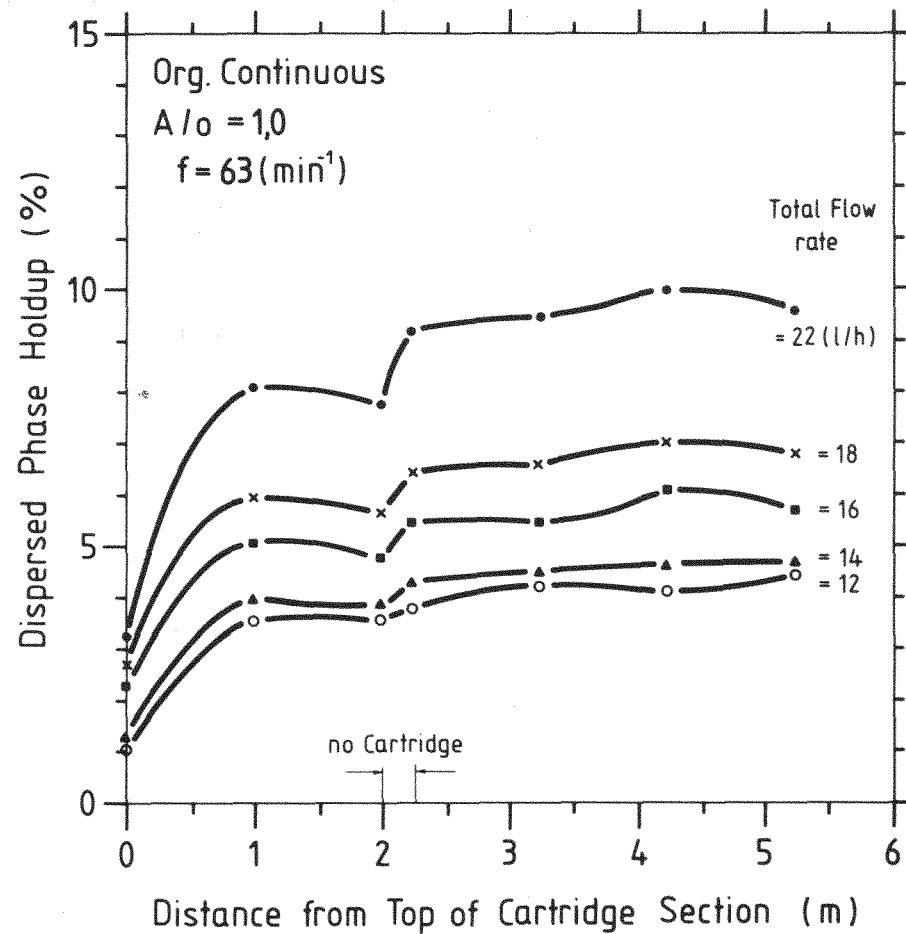
Fig. 6.13: Holdup distribution in the organic continuous column (A/O = 1.0, f = 63)

Table 6-1

Holdup and contact time (solute free)

Continuous phase	$f(min^{-1})$	$U_{aq}(l/h)$	$U_{org}(l/h)$	Holdup (%)	Contact time (min)
Aqueous	32	4	12	5.8	1.8
	32	6	18	12.4	2.5
	77	3.5	10.5	8.8	2.9
	77	4.5	13.5	11.2	3.0
	48	11	11	6.3	2.1
	48	15	15	9.1	2.2
	77	11	11	8.8	2.9
	77	14	14	11.2	3.0
Organic	32	6	18	2.7	1.7
	32	8	24	4.1	1.9
	63	5	15	3.3	2.4
	63	6.5	19.5	4.8	2.7
	32	9	9	4.5	1.8
	32	14	14	9.2	2.4
	63	8	8	5.5	2.5
	63	11	11	9.0	3.0

Regarding the contact time, there is not much difference between the two columns. In order to find the effect of frequency, the flow rate ratio R, defined by the ratio of operating flow rate to the flooding rate, is introduced. Figures 6.14 to 6.17 show the average holdup plotted against R. It is evident that the pulse frequency has no great effect on the holdup.
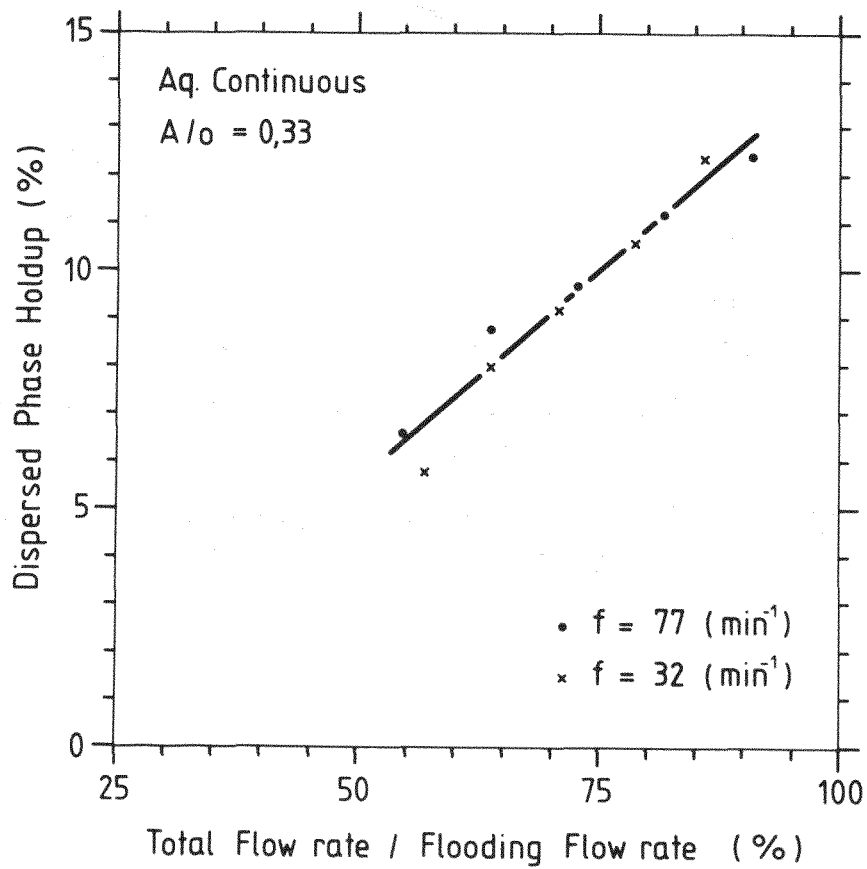
Fig. 6.14: Holdup vs. R in the aqueous continuous column (A/O = 0.33)
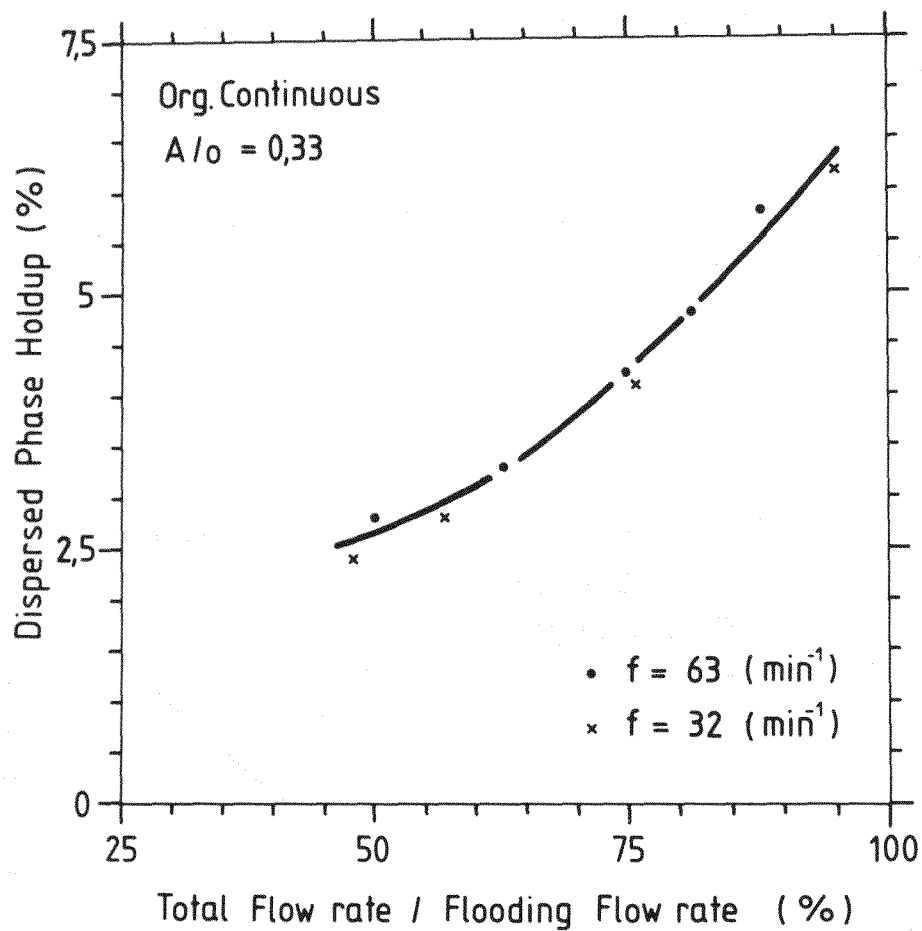
Fig. 6.15: Holdup vs. R in the organic continuous column
(A/O = 0.33)
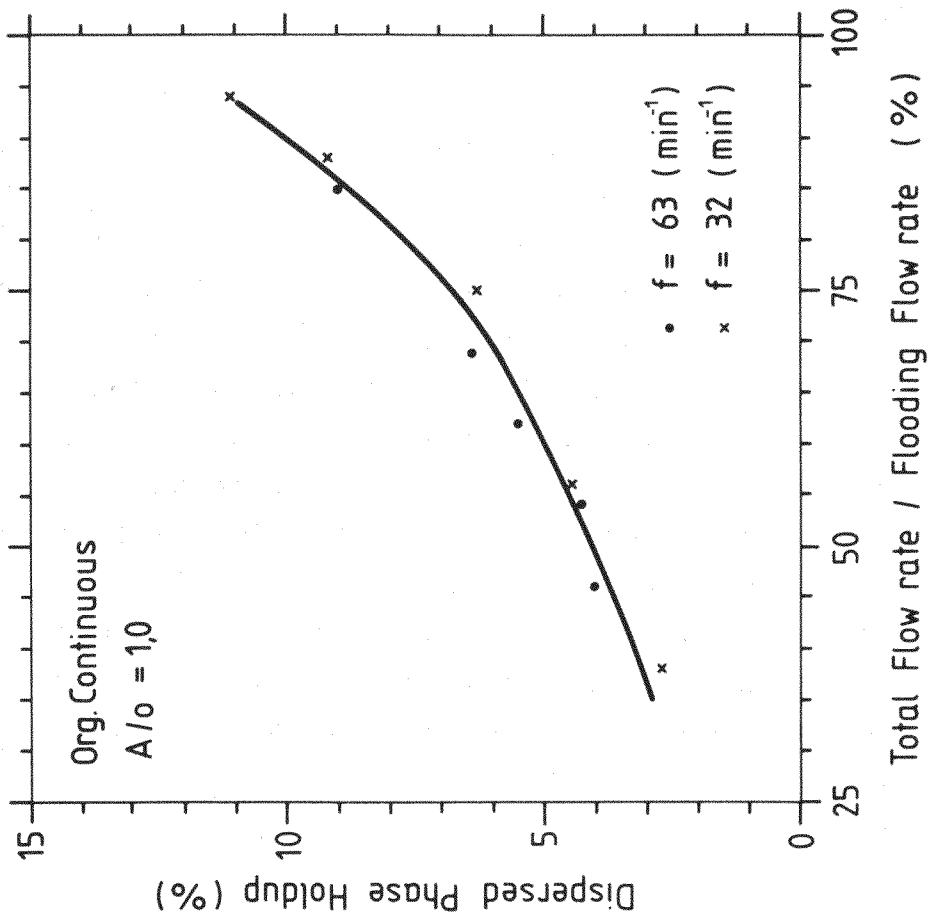
Fig. 6.17: Holdup vs. R in the organic
continuous column
(A/o = 1.0)
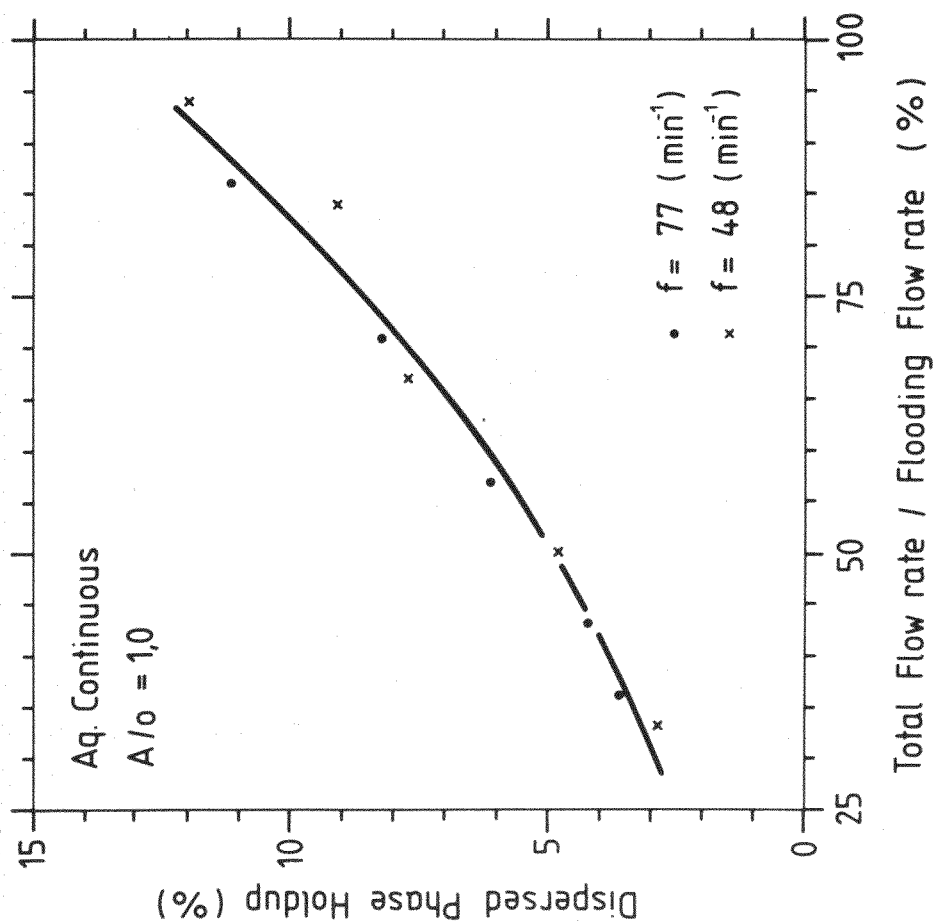
Fig. 6.16: Holdup vs. R in the aqueous
continuous column
(A/O = 1.0)

6.3   Axialmixing

As in other chemical reactors, the effects of longitudinal mixing cannot be avoided in pulse columns. These effects cause the so-called back mixing problem, about which B.W. Mar[18] have given much information. There are two tracing methods for observing the residence time and the back mixing in a continuous flow system. They are called F-diagram and C-diagram, respectively[28]. To explain an F-diagram, one can assume that the colour of the inflowing fluid changes from clear to red at time $\theta = 0$ first. $F(\theta)$ is defined as the fraction of the red tracer at the outlet as a function of θ. The plot $F(\theta)$ against $U \cdot \theta / V_m$ is called an F-diagram. On the other hand, if a quantity Q of a tracer is injected into the inlet, the residence time and the back mixing can be evaluated by observing the concentration in the exit stream. $C(\theta)$ is defined as the tracer concentration in the outlet at time θ.

The plot $\dfrac{V_m \, C(\theta)}{Q}$ vs. $\dfrac{U\theta}{V_m}$ is called a C-diagram.

The continuity equation for the delta injection technique is given by equation[29] (6-1)

$$\frac{dC}{d\theta} = \nabla (E \nabla C) = E \, \frac{d^2 C}{dh^2} \tag{6-1}$$

The equation shows the mixing of the injected tracer with the surrounding fluid. This equation can be solved and modified for a flowing fluid[29].

$$\frac{C V_m}{Q} = \frac{1}{2 \sqrt{\pi \, \dfrac{U\theta}{V_m} \, \dfrac{E}{VL}}} \; e^{\displaystyle - \frac{\left(1 - \dfrac{U\theta}{V_m}\right)^2}{4 \left(\dfrac{U\theta}{V_m}\right) \left(\dfrac{E}{VL}\right)}} \tag{6-2}$$

In this study, the delta injection technique was adopted, using methylene blue for a tracer in the aqueous phase. Since the investigation of the tracer distribution is difficult for the organic phase (solvent recycling), only the tracer distribution in the aqueous phase was examined. Concentration of methylene

blue was determined by photometric analysis. The injecting
concentration of the tracer was 546 mg/l for the aqueous
continuous column and that of 24.1 mg/l was used for the organic
continuous column. The injected volume was 16.4 cm^3 for both
columns. The tracer was injected at the column height of 4 m
in the aqueous continuous column in order to avoid the inter-
ference by the turbulences at the dispersed phase inlet. In
the organic continuous column it was injected at h = 5 m. As
for the aqueous continuous column, the obtained distribution
was plotted against T defined by $U\theta/V_m$. In this case V_m was
estimated by calculating the continuous phase volume as a
fraction of continuous phase holdup, which can be figured by
dispersed holdup in Table 6.1. The experimental condition is
the same as that of holdup study (Table 6.1). Figures 6.18 to
6.21 show the age-distribution to find the effect of the flow
rate. It has been observed that the effect of the flow rate
on the axial mixing is not so important, especially at lower
frequency.
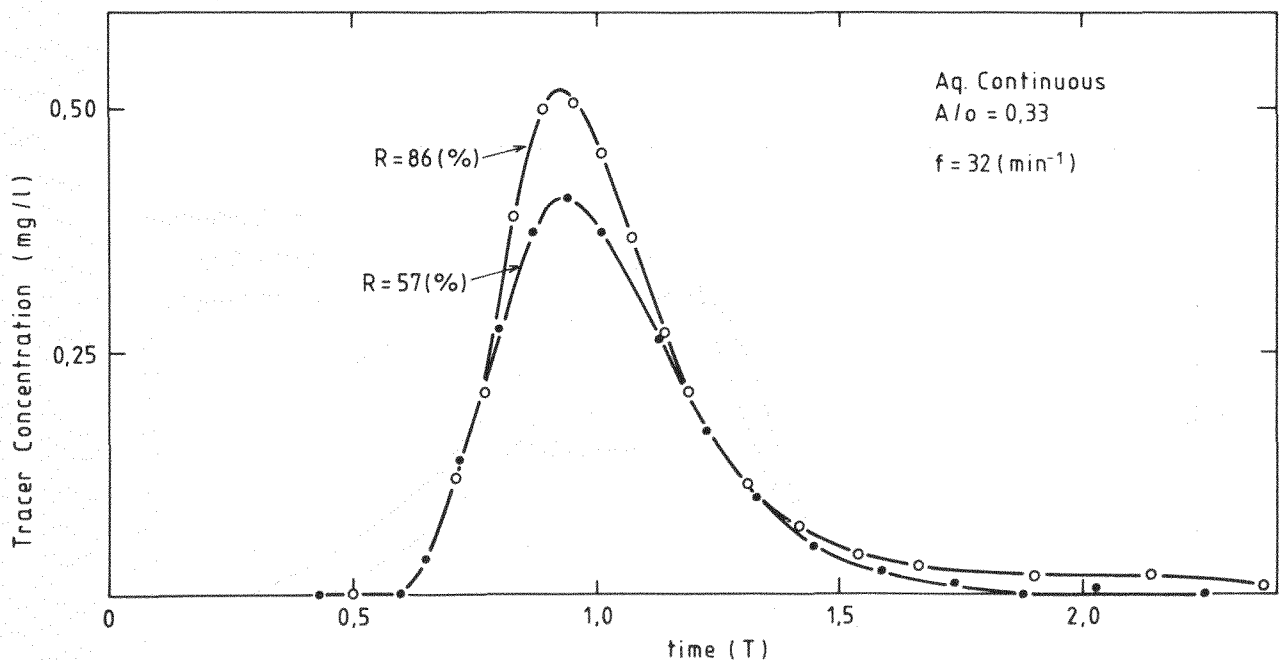
Fig. 6.18: Continuous phase residence time distribution in the
aqueous continuous column (A/O = O.33, f = 32)
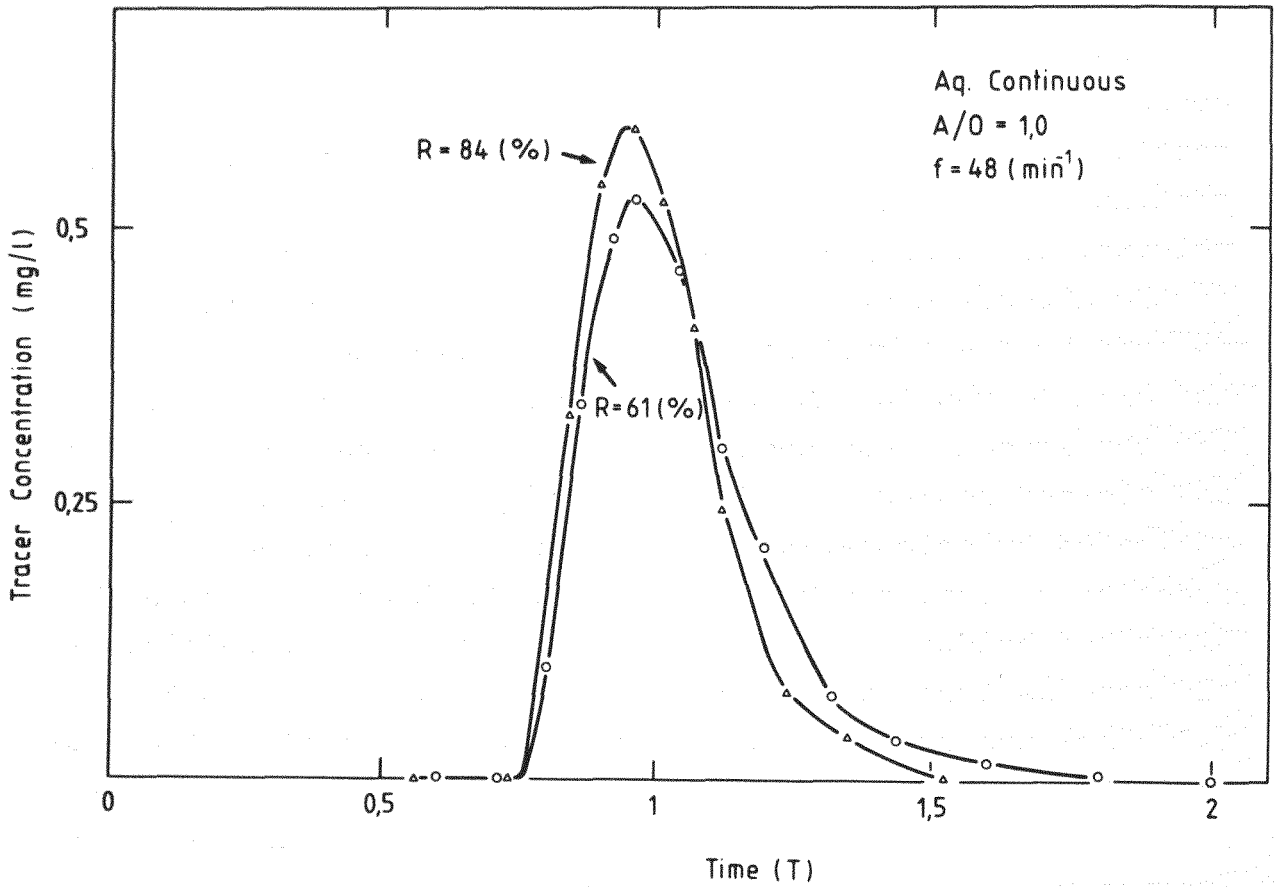
Fig. 6.19: Continuous phase residence time distribution
in the aqueous continuous column
(A/O = 1.O, f = 48)
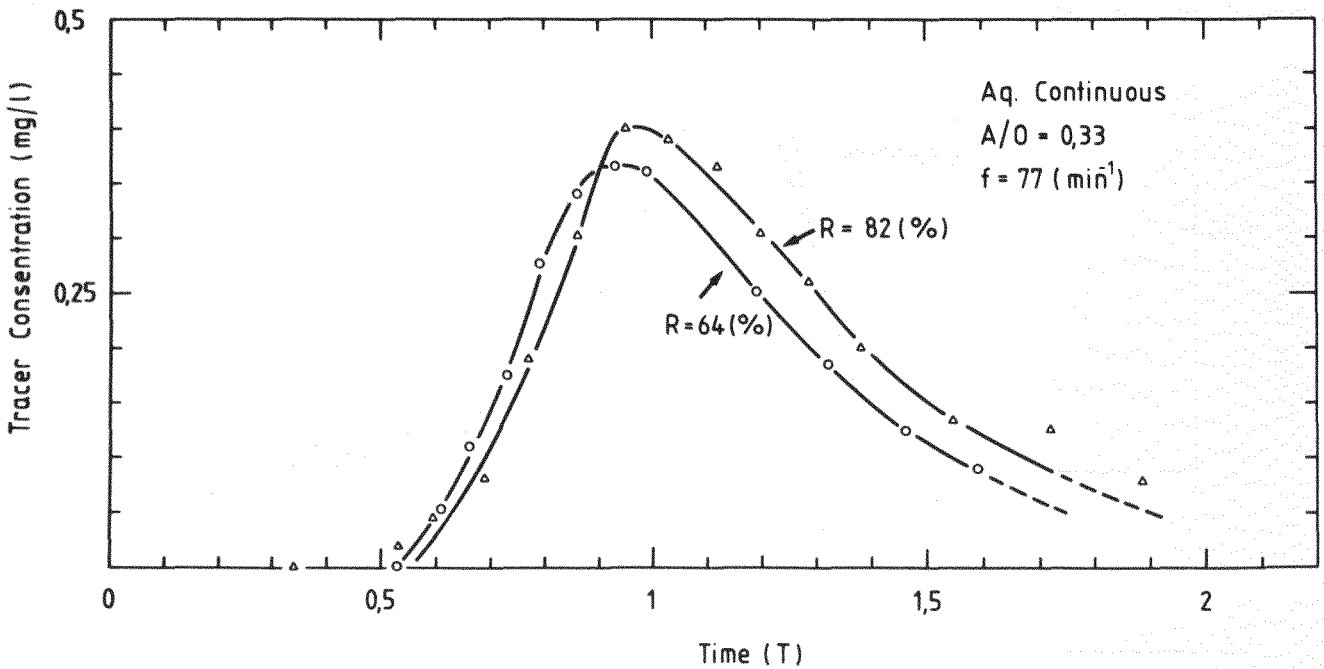
Fig. 6.2O: Continuous phase residence time distribution in the
aqueous continuous column (A/O = O.33, f = 77)
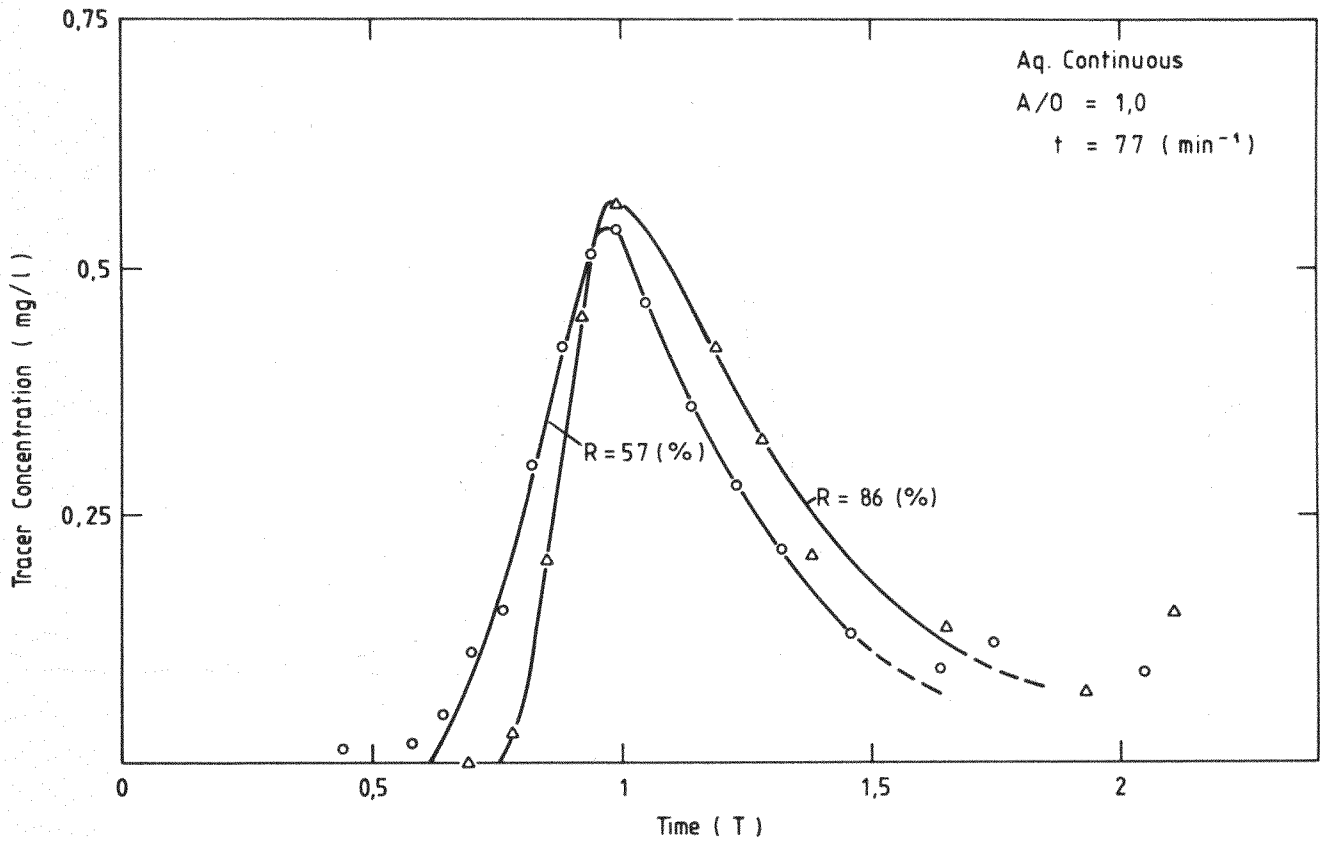
Fig. 6.21: Continuous phase residence time distribution in the aqueous continuous column (A/O = 1.0, f = 77)

On the other hand, Figs. 6.22 to 6.25 shows the effect of pulse frequency on axial mixing.
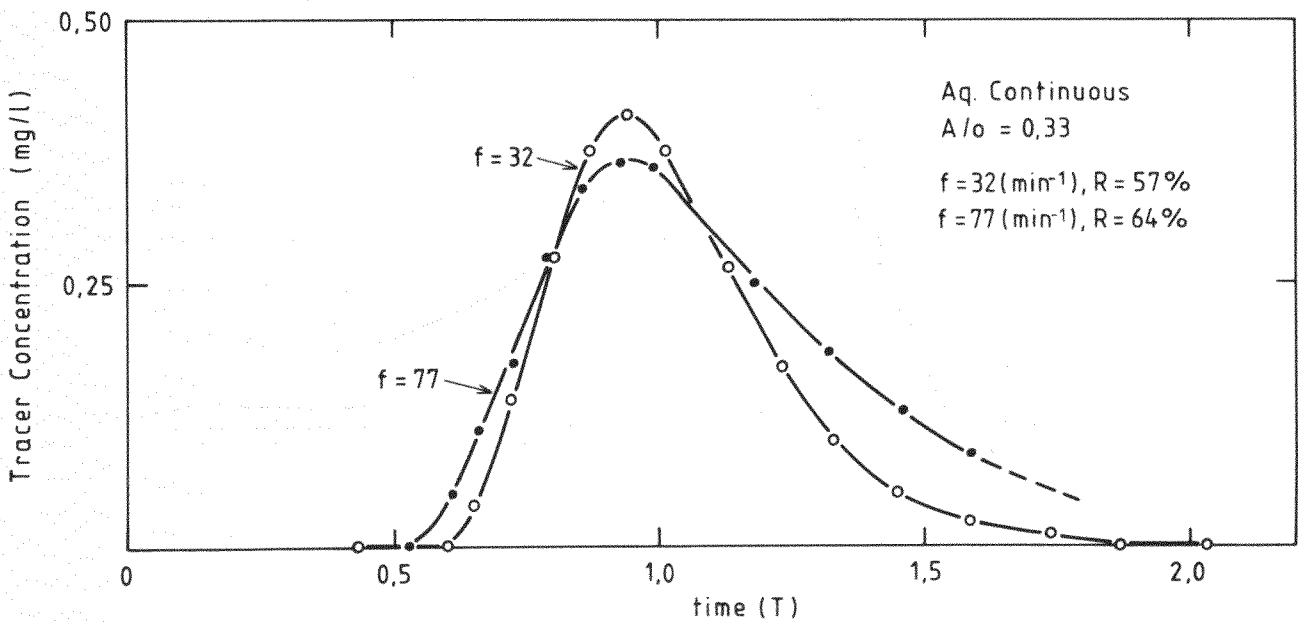
Fig. 6.22: Effect of pulse frequency on axial mixing in the aqueous continuous column (A/O = 0.33, R ≈ 60 %)
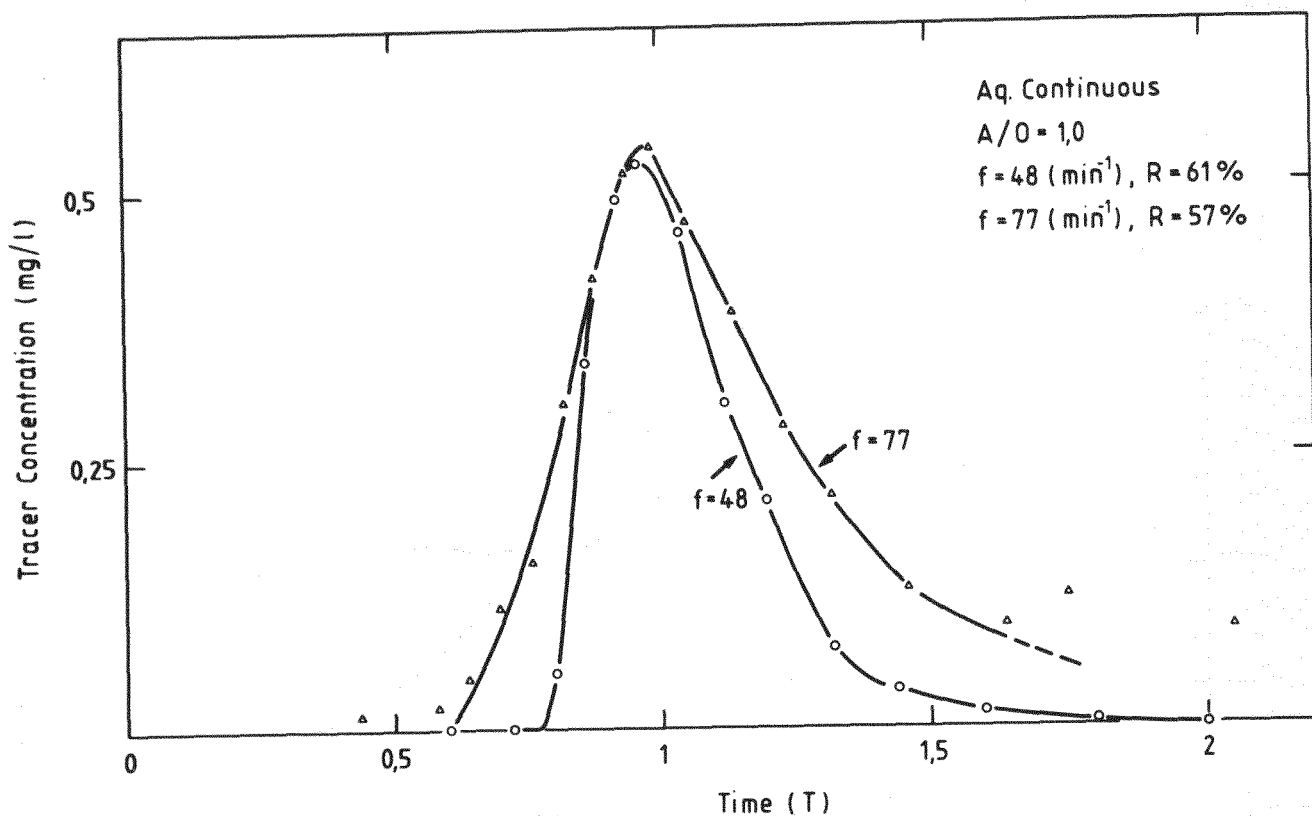
Fig. 6.23: Effect of pulse frequency on axial mixing in the aqueous continuous column (A/O = 1.0, R ≈ 60 %)
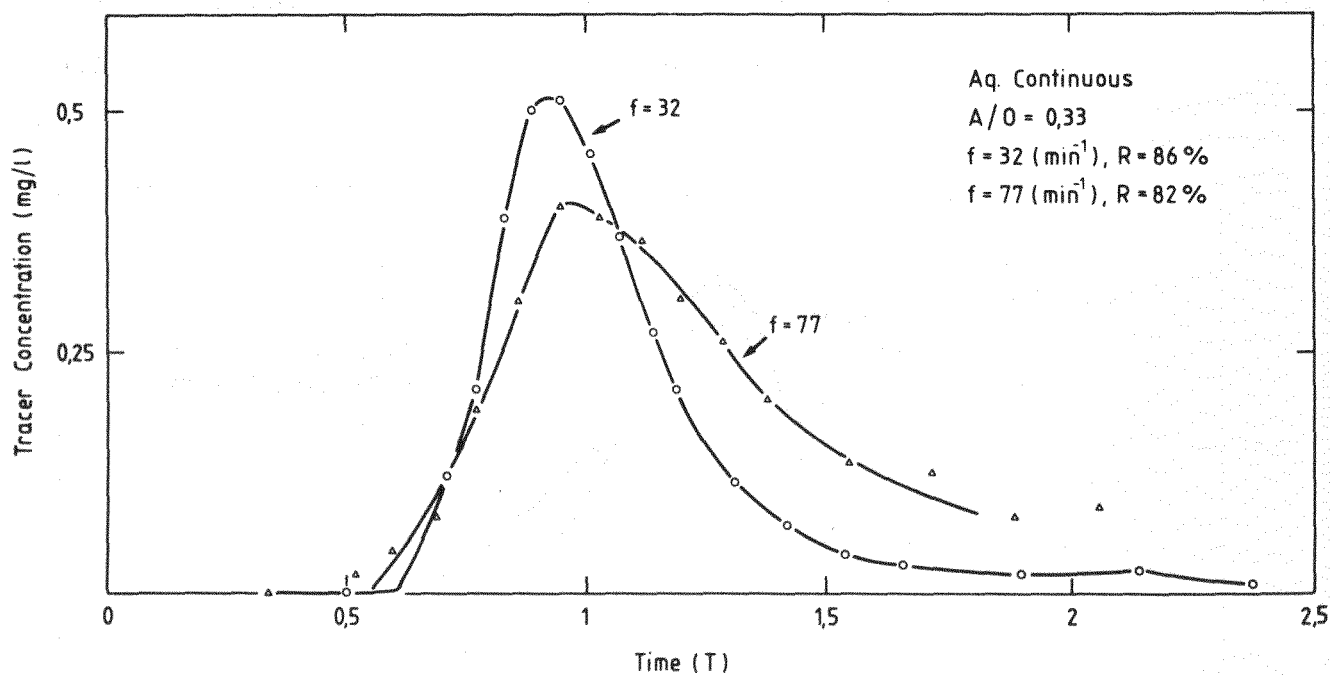
Fig. 6.24: Effect of pulse frequency on axial mixing distribution in the aqueous continuous column (A/O = 0.33, R ≈ 80 %)
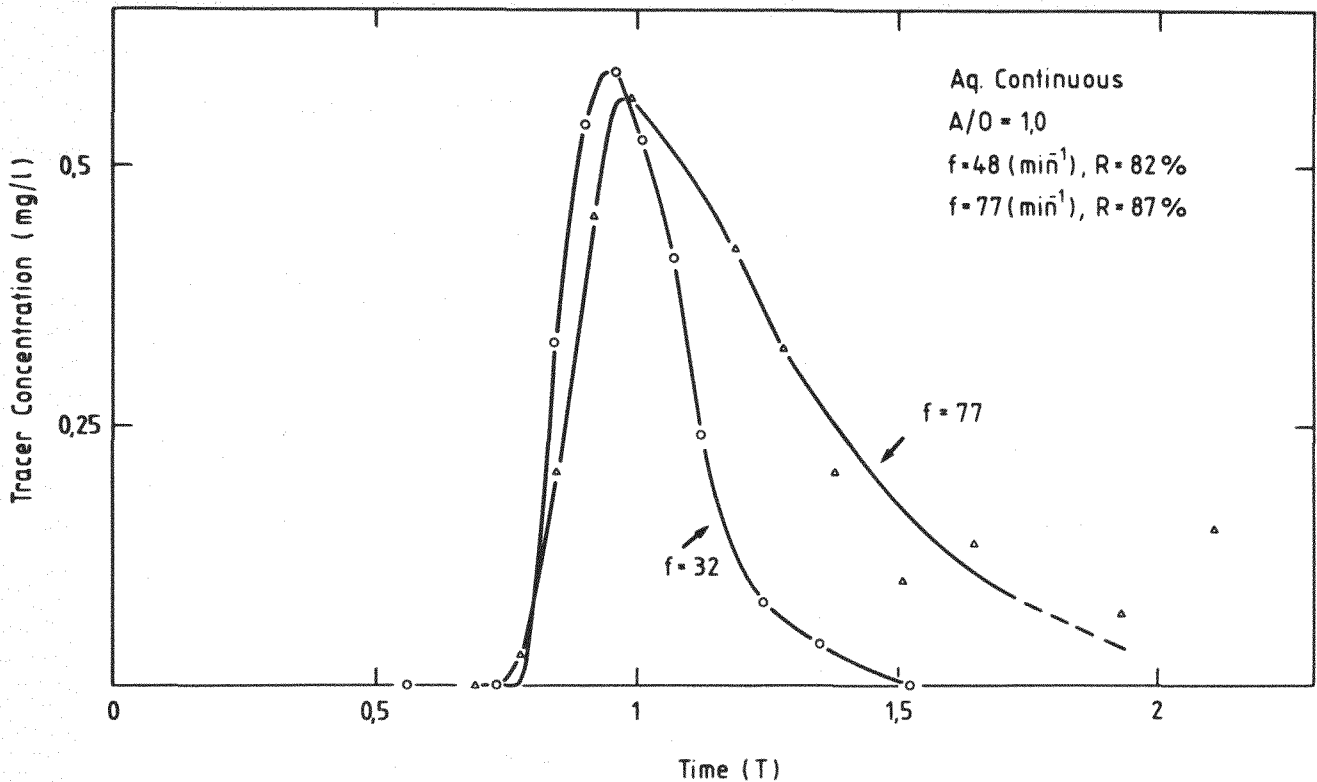
Fig. 6.25: Effect of pulse frequency on axial mixing distribution in the aqueous continuous column (A/O = 1.0, R ≈ 80 %)

From these figures, it is noticed that the longitudinal mixing becomes stronger with increasing frequency.

In the organic continuous column, the dispersed phase residence time and the back mixing were investigated using the same tracer. In this case the fluid was sampled about 1 to 2 cm below the interface in the column.

The ideal residence time, assuming a piston flow system, can be calculated with the dispersed phase holdup. However, in practice the labelled dispersed phase just arriving at the interface cannot be collected immediately. After arriving the interface, the droplets coalesce first and the tracer material is distributed in the aqueous phase. Then, a fraction of the colored aqueous phase is sampled through the sampling outlet for analysis. Since the sampling is made by this complicated procedure, the dimensionless time $T, (\frac{U\theta}{V_m})$ cannot be used for the organic continuous column. Neither the volume V_m nor the

time for coalescence can be determined precisely. Consequently,
the obtained data have been plotted against the absolute time
in minutes. Figures 6.26 to 6.29 show the residence time
distribution in the organic continuous column.
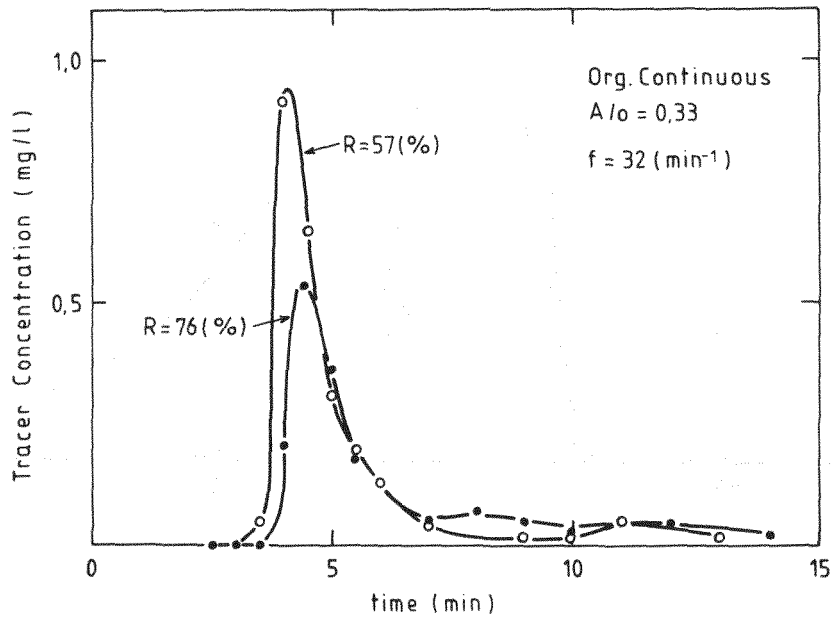
Fig. 6.26: Dispersed phase residence time distribution in the
organic continuous column (A/O = O.33, f = 32)
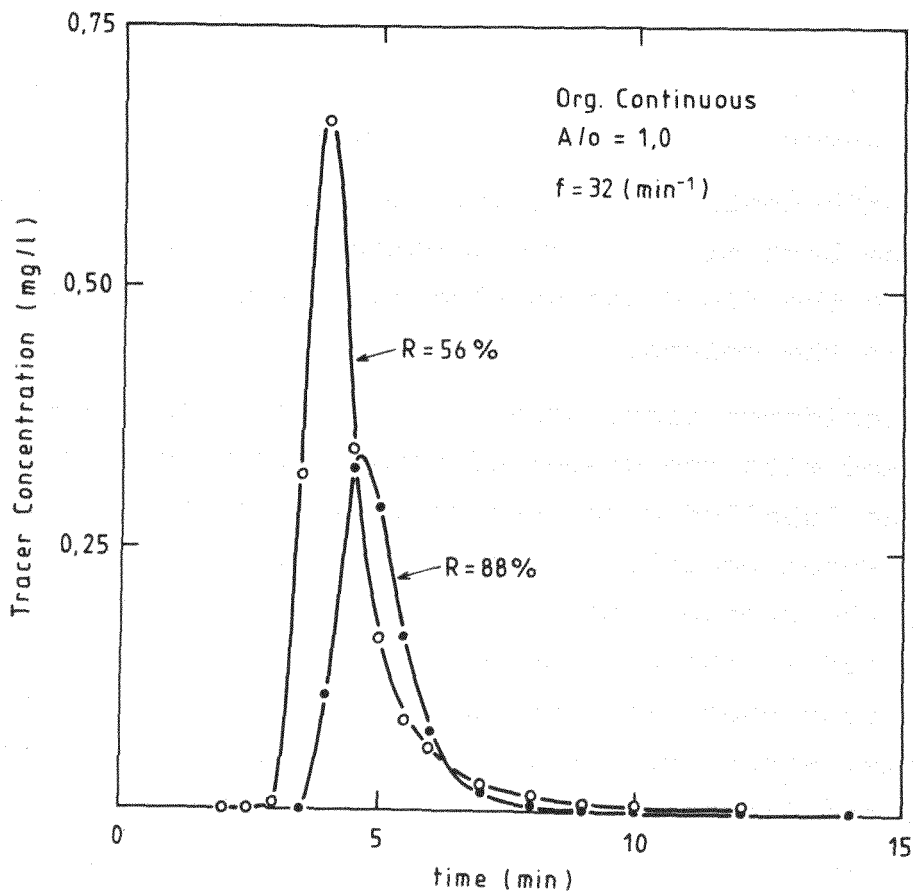
Fig. 6.27: Dispersed phase residence time distribution in the
organic continuous column (A/O = 1.O, f = 32)
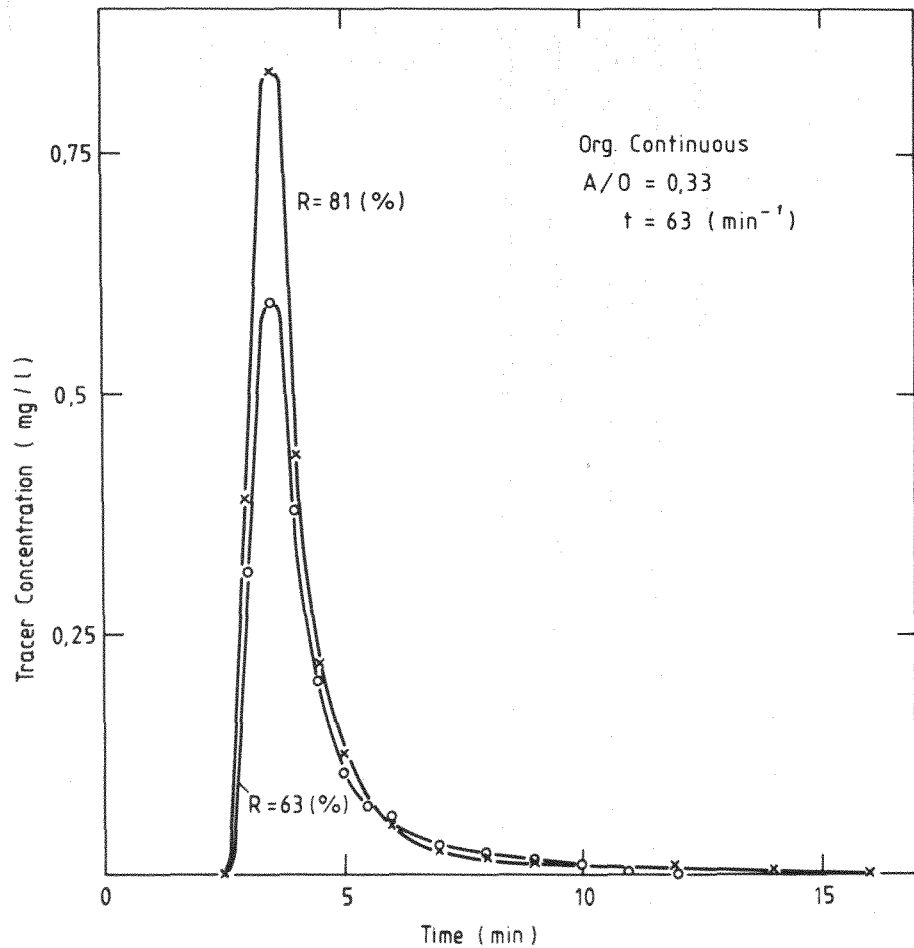
Fig. 6.28: Dispersed phase residence time
distribution in the organic
continuous column
A/O = O.33, f = 63 (min^{-1})
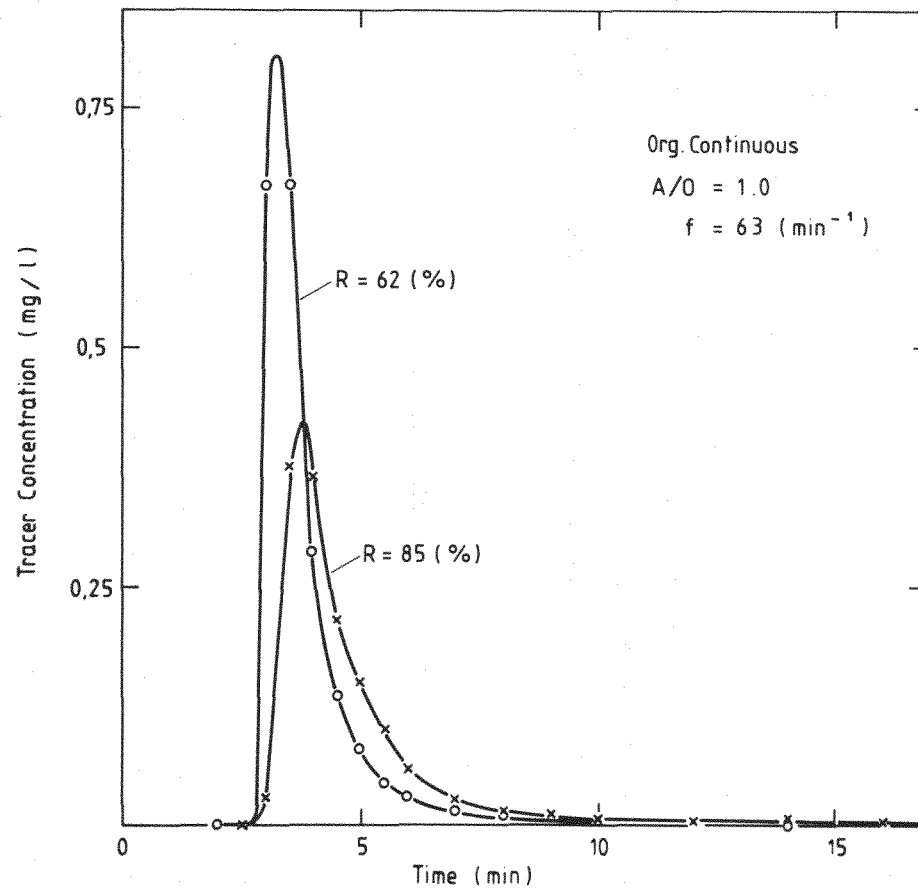
Fig. 6.29: Dispersed phase residence time
distribution in the organic
continuous column
A/O = 1.O, f = 63 (min^{-1})

Contrary to the results of the continuous phase distribution, there is not so much difference in the deviation of the curves.

According to the results, it is qualitatively concluded for the aqueous phase that the flow rates do not play an important role on axial mixing in both the continuous and the dispersed phase. However, with increasing frequency, the longitudinal mixing becomes remarkably stronger in the continuous phase, whereas there is not much effect on axial mixing in the dispersed phase.

7.   Evaluation of the extraction efficiency

7.1   Extraction of acetic acid

A ternary system of 30 % TBP in dodecane-acetic acid-water was applied to the columns to investigate the differences in extraction efficiency. The feed concentration of the acetic acid was chosen so that many extraction stages were necessary to complete the mass-transfer. The operating frequencies are the same in the holdup experiment. That is f = 32 and 64 for the organic continuous and f = 32 (or 48) and 77 for the aqueous continuous column. The throughput was chosen as 60 % or 80 % of the flooding rate in order to find the effect of flow rates on mass-transfer.

The columns were operated for 3 hours at every run to reach the steady state. To confirm the steady state, the mass loaded phase was sampled and titrated regulary. After attaining the steady state, 5 samples along the column height were taken for analysis. Both the extract and the rafinate were also sampled.

7.1.1 Experimental results

Figure 7.1 shows the acetic acid concentration along the column height for extraction and Fig. 7.2 shows that for reextraction.
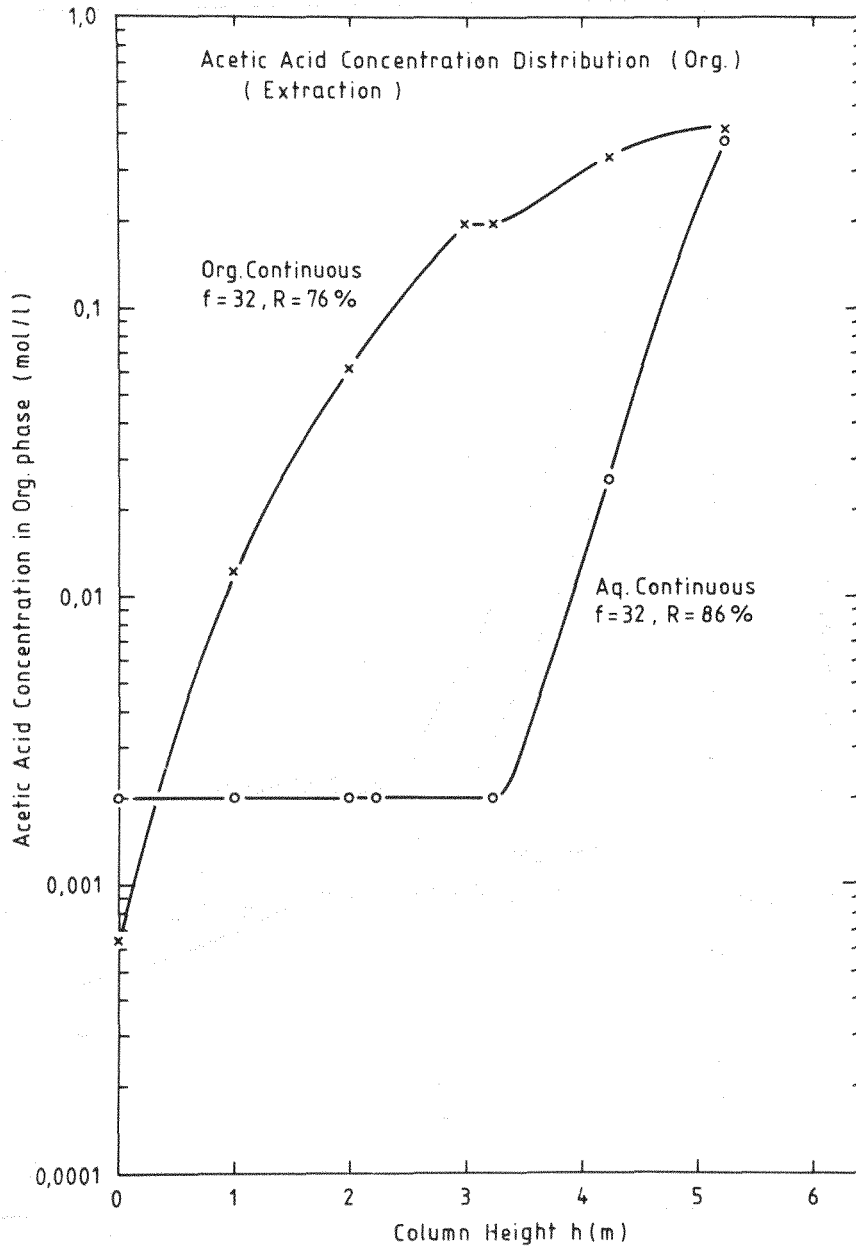
Fig. 7.1: Distribution of acetic acid along the column height in extraction
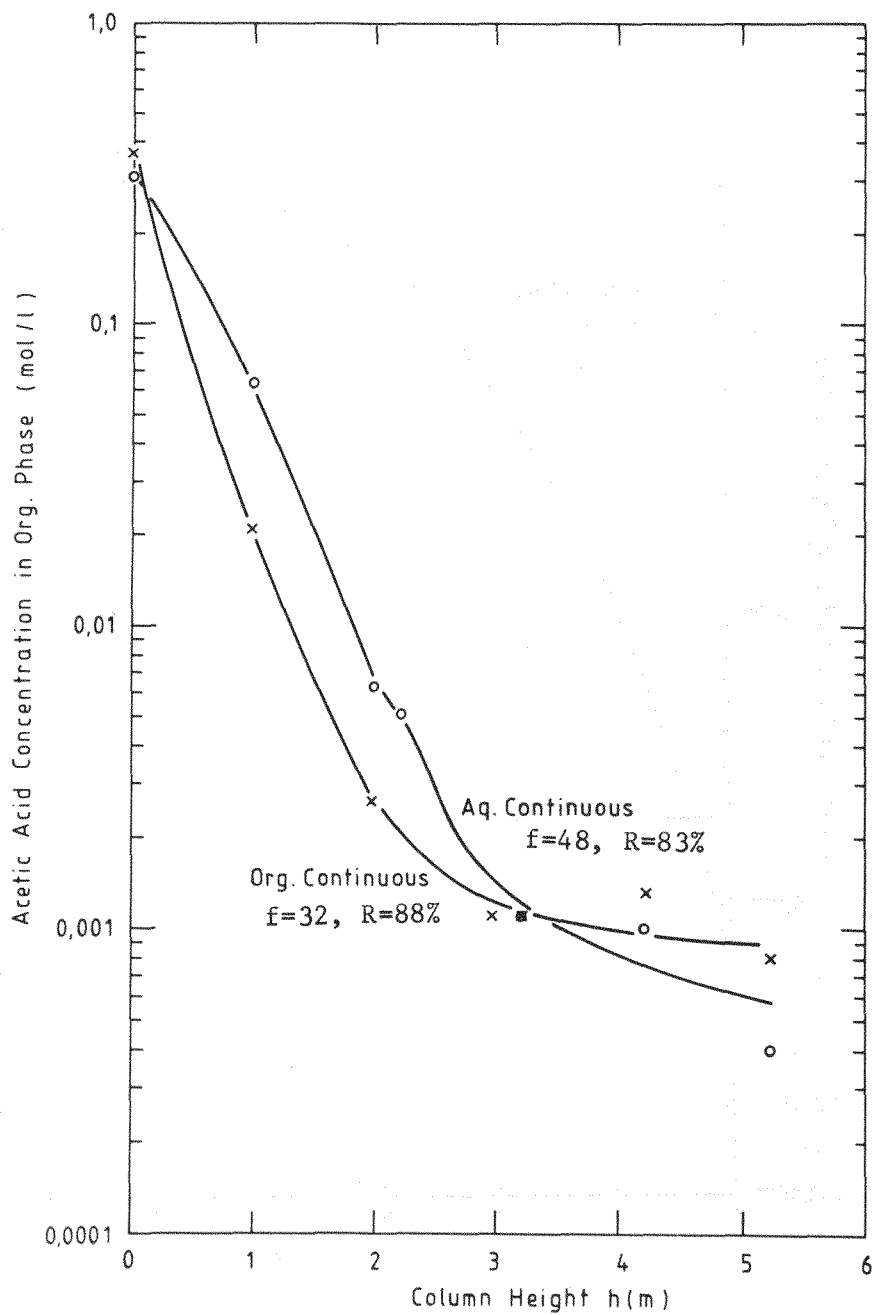
Fig. 7.2: Distribution of acetic acid along the column height in reextraction

In both figures, dispersed phase concentration was estimated
from continuous phase by calculating the material balance.
Figure 7.1 shows that acetic acid is transfered faster in
the aqueous continuous column. However, the relation is opposite
in Fig. 7.2. In Fig. 7.1, the acetic acid concentration in the
raffinate is higher than that of the organic continuous column.
But this may be caused by the acetic acid left in organic feed
from an inadequate solvent washing. In the organic phase for the
evaluation of the results, it must be emphasized that acetic
acid concentrations < 0.01 (mol/l) can be analysed only with
high error. Therefore, only the upper 1 m for extraction and
the lower 1 m for reextraction can be used for the evaluation
of characteristic differences. The equilibrium curve for the
system, 30 % TBP in Dodecane-acetic acid-water is shown in
Fig. 7.3. The acetic acid determination was carried out as
described in chapter 11.
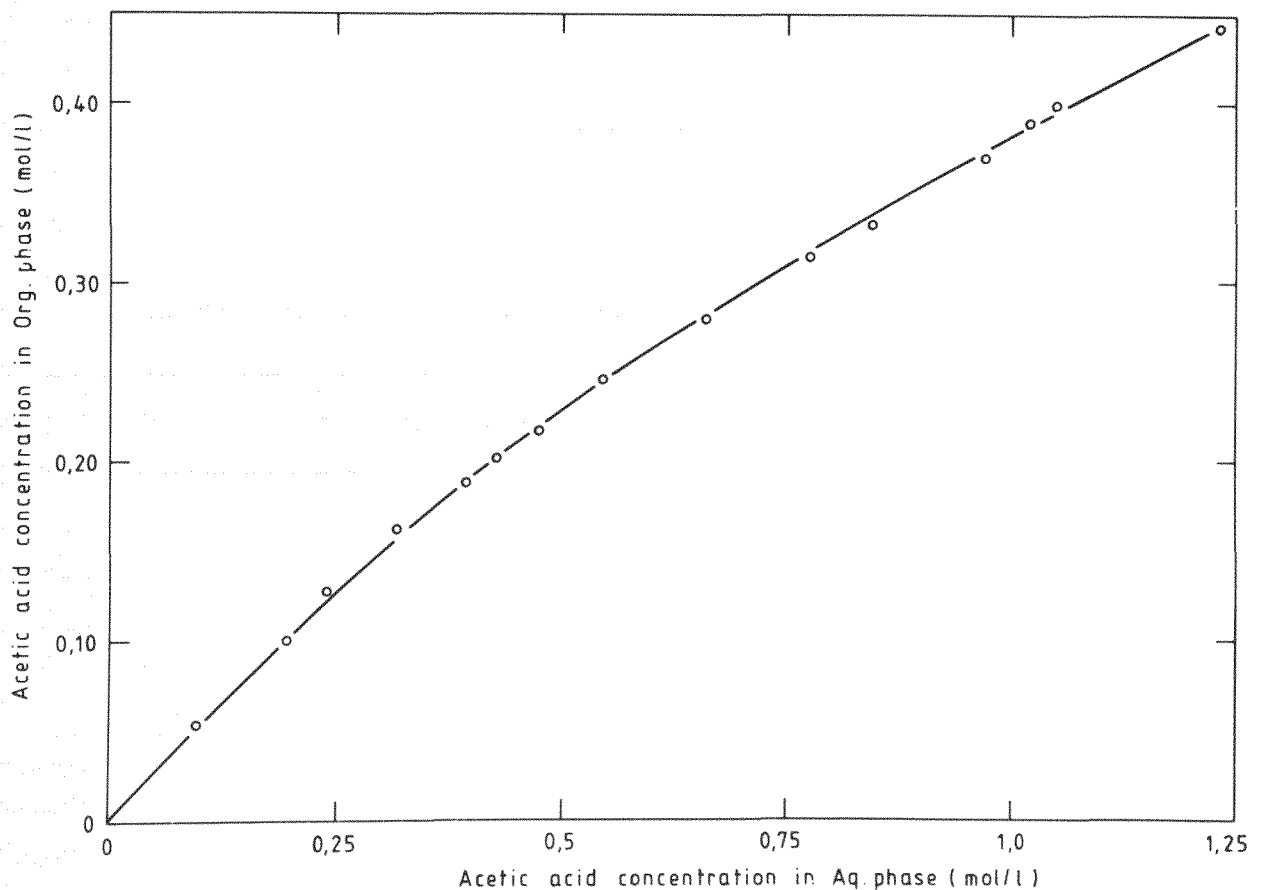
Fig. 7.3: Equilibrium curve of 30 % TBP in dodecane-acetic
acid-water

7.1.2 Evaluation of HETS and HTU

Table 7.1 shows the HETS in extraction at the upper 1 m obtained in this experiment and Table 7.2 shows the HETS in reextraction.

Table 7.1

Upper 1 m HETS for acetic acid in extraction

Continuous phase	R (%)	Pulse frequency (min^{-1})	HETS (cm)
Organic	57	32	59
Organic	86	32	50
Organic	63	63	45
Organic	81	63	34
Aqueous	57	32	17
Aqueous	86	32	15
Aqueous	64	77	15
Aqueous	82	77	11

Table 7.2

Lower 1 m HETS for acetic acid in reextraction

Continuous phase	R (%)	Pulse frequency (min^{-1})	HETS (cm)
Organic	56	32	31
Organic	88	32	27
Organic	62	63	29
Organic	85	63	25
Aqueous	61	48	44
Aqueous	83	48	36
Aqueous	57	77	33
Aqueous	86	77	33

It will be seen that in extraction, the aqueous continuous column
has much shorter HETS at the upper 1 m. On the other hand, in
reextraction, the organic continuous column has shorter HETS.
Figures 7.1 and 7.2 will show the situation clearly. Through
this experiment, it is ensured that HETS becomes shorter by
increasing the pulse frequency from f = 32 to 64 (organic
continuous column) or f = 32 (48) to 77 (aqueous continuous
column). Except for the case of extraction in the organic
continuous operation at a frequency of 32 per minute, a larger
flow rate of about 80 % of a flooding rate gives a shorter HETS
than that of lower flow rate around 60 %. This may suggest that
the pulse column can be operated stably even at a flow rate
over 80 % of the flooding flow rate.

Next, HTU was calculated to evaluate the overall mass-transfer
coefficient based on aqueous phase. NTU (Number of Transfer
Units) can be calculated by integrating equation (3-7).

$$NTU = \int_{x_i}^{x_o} \frac{dx}{x - x_e} \qquad (3-7)$$

In this study, it is assumed that the operating line is linear.
Table 7.3 shows the NTU and HTU obtained for a flow rate of
80 % of the flooding rate.

7.1.3 Comparison of the two modes of operation

NTU can also be defined with respect to $K_x A$ by equation (7-1)[19],

$$NTU = K_x A \, h/V \qquad (7-1)$$

If the NTU values are known, $K_x A$ can be determined. The values
of $K_x A$ and holdup are also shown in table 7.3. As for $K_x A$,
there is not much difference in the aqueous continuous operation
between extraction and reextraction. However, in the organic
continuous column the difference is significant. Comparing $K_x A$
with holdup of the two columns, some kind of mutual relation is
observed; that is in extraction

Table 7.3

HTU, K_xA, and holdup at 80 % of flooding flow rate

	f (min^{-1})	R (%)	HTU (cm)	NTU	K_xA (h^{-1})	Holdup (%)
Extraction Org. continuous	32	86	61	1.6	12	2.8
Extraction Aq. continuous	32	86	12	8.2	43	13
Reextraction Org. continuous	32	88	15	6.9	84	10
Reextraction Aq. continuous	48	83	28	3.5	48	6.0

$$(K_x A)_{aq} = 4.7 (K_x A)_{org} \qquad (7-2)$$

$$Holdup_{aq} = 3.8 Holdup_{org} \qquad (7-3)$$

and in reextraction

$$(K_x A)_{org} = 1.6 (K_x A)_{aq} \qquad (7-4)$$

$$Holdup_{org} = 1.8 Holdup_{aq} \qquad (7-5)$$

This may suggest $K_x A$ is nearly proportional to holdup. Observing the droplets by photos, there is not much difference between the diameters observed in the aqueous continuous column and the organic continuous column. Figures 7.4 and 7.5 shows the droplets in the both columns.

If it is accepted that drop diameters are the same, the specific contact surface area, A, is proportional to holdup. Therefore, it follows that $(K_x)_{aq}$ and $(K_x)_{org}$ would have the similar value. Although this may be a rough estimation, the assumption was applicable for both extraction and reextraction systems in this experiment. The same idea might be expected to apply to other systems.

7.2   Extraction of thorium

Next, HTU and HETS were evaluated for thorium nitrate in both modes of operation. The solvent was 30 % TBP in dodecane as in the prior experiment. The A/O ratio of 1/3 was chosen for extraction and that of 1/1 for reextraction. The nitric acid concentration plays an important role on the equilibrium line for uranium and thorium. In this study, in order to use the equilibrium line, which is given by Siddall[30], the nitric acid concentration of 1.1 (mol/l) was chosen for the aqueous feed solution and that of 0.01 (mol/l) for the aqueous strip. Since no scrub was used in this extraction experiment, the thorium feed concentration was confined to 0.4 (mol/l) for
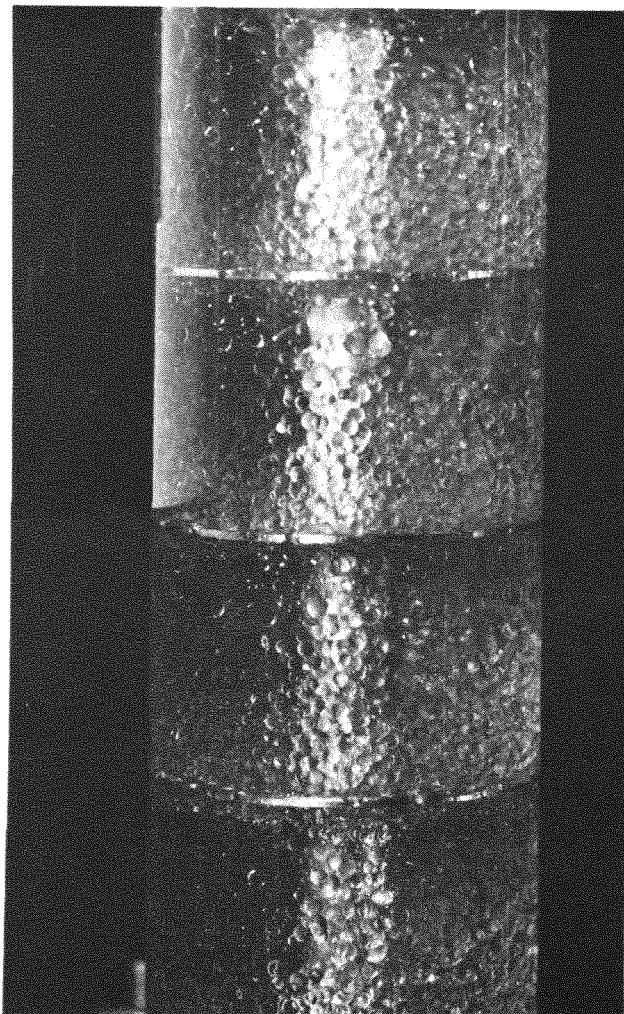
Fig. 7.4: Dispersion of droplets in
the aqueous continuous column
$V_{aq} = 5$ (l/h), $V_{org} = 15$ (l/n)
$f = 32$ (min^{-1})

Fig. 7.5: Dispersion of droplets in
the organic continuous column
$V_{aq} = 5$ (l/h), $V_{org} = 15$ (l/h)
$f = 32$ (min^{-1})

fear of the third phase formation. The same flow rates as in the experiment before were chosen, i.e. 80 % of the flooding flow rate. The pulse frequency was chosen to be 48 per minute for reextraction in the aqueous continuous column and 32 per minute for other cases. To confirm that the steady state was reached, samples for analysis were taken regularly at the organic and the aqueous outlets. After attaining the steady state, 5 samples along the axis of the columns were taken to obtain the thorium concentration profile.

During extraction, the droplets tend to be larger than in the absence of thorium, since the interfacial tension increases with thorium concentration. Figures 7.6 and 7.7 illustrate the situation clearly.

In these figures, the column was operated in the aqueous continuous mode. They show the difference of the droplets behavior in the column. It can be seen that coalescence occured much more rapidly in Fig. 7.7 than in 7.6. In Fig. 7.7, the organic phase has coalesced, making a layer under the sieve plates, while coalescence has taken place to a lesser extent in Fig. 7.6. Holdup was expected to increase with the thorium concentration because of the increasing interfacial tension. Table 7.4 shows the experimental conditions. It can be seen in this table that the aqueous continuous column has a longer contact time than the organic continuous column, whereas they have about the same value in Table 6.1

7.2.1 Start up characteristics of the columns

Figures 7.7 and 7.8 show how the aqueous and the organic out- let phases attain the steady state in extraction.

It is noticed that the thorium concentration in the raffinate is remarkably high at the beginning of the operation. It took two hours to reach the steady state in the organic continuous column. On the other hand in the aqueous continuous column, the thorium concentration in the aqueous outlet attains the steady state in one hour. The difference comes from the different modes
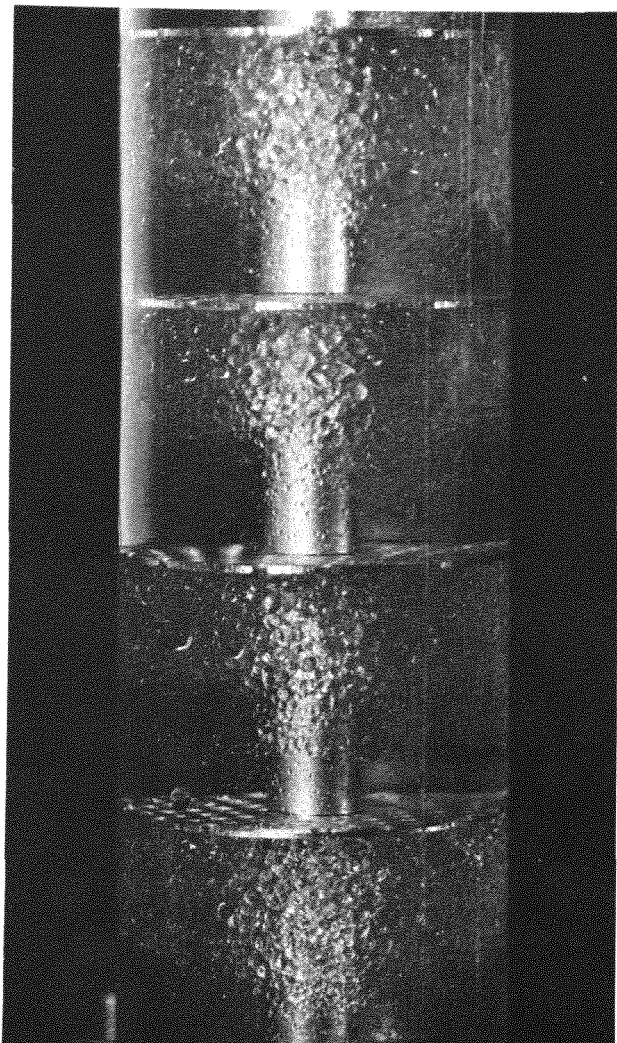
Fig. 7.6: Dispersion of droplets in the
aqueous continuous column in
the absence of thorium
$V_{aq} = 6$ (l/h), $V_{org} = 18$ (l/h),
$f = 32$ min^{-1})
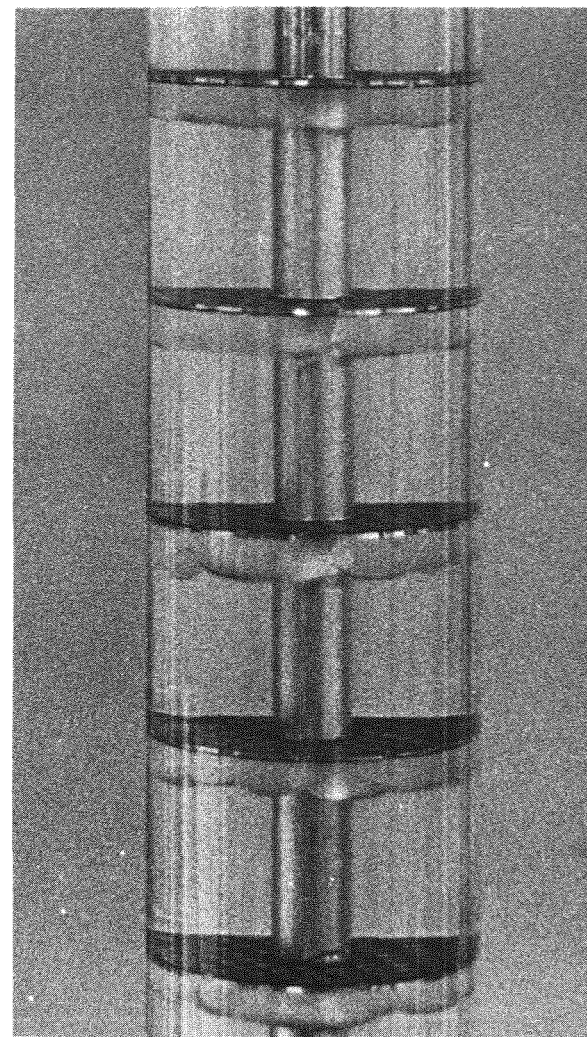
Fig. 7.7: Dispersion of droplets in the
aqueous continuous column in
the presence of thorium
$V_{aq} = 6.1$ (l/h), $V_{org} = 18.2$ (l/h),
$f = 32$ (min^{-1})

Table 7.4

Experimental conditions for thorium extraction

	Continuous phase	U_{aq} (1/h)	U_{org} (1/h)	f (min^{-1})	Holdup (%)	Contact time (min)
Extraction	Organic	8.1	24.2	32	5.9	2.7
	Aqueous	6.1	18.2	32	18	3.7
Reextraction	Organic	14.2	14.0	32	14	3.6
	Aqueous	15.3	15.1	48	16	3.7
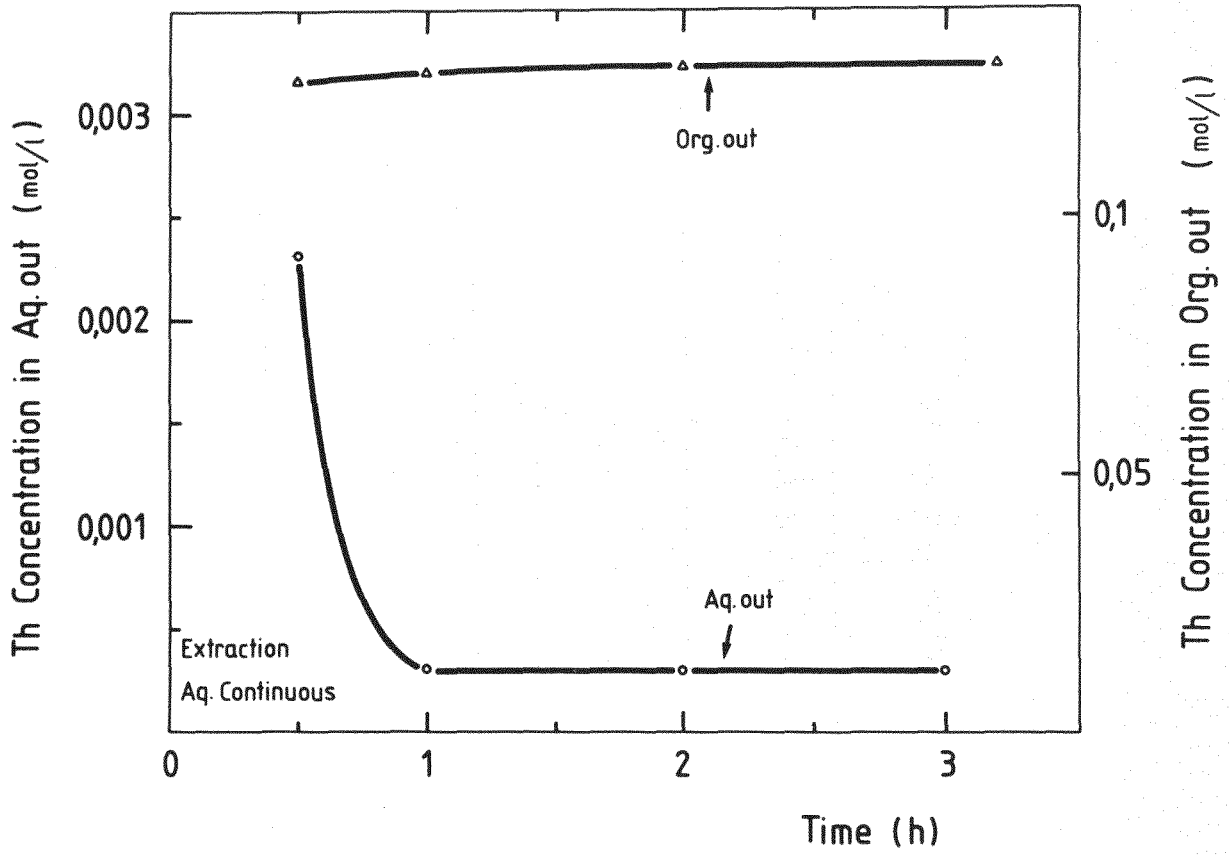
Fig. 7.8: Transient curve of thorium (aqueous continuous column in extraction)
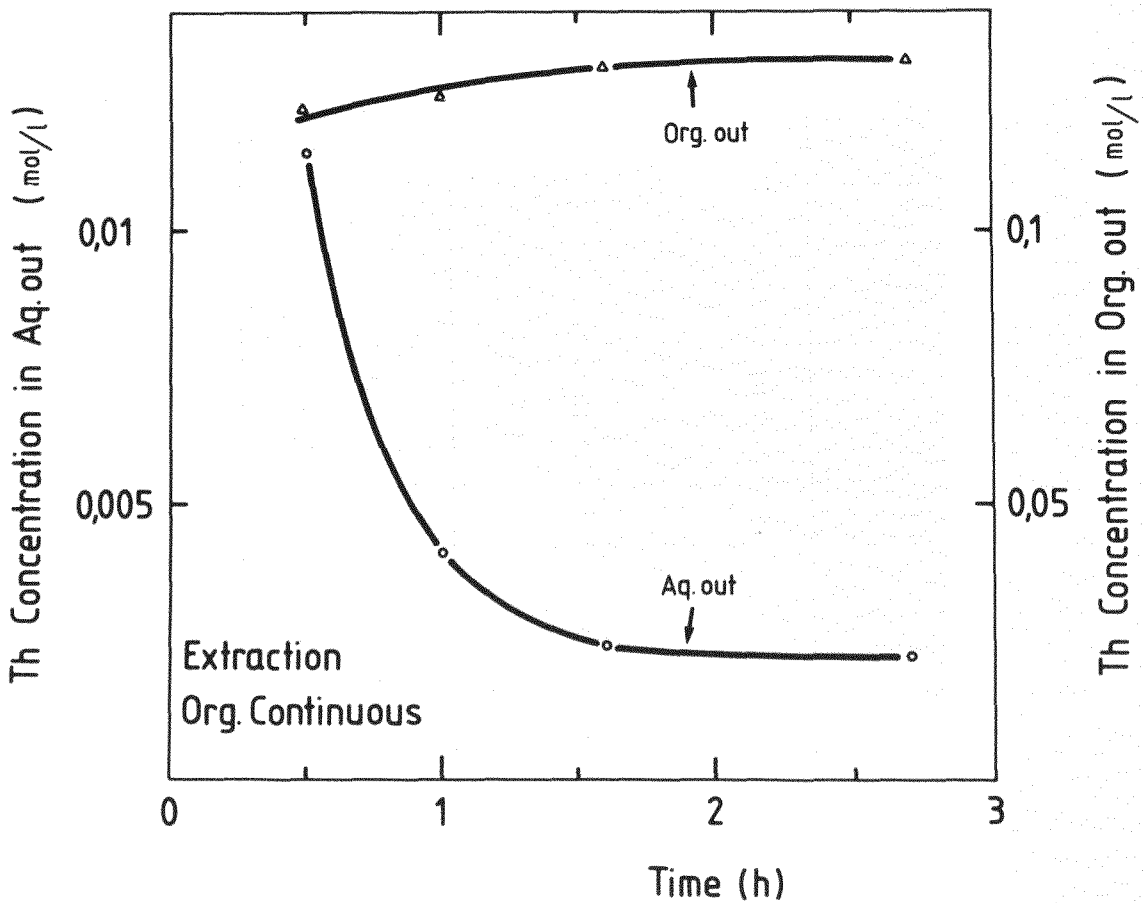
Fig. 7.9: Transient curve of thorium (organic continuous column in extraction)

of start-up operation in the two columns. In the first run,
the aqueous continuous column was started up,filled with
distilled water. However, the column could not attain the
steady state within three hours. Then, in the next run, at
the beginning of extraction the aqueous continuous column was
filled with 1.1 $\underline{M}$ HNO_3, while the organic continuous column
was filled with solute-free solvent. As expected, the aqueous
continuous column attained the steady state faster than the
organic continuous column. From this fact, it is concluded
that the aqueous continuous mode of operation needs longer
time to reach the steady state than the organic continuous
mode of operation.

Figures 7.10 and 7.11 show how the thorium concentration at
the outlets attain the steady state in reextraction.
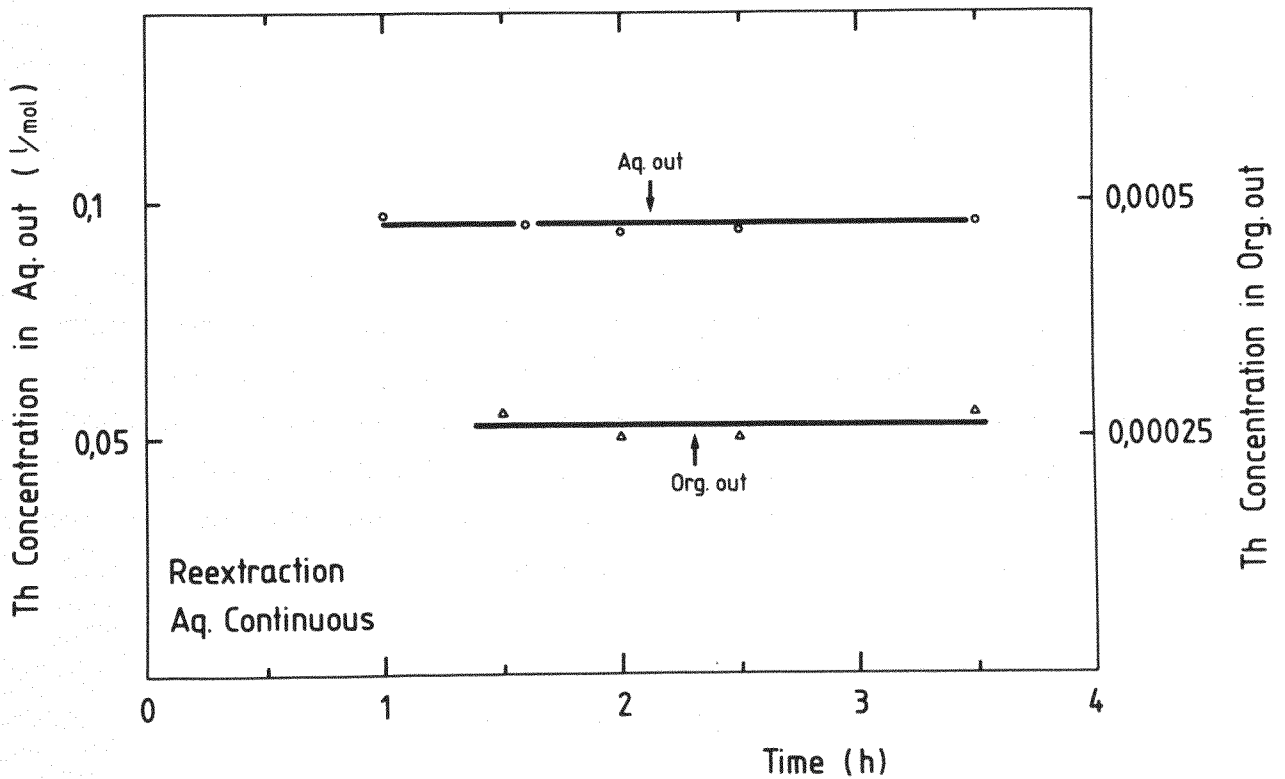
Fig. 7.10:   Transient curve of thorium (aqueous continuous
column in reextraction)

It was observed that the concentration at the organic outlet
attained the steady state in 1.5 hours in the aqueous and in
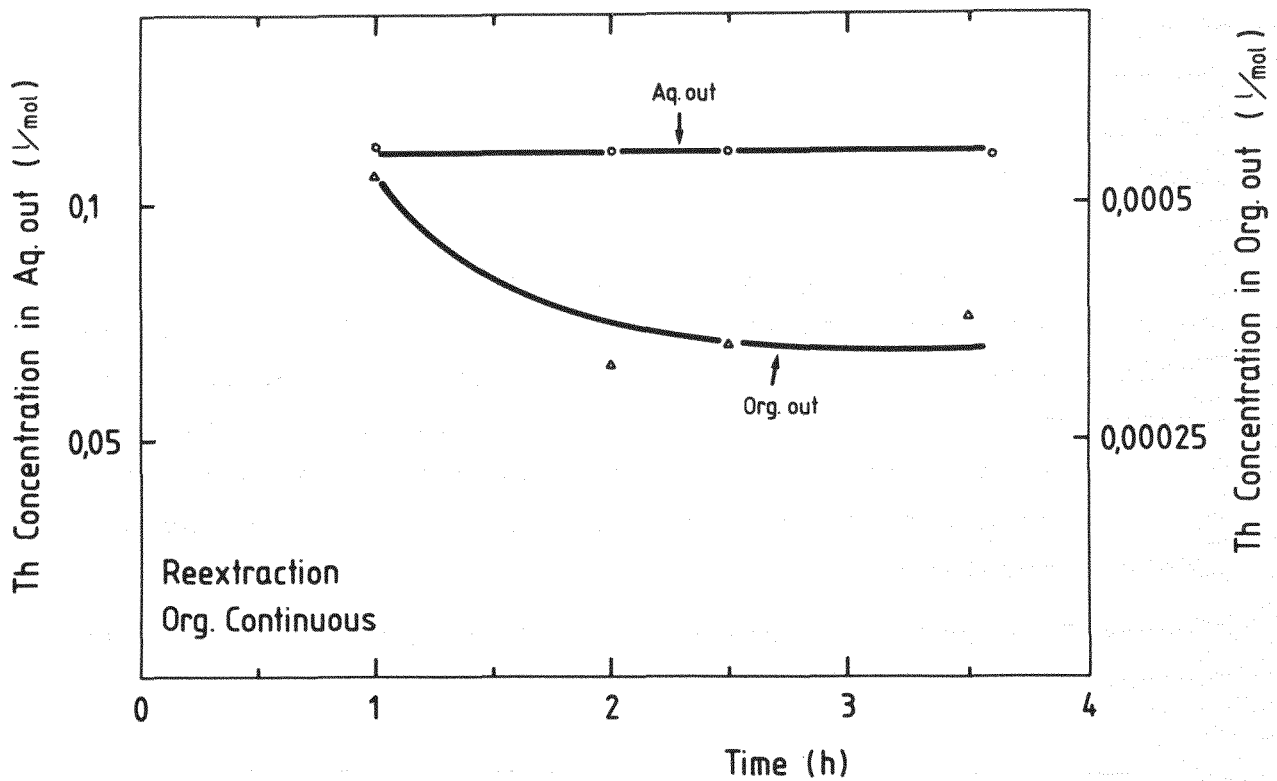
Fig. 7.11: Transient curve of thorium (organic continuous column in reextraction)

2.5 hours in the organic continuous column. In reextraction, the organic continuous mode of operation needs more time to reach the steady than the aqueous continuous mode of operation. In this extraction experiment with thorium, it was observed that the mass-transfer from the continuous to the dispersed phase needs more time to attain the steady state than the mass-transfer from the dispersed to the continuous phase.

7.2.2 Experimental results of extraction

Figures 7.12 and 7.13 show the thorium concentration plotted along the column height in the steady state. Figure 7.12 shows the profile in extraction and Fig. 7.13 shows that in re-extraction.

In order to find the effect of nitric acid, the nitric acid concentration was also measured. Figure 7.14 shows the nitric acid concentration along the column height in extraction and
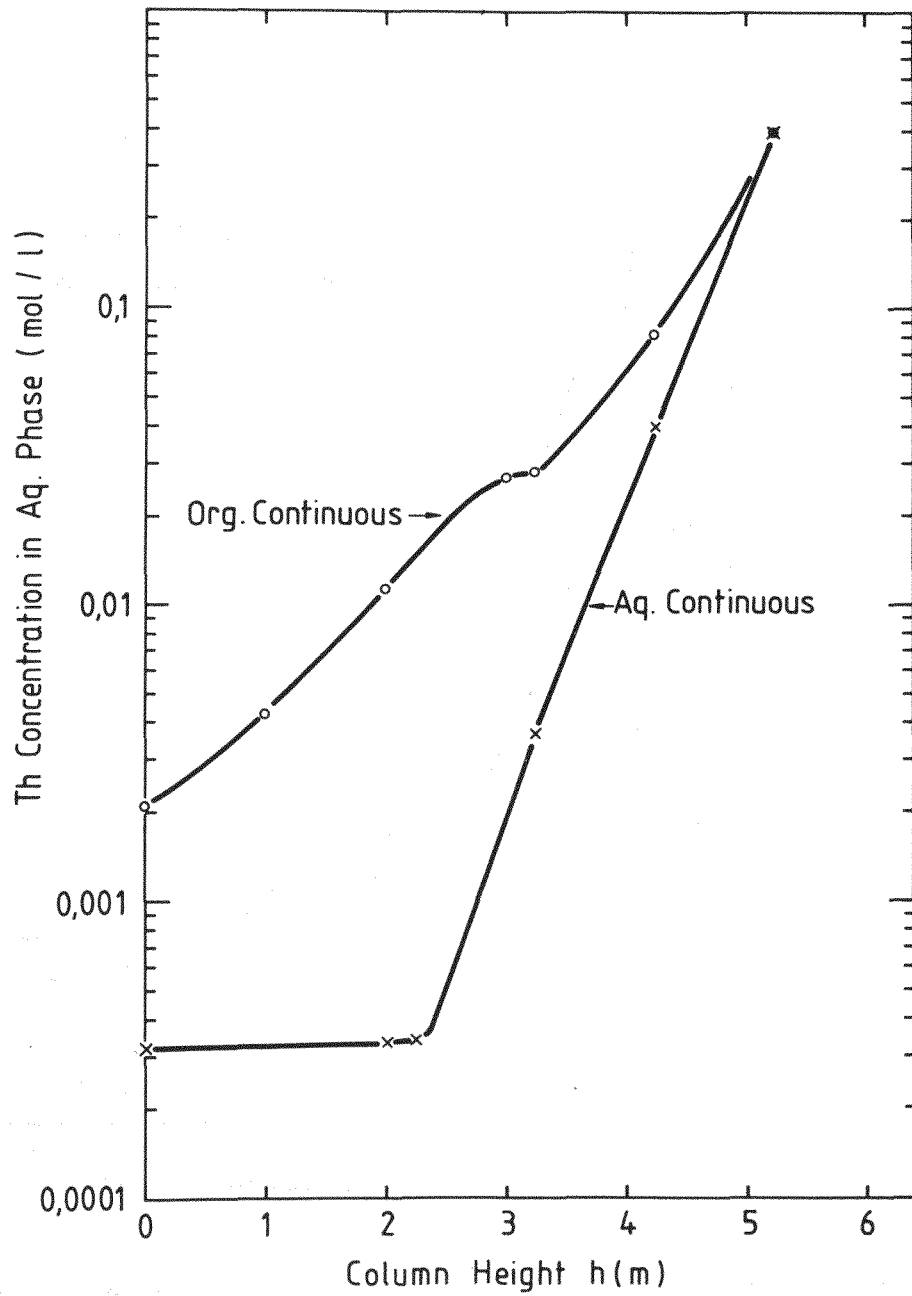
Fig. 7.12: Thorium concentration profile along the column height in extraction
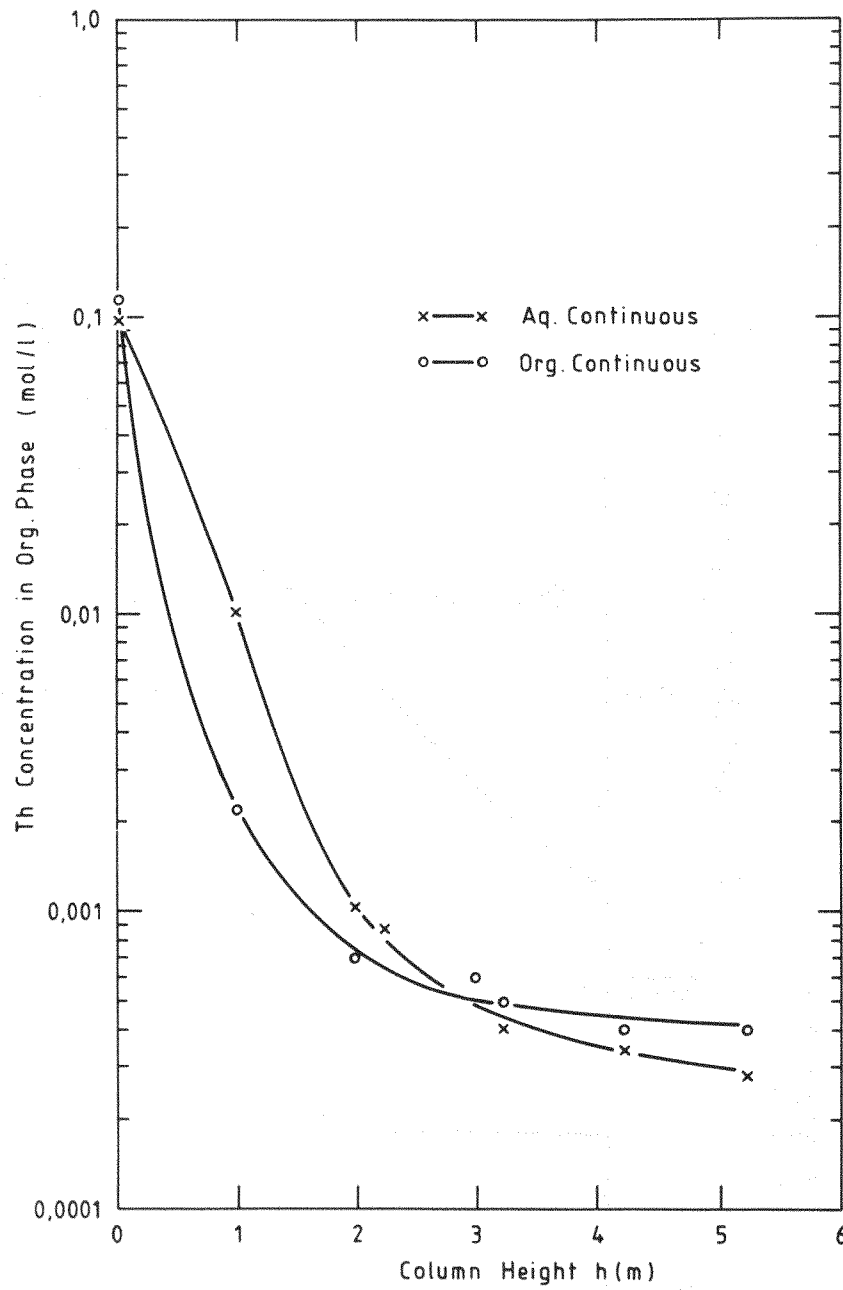
Fig. 7.13: Thorium concentration profile along the column height in reextraction

Fig. 7.15 shows that in reextraction.
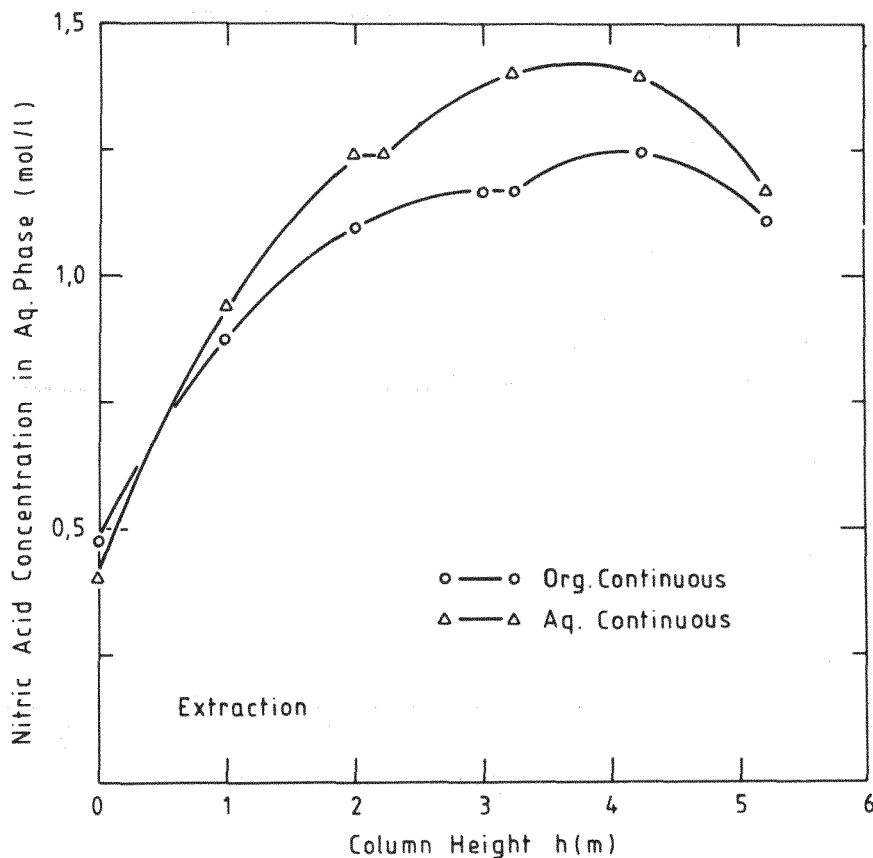
Fig. 7.14: HNO_3 concentration profile along the column height in extraction

In Fig. 7.14, the nitric acid concentration increases at first with distance from the feed point at 5.24 m. However, below the column height of about 4 m, it decreases slowly to the value of the aqueous outlet. The outlet concentration agrees with the material balance. On the other hand, the nitric acid concentration decreases very fast in the reextraction columns. It reaches about 0.01 (mol/l) at the height of 1.5 m. There is not much difference between the aqueous continuous and the organic continuous columns concerning the nitric acid distribution along the column height. From the results, it seems to be reasonable for a first approximation that the nitric acid concentration is constant along the column height. Therefore, the thorium equilibrium curve at the nitric acid concentration of 1.1 (mol/l) was used for the extraction and that of 0.01 (mol/l) was used for the reextraction.
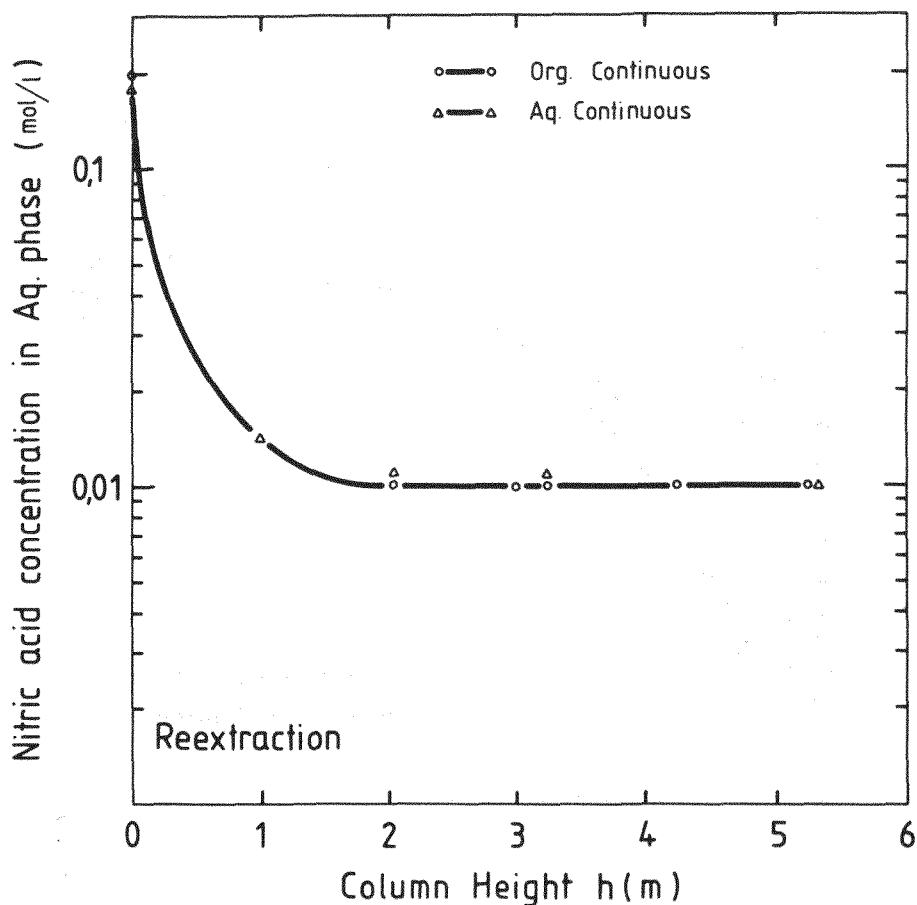
Fig. 7.15: HNO$_3$ concentration profile along the column height
            in reextraction

7.2.3 Evaluation of HETS and HTU

The experimental results shown in Figs. 7.12 and 7.13 were
analysed by McCABE-THIELE diagrams. Table 7.5 shows the HETS
obtained in this study assuming the operating line to be
linear. The value is 28 to 98 cm for extraction and 62 to
130 cm for reextraction.

Table 7.6 shows the HTU calculated by equation (3-7)

$$NTU = \int_{x_i}^{x_0} \frac{dx}{x-x_e} \qquad (3-7)$$

The operating line was also assumed to be linear. In this case,
the integration of equation (3-7) was carried out numerically
by computer. The equilibrium curve was approximated as follows;

in extraction, $\quad y = 0.688\ x\ (x \leq 0.138) \qquad (7\text{-}6)$

$\qquad\qquad\qquad\qquad y = 0.386\ x^{0.708}\ (x > 0.138) \quad (7\text{-}7)$

in reextraction, $\quad y = 4.84\ x^{3.08}$

Table 7.5

HETS for thorium (cm)

Column height (m)	0~1	1~2	2~3	3~4	4~5	overall
Extraction (Org. continuous)	75	98	93	71	42	78
Extraction (Aq. continuous)	–	–	36	31	28	32
Reextraction (Org. continuous)	62	–	–	–	–	–
Reextraction (Aq. continuous)	108	130	–	–	–	–

It is noticed in Table 7.6 that the aqueous continuous column has the better performance of shorter HTU than the organic continuous column in extraction. On the other hand in re-extraction, the organic continuous column gives shorter HTU than the aqueous continuous column. However, the difference is greater in extraction. Corresponding to this fact, the difference of the contact time between the two modes of operation is much greater in extraction than in reextraction. HTU can be expected to decrease with increasing contact time, if it is assumed that the droplets diameters are the same between the two modes of operation. If the droplets diameters are the same, the specific surface area A is proportional to holdup η while contact time is proportional to η/V_d. Consequently,

the contact time is proportional to A/V. On the other hand, in equation (7-1). NTU is proportional to A/V

$$NTU = K_xA \, h/V \qquad (7-1)$$

Thus, NTU might be expected to increase with increasing contact time. The great difference of HTU in extraction might be explained as above.

Table 7.6

HTU of thorium (cm)

Column height (m)	0~1	1~2	2~3	3~4	4~5	overall
Extraction (Org. continuous)	128	69	65	50	34	58
Extraction (Aq. continuous)	–	–	28	22	32	24
Reextraction (Org. continuous)	146	–	–	–	–	–
Reextraction (Aq. continuous)	195	–	–	–	–	–

8.   Thorex process

Uranium and thorium were co-extracted, co-stripped, and
partitioned, using the columns. The thorium/uranium concen-
tration ratio was chosen to be 10 : 1 as is the case for HTR
fuel. The organic continuous flow was adopted for the ex-
traction column since in actual reprocessing, this mode
reduces the penetration of fission products to the organic
product at the interface. For the same reason, i.e. to obtain
a pure product, the aqueous continuous flow was chosen for the
partitioning and the co-stripping column. The extraction column
has a 2 m high scrub and 3 m high extraction section. In this
column, the salting agent of 13 $\underline{M}$ HNO$_3$ solution was fed at 1 m
above the bottom. In the partitioning column, the uranium
scrub section is 2 m high and the thorium strip section is 3 m.
The pulse frequencies were 64 per minute for the extraction
column and 77 per minute for the partitioning and the co-
stripping column.

The obtained data were analysed by the McCABE-THIELE diagram
to evaluate HETS for uranium and thorium. In this calculation,
the uranium equilibrium curve was constructed by assuming that
the salting effect of thorium was equivalent to that of nitric
acid[31]. The equilibrium data by J.W. Codding for uranium[32]
were used in this study. The equilibrium data for thorium by
T.H. Siddall[30] were used to set up the McCABE-THIELE diagram.

In this experiment the feed, the scrub, and the salting agent
were supplied to the extraction column by proportionating
pumps. The solvent of 30 % TBP in dodecane was fed by a gear
pump. In the partitioning column, the organic feed and the
thorium strip were supplied by gear pumps and the uranium scrub
solvent was fed by a proportionating pump. In the co-stripping
column, both the organic feed and the strip were supplied by
gear pumps. The flow rates through the pumps were determined
as explained in chapter 5.

The acid deficient feed solution was prepared by a evaporator
without steam stripping as explained in Chap. 3.3. The solution
was made acid deficient by evaporating to a boiling point of
155°C.

8.1   Co-extraction process with acid feed solution

Figure 8.1 shows the schematic diagram of this experiment.
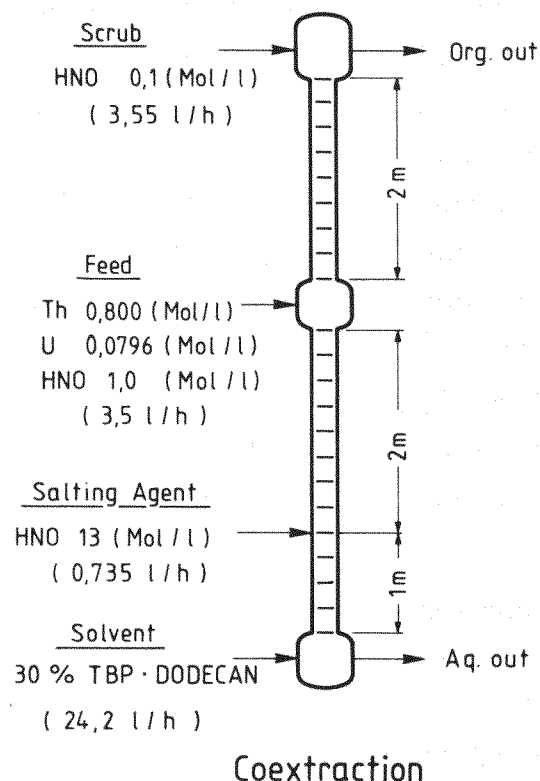
Fig. 8.1:   Schematic diagram of the co-extraction process
(acid feed solution)

The feed concentrations of thorium, uranium, and nitric acid
were 0.800, 0.0796, and 1.0 (mol/l) respectively. The nitric
acid concentration of the scrub solution was chosen as 0.1 $\underline{M}$
and that of salting agent as 13 $\underline{M}$. The flow rates of the feed,
scrub, salting agent, and solvent were 3.5, 3.55, 0.735, and
24.2 (1/h) respectively.

8.1.1 Experimental results

Figure 8.2 shows the distribution of thorium, uranium and nitric acid along the column height in the co-extraction process.
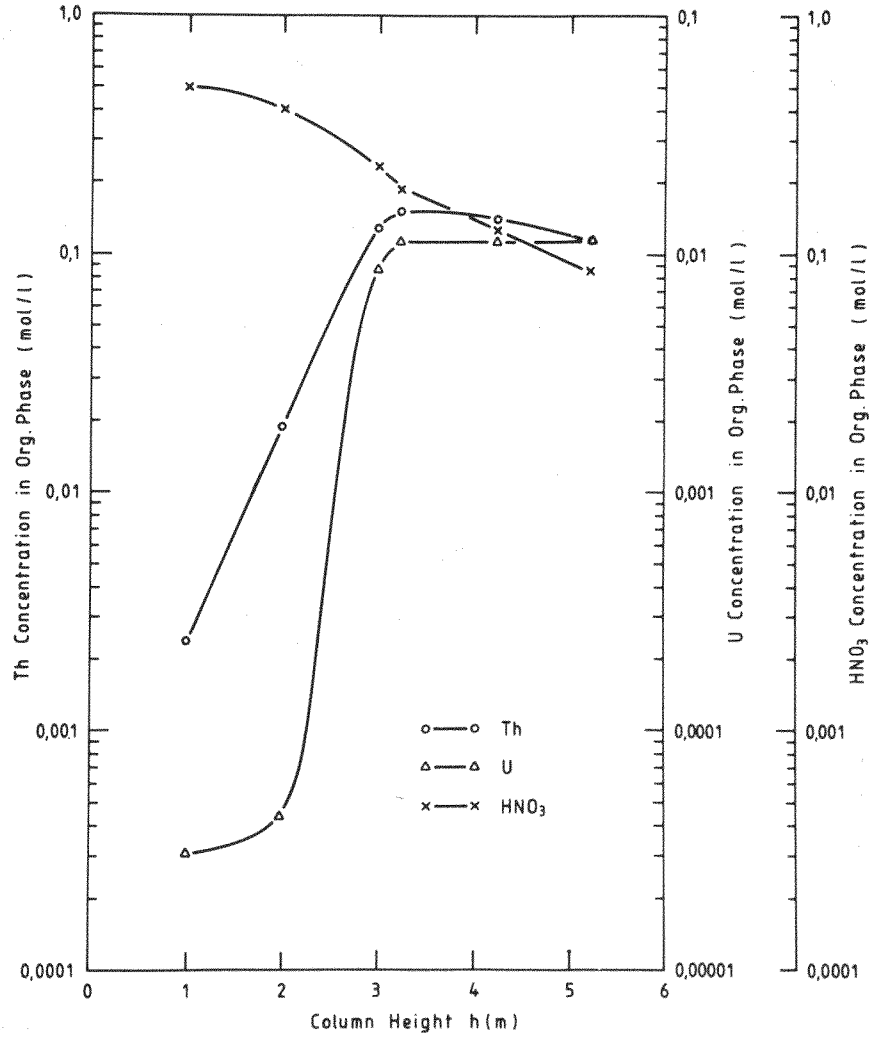
<u>Fig. 8.2:</u> Distribution profiles of thorium, uranium, and nitric acid along the column height in the co-extraction process (acid feed solution)

It can easily be seen that the uranium concentration decreases much faster than thorium in the extraction section. In contrast, in the scrub section the uranium concentration does not change, while the thorium concentration decreases from the feed point to the top of the column.

In this experiment, the extraction column was operated first about 2 hours without thorium and uranium in order to attain the steady state of nitric acid distribution. The feed solution was an 1.0 $\underline{M}$ HNO$_3$. After two hours, a solution of 0.800 $\underline{M}$ Th, 0,08 $\underline{M}$ U, and 1.0 $\underline{M}$ HNO$_3$ was fed into the column turning a three-way valve which is located at the inlet of the proportionating pump. Fig. 8.3 shows the transient curve of thorium in the aqueous and the organic outlet.
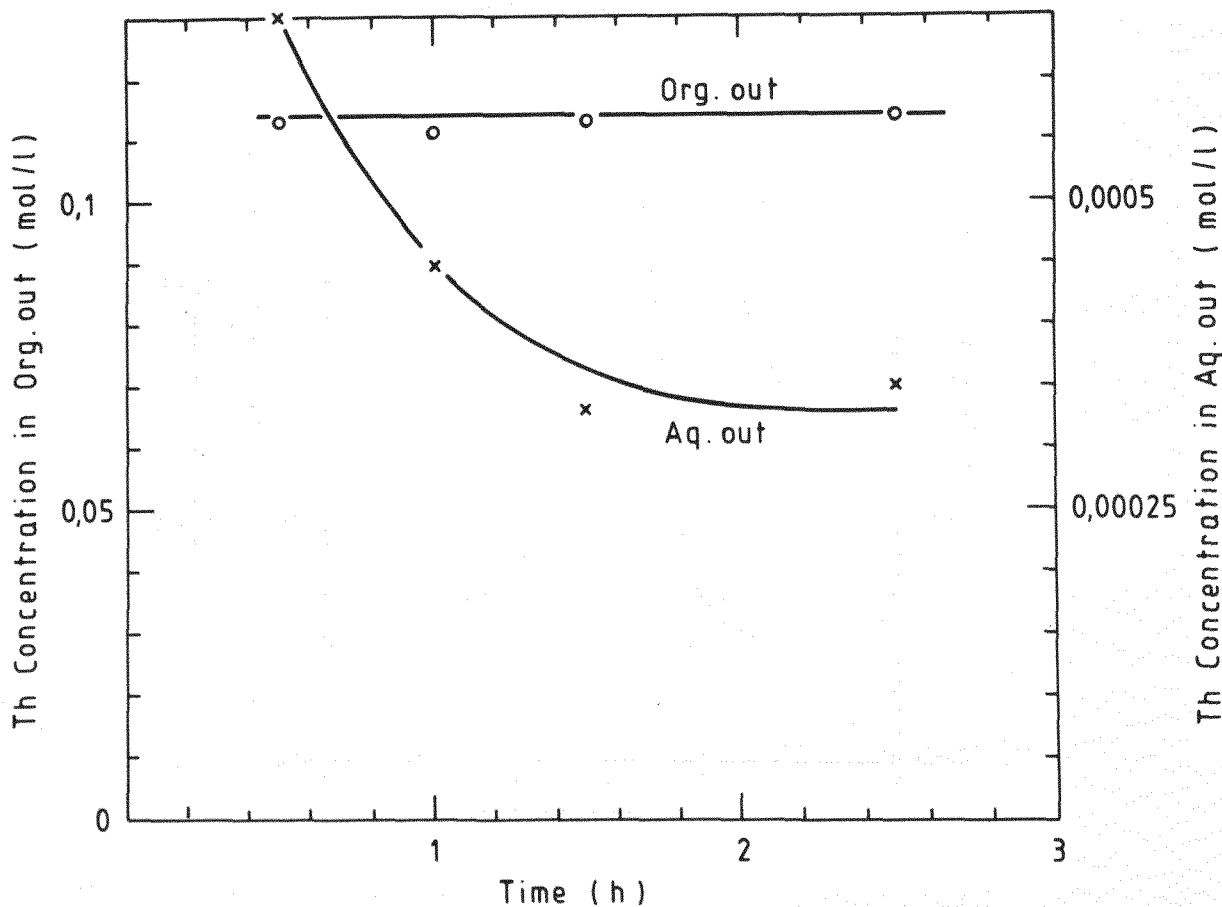
Fig. 8.3: Transient curve of thorium in the co-extraction process (acid feed solution)

Figures 8.4 and 8.5 show the same transient curves for uranium and nitric acid.

It is noticed that thorium takes about 2 hours to reach the steady state, while uranium needs only 1 hour.
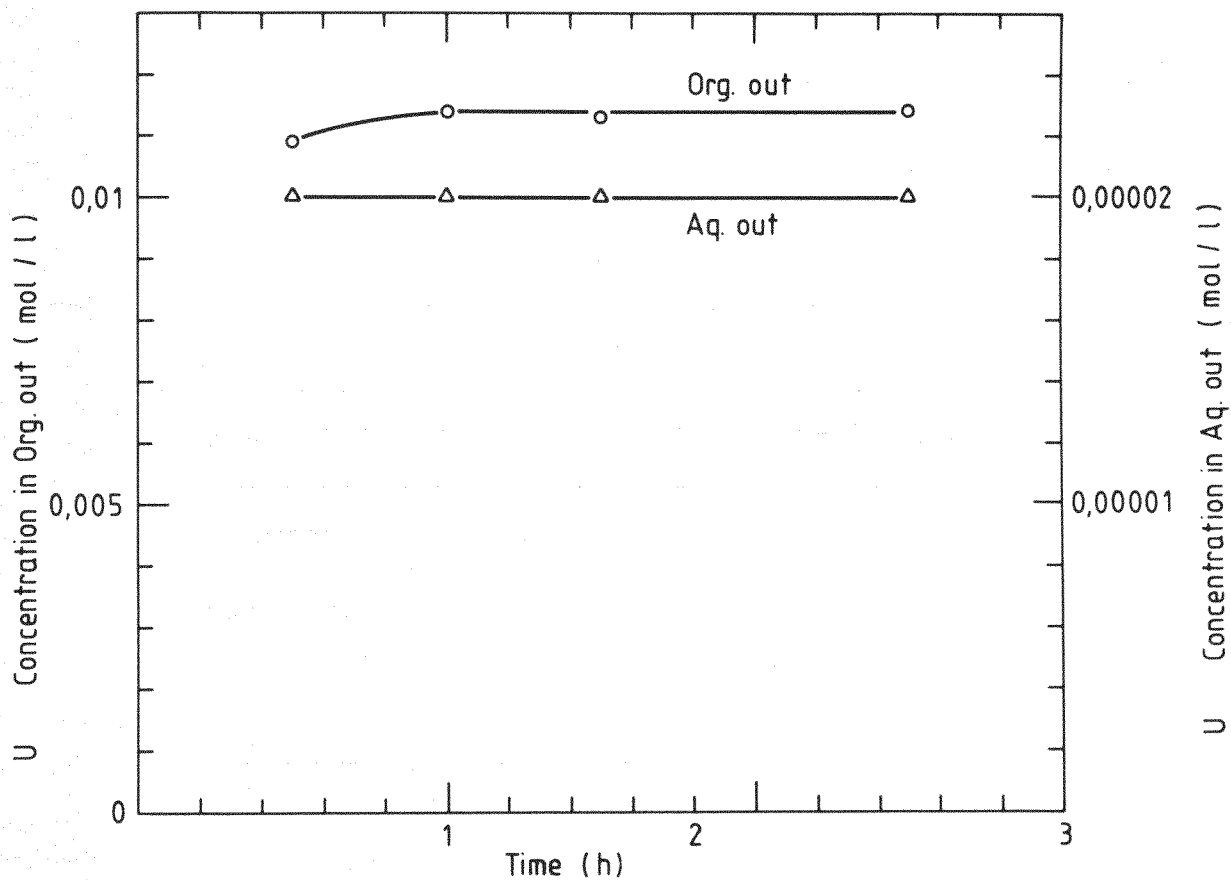
Fig. 8.4: Transient curve of uranium in the co-extraction process (acid feed solution)
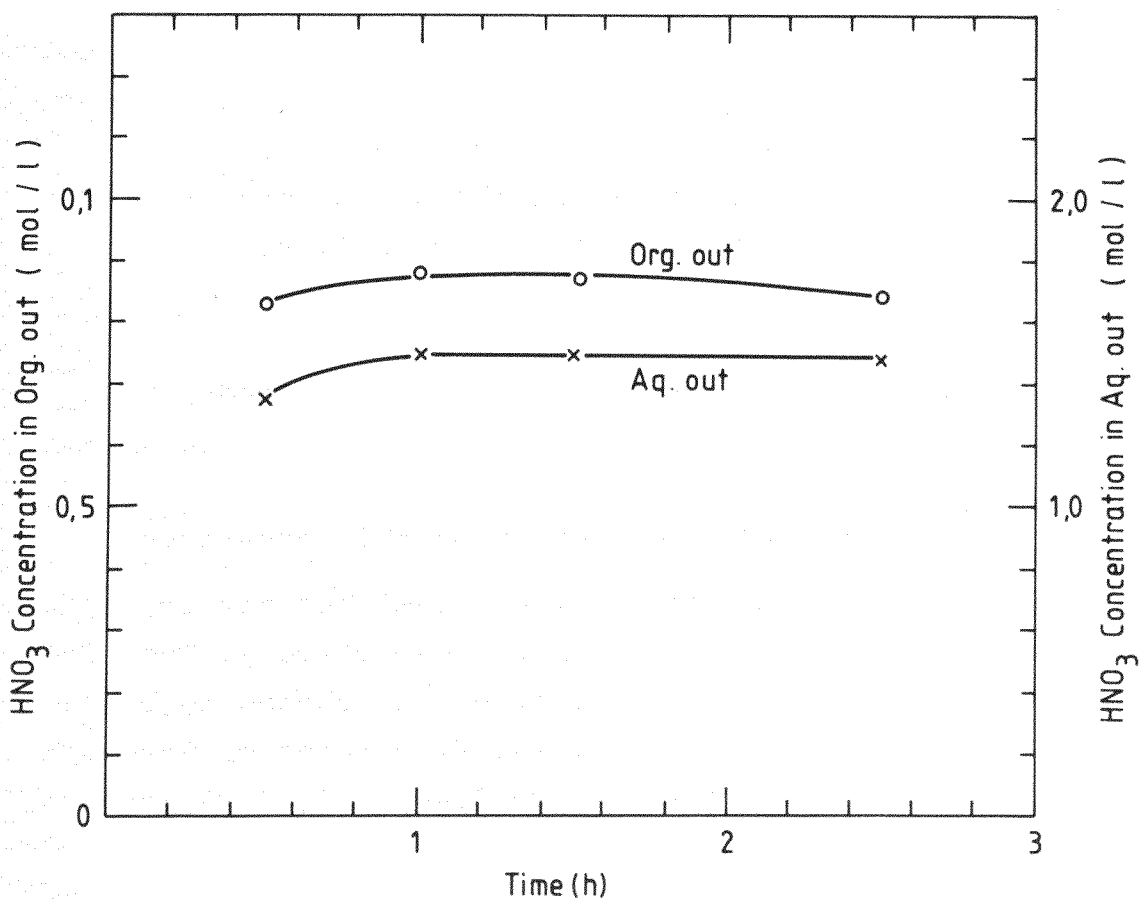
Fig. 8.5: Transient curve of nitric acid in the co-extraction process (acid feed solution)

8.1.2 Evaluation of HETS

Table 8.1 shows the obtained HETS for this process.

Table 8.1

HETS in the co-extraction process with acid feed solution (cm)

Column height (m)	0~1	1~2	2~3	3~4	4~5
	extraction			scrub	
HETS for thorium	50	62	56	183	143
HETS for uranium	–	–	55	–	–

HETS of about 55 cm was obtained in the extraction section for both uranium and thorium. No great difference was observed in the extraction section for the HETS values of thorium and uranium. Since uranium is extracted into the organic phase faster than thorium, it is impossible to obtain its HETS values in the column parts from 0 to 2 m. On the other hand, in the scrub section HETS of about 160 cm was obtained for thorium, and no back washing was observed for uranium. In the scrub section HETS becomes shorter with increasing the column height.

8.2　Co-extraction process with acid deficient feed solution

Figure 8.6 shows the schematic diagram of this experiment.

The feed concentrations of thorium, uranium, and nitric acid were 0.805, 0.0810 and -0.143 (mol/l), respectively. The nitric acid concentration of the scrub solution was chosen to be 1.0 $\underline{M}$ and that of salting agent as 13 $\underline{M}$. The flow rates of the scrub, feed, salting agent, and solvent were 3.46, 3.5, 1.02, and 24.0 (l/h) respectively.
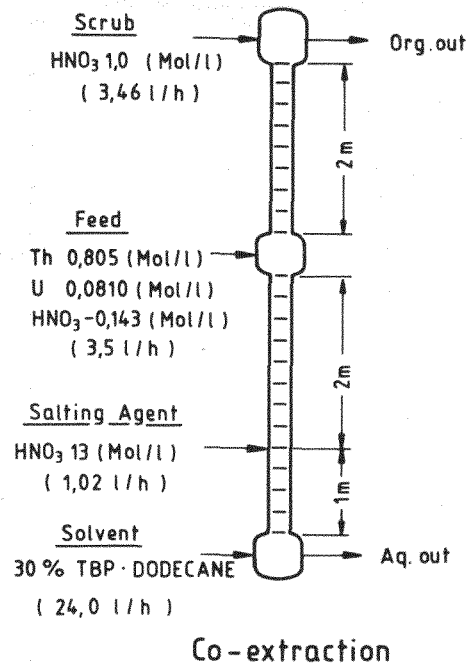
Co-extraction

Fig. 8.6: Schematic diagram of the co-extraction process (acid deficient feed solution)

8.2.1 Experimental results

Figure 8.7 shows the concentration profiles of thorium, uranium, and nitric acid.

It is noticed in Fig. 8.7 that in the extraction section the nitric acid concentration decreases faster than that of acid feed solution with increasing column height $(h>1)$. And the thorium and the uranium concentrations decrease more slowly from the feed point $(h \approx 3 \, m)$ to the bottom compared with those of acid feed solution. On the other hand, in the scrub section the profile of the uranium and the thorium concentrations is about the same as that of acid feed solution. Uranium was not washed back there. The nitric acid concentration increases from
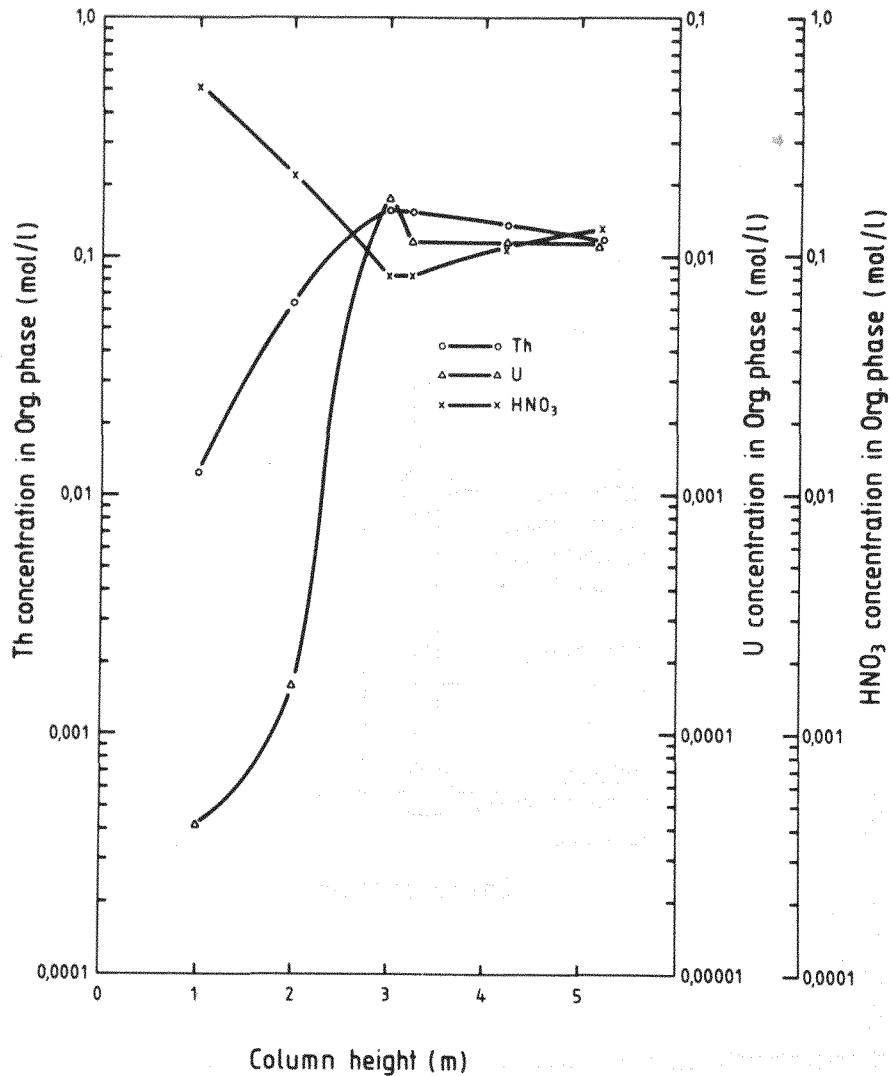
Fig. 8.7: Distribution profiles of thorium, uranium, and nitric acid along the column height in the co-extraction process (acid deficient feed solution)

the feed point to the top with acid deficient feed solution, while it decreases with acid feed solution.

Figures 8.8 to 8.10 show the transient curves of this experiment for thorium, uranium, and nitric acid.

Prior to the heavy metal extraction, the column was operated 1.5 hours with distilled water as feed to reach the hydraulic stability, but the scrub and the salting agent were fed as usual during this time. Fig. 8.10 shows that the HNO_3 concentration in the organic outlet decreases after starting the acid deficient feed solution, whereas the HNO_3 concentration
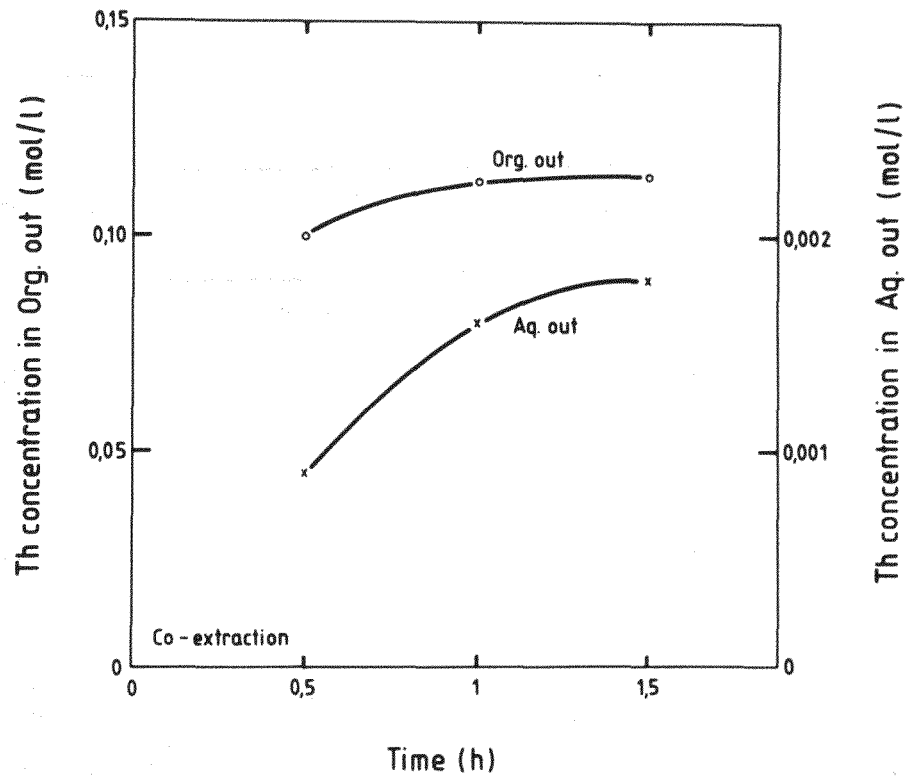
Fig. 8.8: Transient curve of thorium in the co-extraction process (acid deficient feed solution)
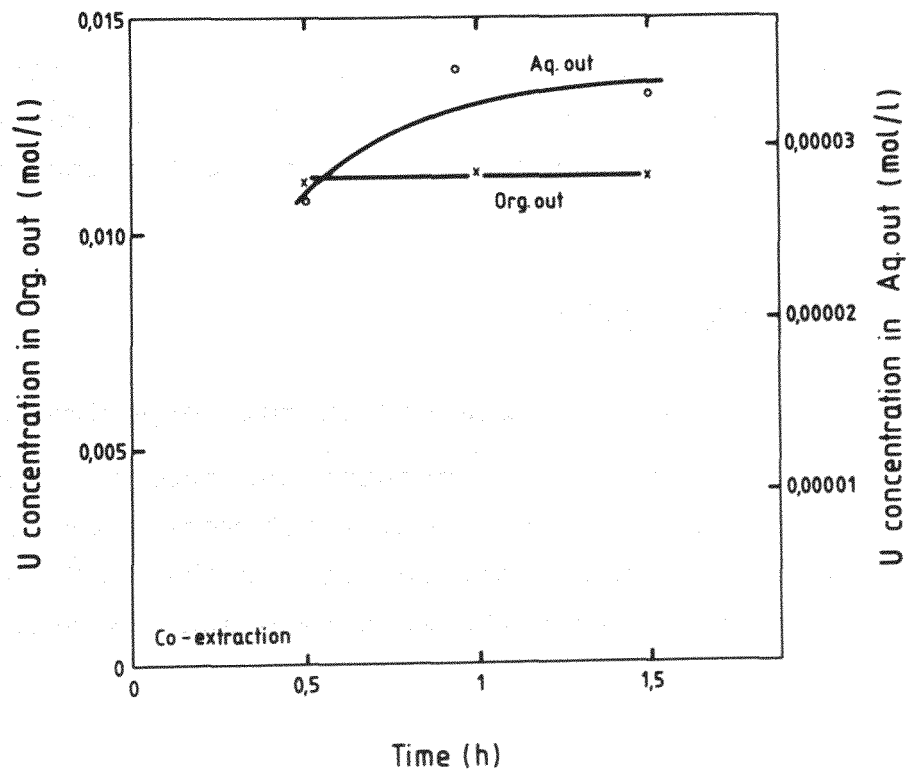
Fig. 8.9: Transient curve of uranium in the co-extraction process (acid deficient feed solution)
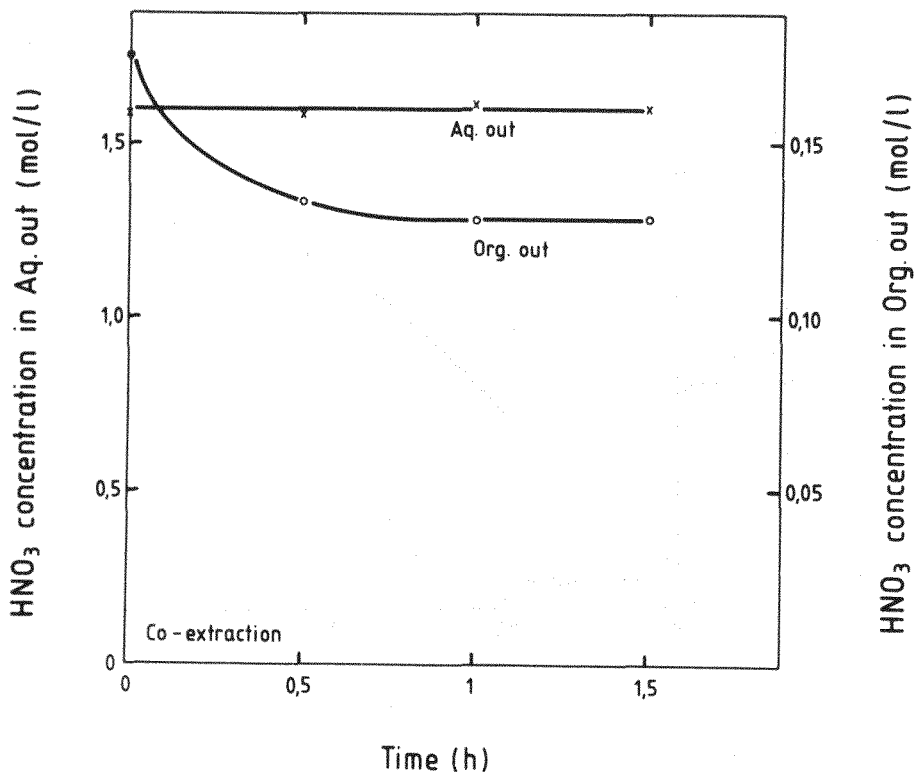
Fig. 8.10: Transient curve of nitric acid in the co-extraction process (acid deficient feed solution)

in the aqueous outlet keeps the same value. The nitric acid needs 1 h to reach the steady state, while the uranium in the product (organic out) needs only 0.5 h and the thorium 1.5 h.

8.2.2 Evaluation of HETS

Table 8.2 shows the HETS obtained in this experiment.

The obtained values both for uranium and thorium agree well with those of acid feed solution, which were shown in Table 8.1. No great difference was observed as for the HETS values of the extraction column between the acid feed and the acid deficient feed operations.

Table 8.2

HETS in the co-extraction process (acid
deficient feed solution) (cm)

Column height (m)	0~1	1~2	2~3	3~4	4~5
	extraction			scrub	
HETS for thorium	49	70	43	186	152
HETS for uranium	–	–	56	–	–

8.3 Co-strip process

Fig. 8.11 shows the flow sheet of this process.
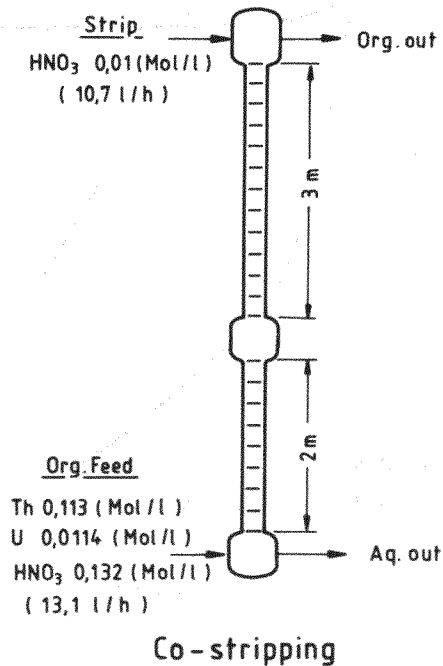
Co-stripping

Fig. 8.11: Schematic diagram of the co-stripping process

The organic feed concentrations of thorium, uranium, and nitric acid were 0.113, 0.0114, and 0.132 (mol/l) respectively. The stripping nitric acid concentration was 0.01 $\underline{M}$. The flow rates of feed and strip were 13.1 and 10.7 (l/h) respectively.

8.3.1 Experimental results

Figure 8.12 shows the profiles of the thorium, uranium, and nitric acid concentrations along the column height after attaining the steady state.
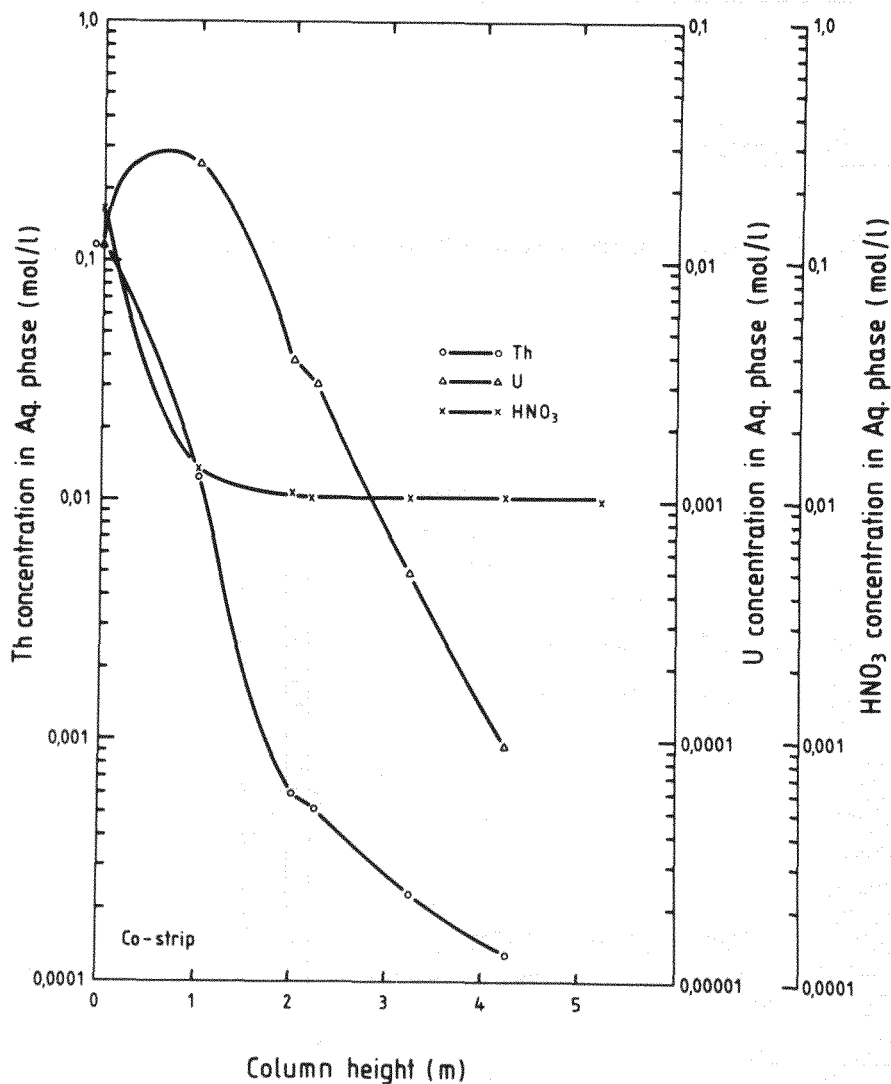
Fig. 8.12: Distribution profiles of thorium, uranium, and nitric acid along the column height in the co-stripping process

It is noticed in Fig. 8.12 that the uranium concentration increases with column height in the lower part of the stripping column (h: $0 \sim 1$ m). This may be caused by the presence of thorium. The uranium was reextracted well in higher parts of the column where the thorium concentration is < 0.01 $\underline{M}$. The nitric acid concentration was decreased very fast with column height as already observed in Chap. 7.2.2.

Fig. 8.13 to 15 show the transient curve of thorium, uranium, and nitric acid.
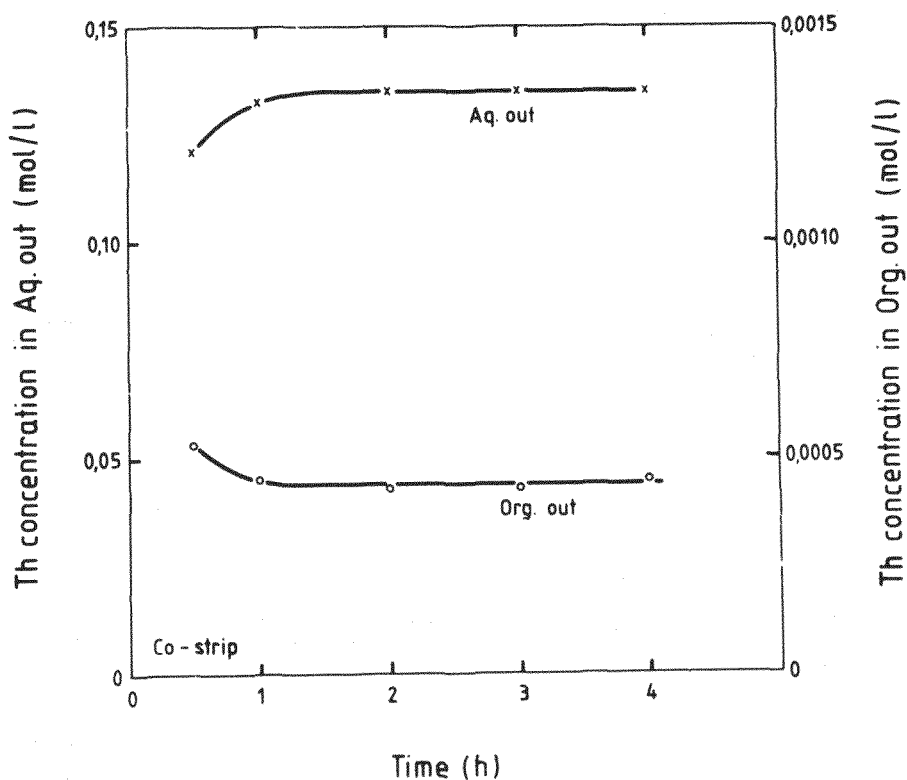
Fig. 8.13: Transient curve of thorium in the co-stripping process

In this experiment the column was filled with water before starting. At time = 0, the organic feed was started. Though the hydraulic steady state was not attained on starting, the column reached steady state in 3 hours. These figures show that the uranium needs more time than the thorium. However,
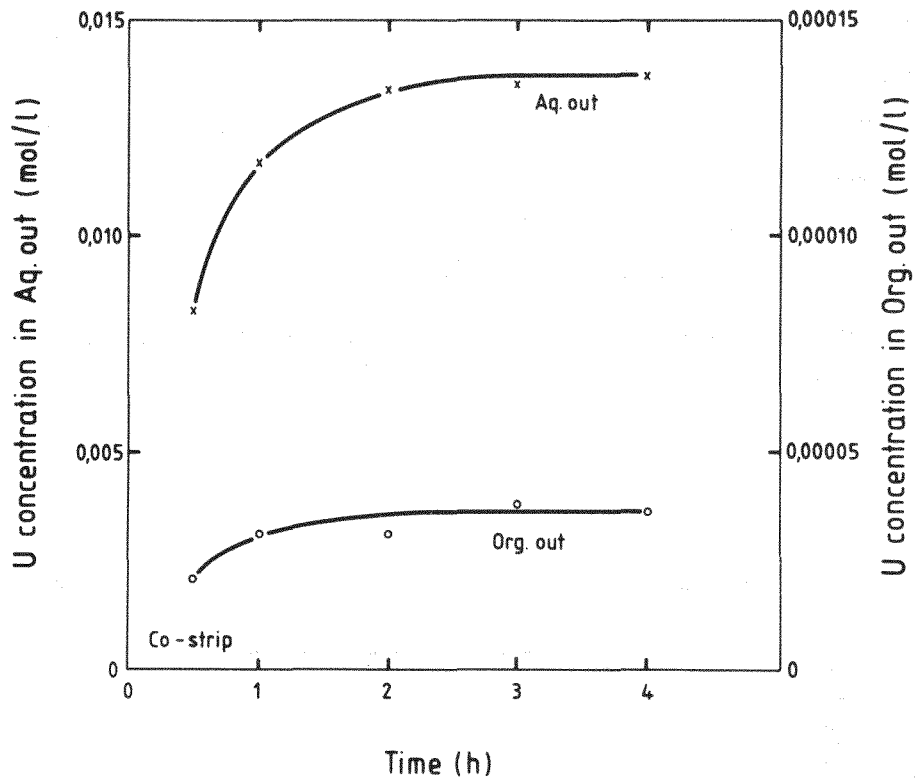
Fig. 8.14: Transient curve of uranium in the co-stripping process
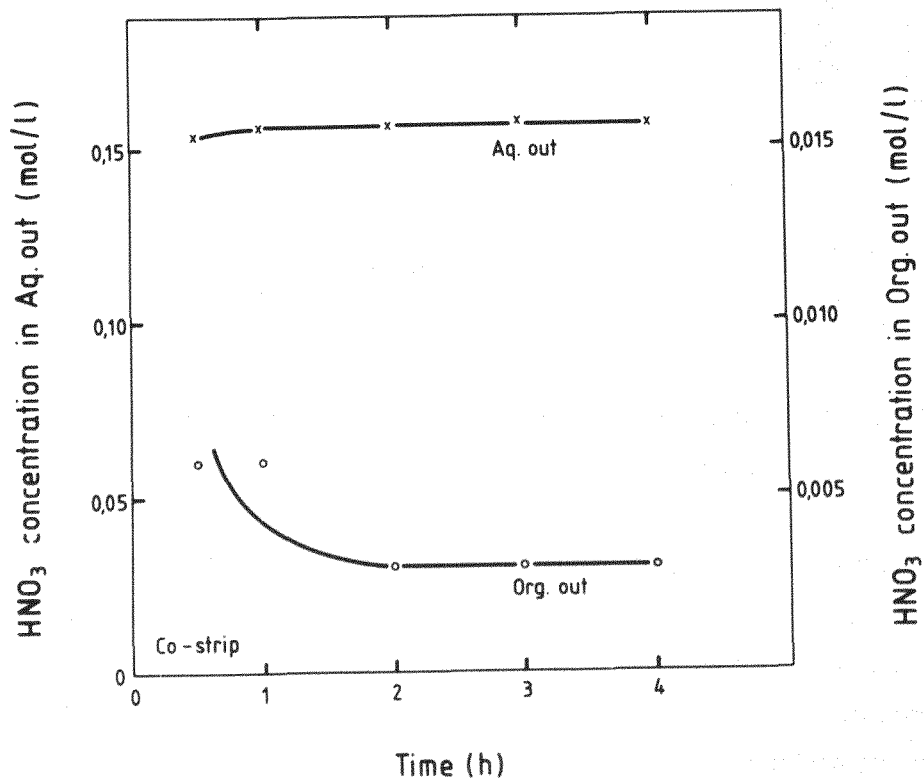
Fig. 8.15: Transient curve of nitric acid in the co-stripping process

it may be explained by the fact that the column contains a
relative larger quantity of uranium than thorium in the steady
state.

8.3.2 Evaluation of HETS

Table 8.3 shows the HETS obtained in this experiment.

Table 8.3

HETS in the co-stripping process (cm)

Column height (m)	0~1	1~2	2~3	3~4	4~5
HETS for thorium	100	105	–	–	–
HETS for uranium	–	112	147	–	–

According the results, this stripping column gives shorter
HETS for thorium than for uranium. However, the difference
is not so great.

Contrary to these results, a report by General Atomic[33] gives
HETS for uranium as 59 cm and that for thorium as 153 cm.

8.4   Partitioning process

Fig. 8.16 shows the flow sheet of this process.

The organic feed concentrations of thorium, uranium, and nitric
acid were 0.111, 0.0114, and 0.088 (mol/l) respectively. The
stripping HNO_3 concentration was 0.01 $\underline{M}$. The flow rates of
the feed, strip, and uranium scrub were 13.2, 7.91, and
2.73 (l/h) respectively.
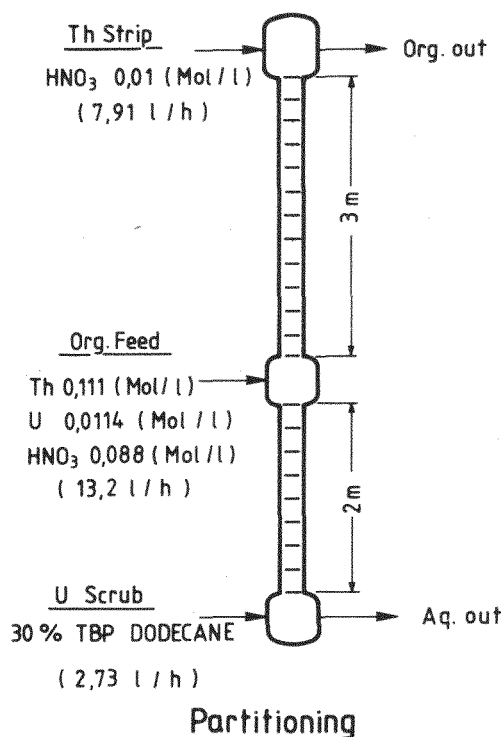
Fig. 8.16: Schematic diagram of the partitioning process

8.4.1 Experimental results

Figure 8.17 shows the uranium, thorium and nitric acid concentration along the column height in the partitioning column.

It is noticed in this figure that the highest concentration of uranium appears at the height of about 4 m in the thorium strip section; this despite the fact that the organic feed point is located at the height of 2 m. This may be caused by the presence of thorium in the strip section. The figure also shows that the nitric acid concentration decreases sharply in the strip section as in Fig. 7.15.
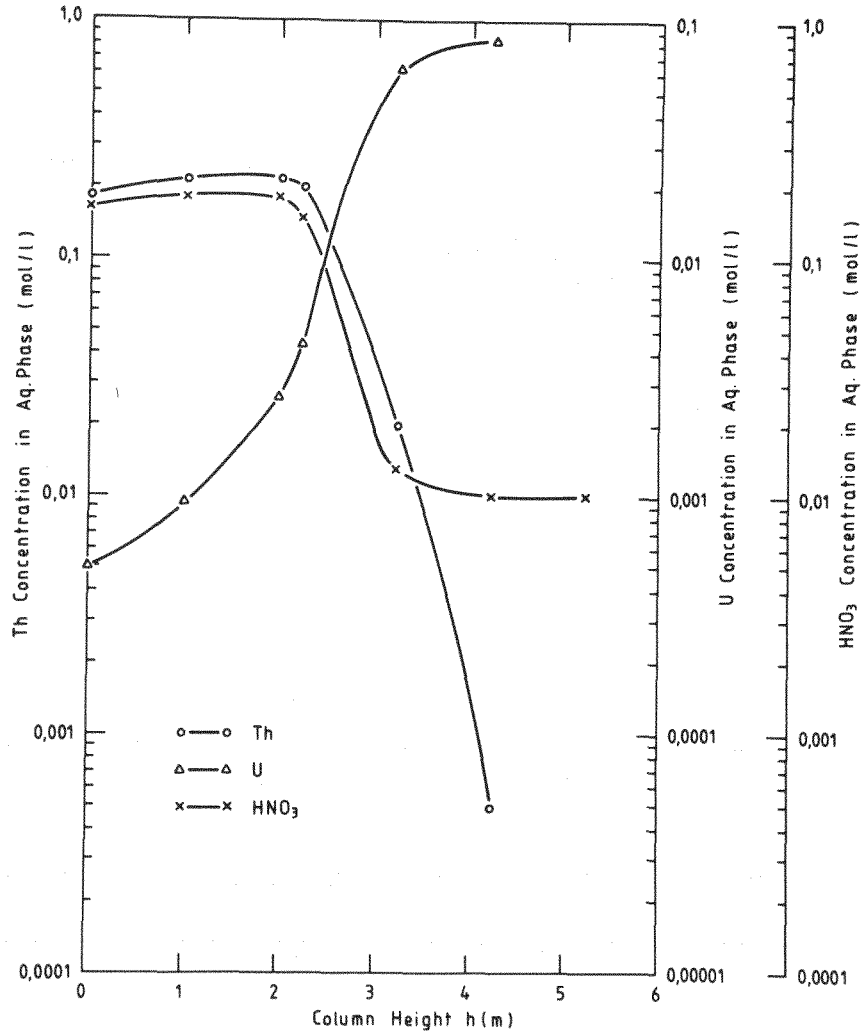
Fig. 8.17: Distribution profiles of thorium, uranium, and nitric acid along the column height in the partitioning process

Figures 8.18 to 20 shows the transient curve of thorium, uranium, and nitric acid in this experiment.

In these figures, the thorium and the uranium concentrations at the outlets seem not to reach the steady state perfectly within 3 hours. However, the error of material balance was within 3 % (see Appendix). From this fact, it may be reasonable to analyse the results by McCABE-THIELE diagrams.
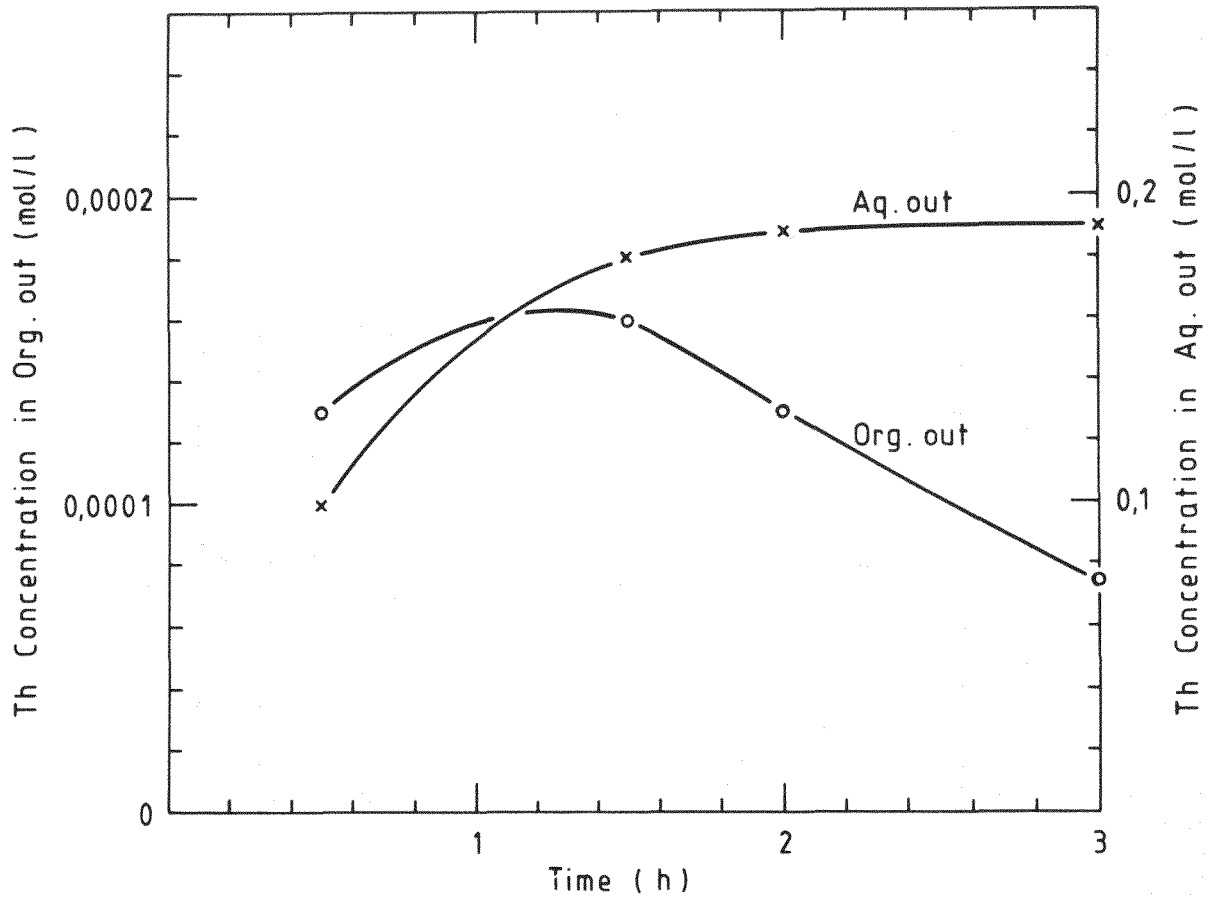
Fig. 8.18: Transient curve of thorium in the partitioning process
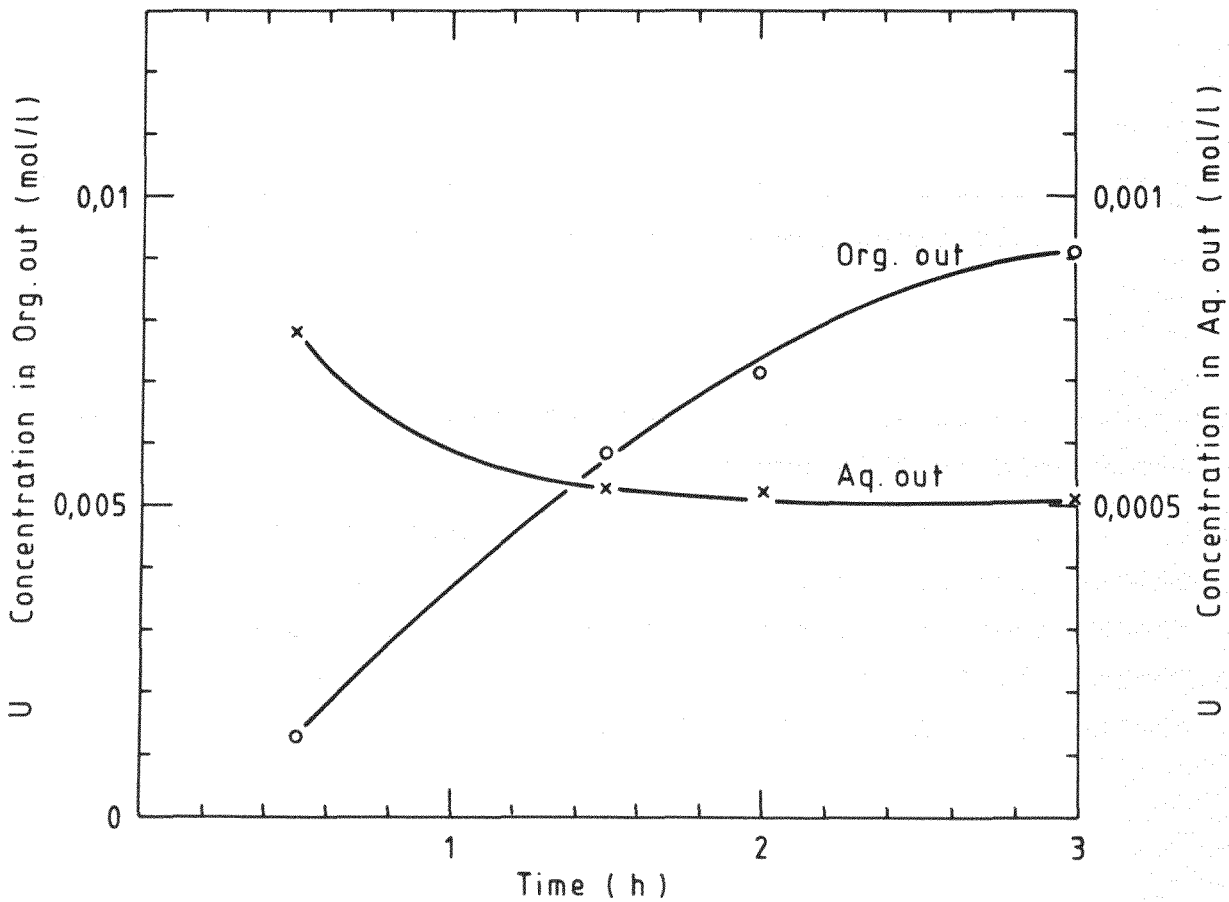
Fig. 8.19: Transient curve of uranium in the partitioning process
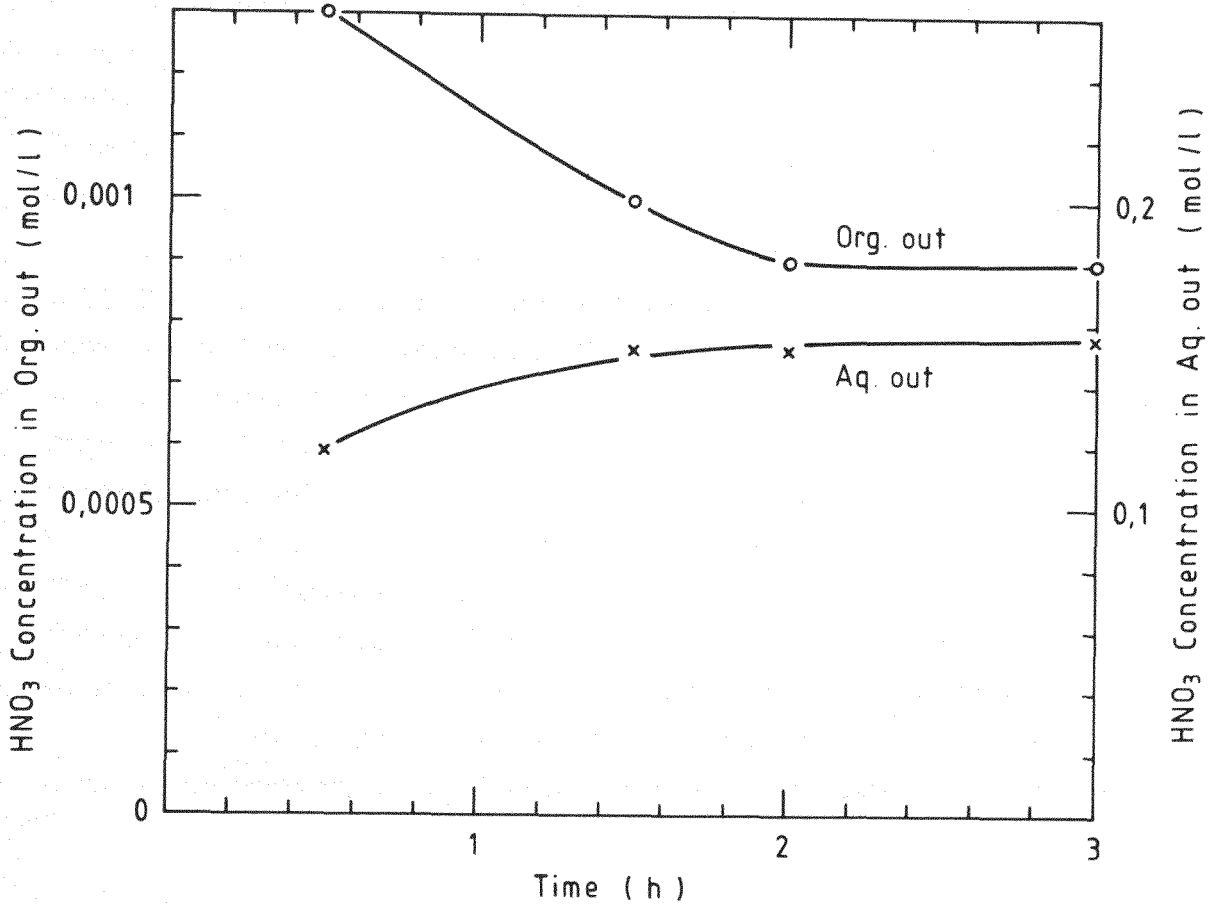
Fig. 8.20: Transient curve of nitric acid in the partitioning process

8.4.2 Evaluation with McCABE-THIELE diagrams

For the thorium strip section of the partitioning column, it was too complicated to calculate HETS for uranium, since the thorium concentration changed extremely there. Therefore, only the thorium was analysed to evaluate HETS. Table 8.4 shows the obtained HETS.

Table 8.4

HETS in the partitioning process

Column height (m)	0~1	1~2	2~3	3~4	4~5
	U scrub		Th strip		
HETS for thorium	–	–	81	71	–

In the uranium scrub section, both uranium and thorium were
pinched out, according to the McCABE-THIELE diagram. Thorium
was pinched at the concentration of 0.204 (mol/l), following
the McCABE-THIELE diagram. In this experiment, the thorium
concentration of 0.218 (mol/l) was obtained. The values agree
fairly well. In the uranium scrub section of the partitioning
column, uranium was pinched at the concentration of 0.00113
(mol/l) according to the McCABE-THIELE diagram, while it was
0.00616 in experiment. The nitric acid concentration was
0.18 (mol/l) and that of thorium was 0.22 (mol/l) in the scrub
section. Therefore, for a first approximation the equilibrium
curve at a nitric acid concentration of 0.40 (mol/l) was used
in this case for the diagram. The uranium distribution coefficient
was 1.8 at that nitric acid concentration, although it must be
2.3 following the experimental results. If the equilibrium data
of uranium in the presence of thorium were available, the
results of this experiment might show better agreement with the
theory.

9.   Discussion

9.1   Comparison of the aqueous continuous and the organic
        continuous mode of operation

In Chap. 6, general flow characteristics have been investigated
for the comparison between the two different modes of operation.
Concerning the extraction process (A/O ≈ 1/3) the organic
continuous column is favorable since this mode of operation has
a larger capacity than the aqueous continuous mode. As for the
extraction of acetic acid (Chap. 7.1), it is observed that the
overall mass-transfer coefficient K_x is independent of whether
the column is being operated in the aqueous continuous or in the
organic continuous mode. In addition, in a solute free condition,
the two modes of operation do not give greatly different contact
times.

In Chap. 7.2, the two modes of operation was examined with
thorium nitrate. The aqueous continuous column shows better

performances (lower thorium loss and shorter HTU). However, it is noticed that the contact time is much longer in the aqueous continuous column than in the organic continuous column. The difference might be explained by the different holdups.

In reextraction (A/O $\approx$ 1/1) the aqueous continuous column has a larger capacity than the organic continuous column. No difference of overall mass-transfer coefficient K_x was observed in re-extraction of acetic acid between the two modes of operation. However, in the operation with thorium, a problem of wetting was observed in the aqeuous continuous column.
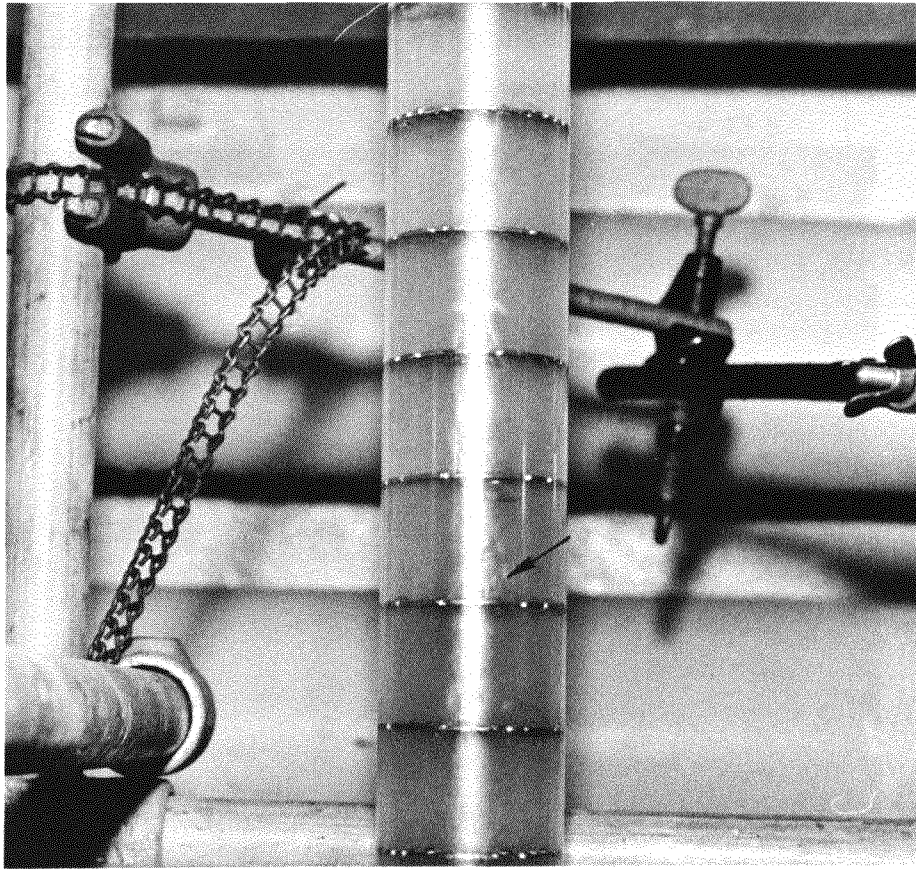
Fig. 9.1: Concentration of organic phase in the middle of the aqueous continuous column

It can be seen in Fig. 9.1 that the organic phase passes upward along the center spacing pipes without forming droplets. The plates are wetted with the organic phase, forming a film on the plates. This phenomenon was observed after recycling the solvent three times. In the presence of higher uranium, thorium or

nitric acid concentration, this problem was not encountered.
Since extraction was made at higher HNO_3 concentrations, the
wetting problem never occurred in extraction. Once wetting
occurs, the column must be washed perfectly for the next
operation. This may be caused by thorium containing organic
compound adhered to the plates.

9.2   Co-extraction process

A co-extraction process was carried out in the organic
continuous mode of operation. Flow problems also occurred here,
which disturbed the performance in the scrub section. Figure
9.2 shows the wetting problem.
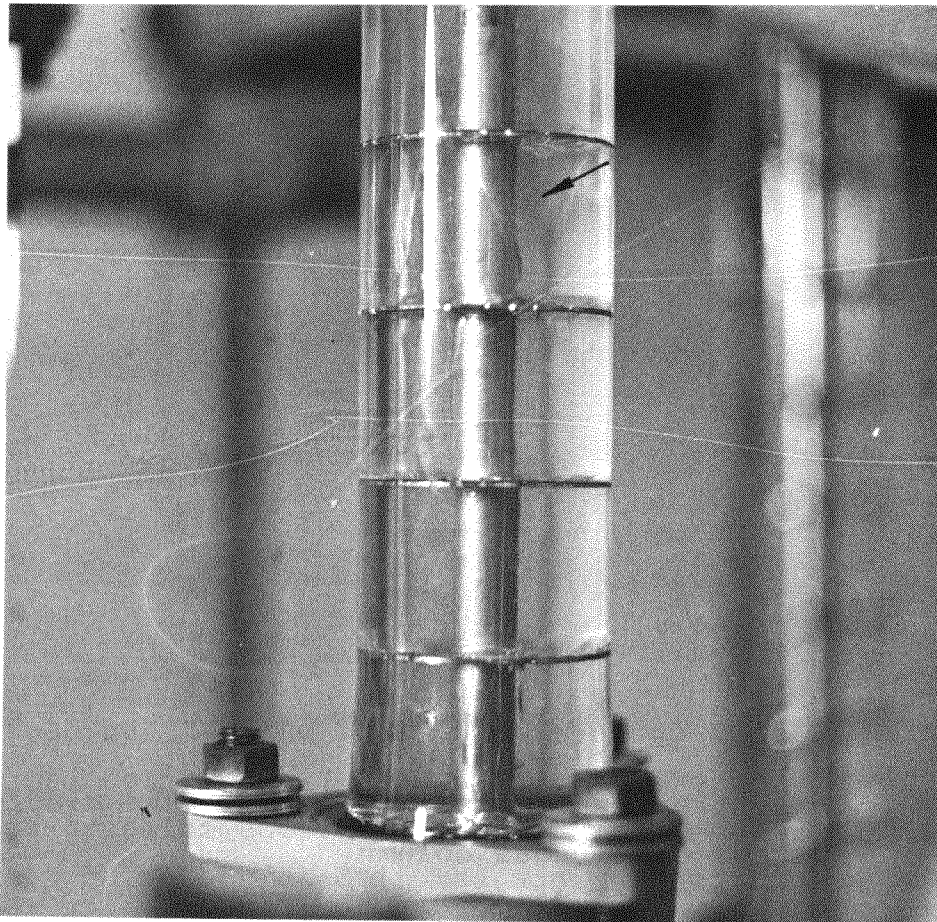
Fig. 9.2:   Concentration of aqueous phase at the wall of the
organic continuous column

It can be seen that the aqueous phase (dispersed phase) goes
down through the column along the inside wall of the glass tube
and no droplets are formed. The column was operated at the pulse
frequency of 32 per minute. This problem was solved by increasing
the frequency. At the frequency of 63 per minute, this kind of
problem has never occurred.

Figure 9.3 shows the difference of the nitric acid distribution
between the acid feed solution and the acid deficient feed
solution along the column height.
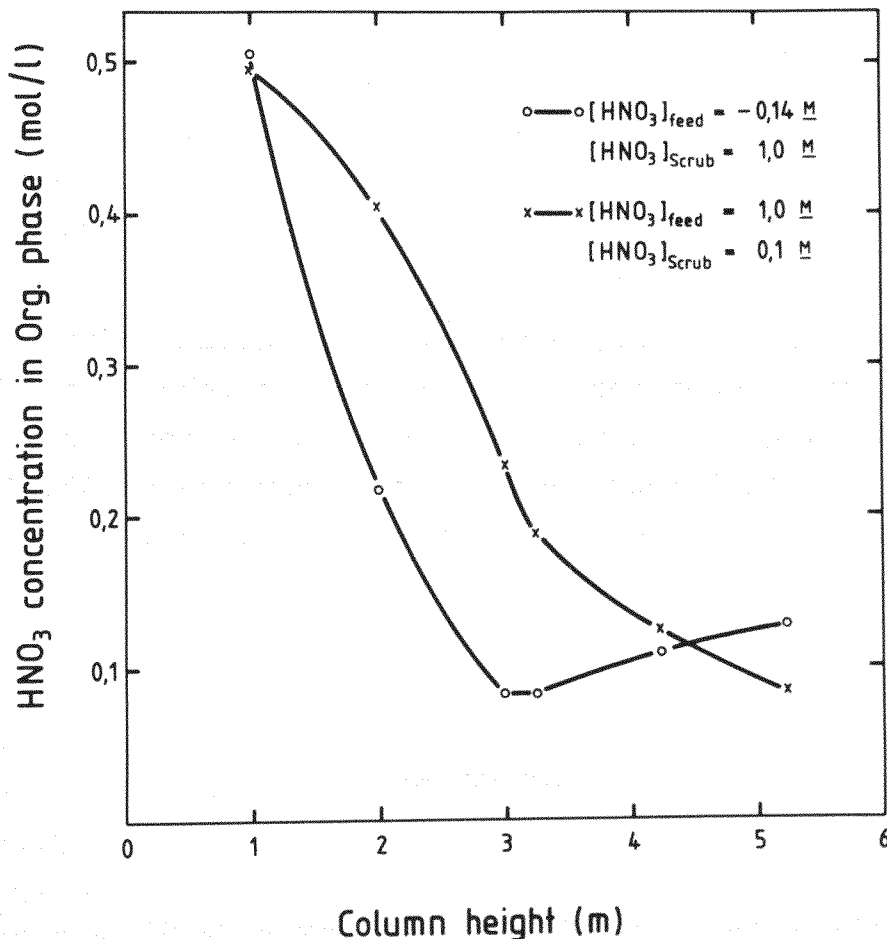
Fig. 9.3: Nitric acid concentration vs. column height (co-
           extraction process)

It is observed that the acid deficient feed solution gives
lower HNO_3 concentration between the column height of 1 to 4 m.
Acidity plays an important role on decontamination factors.
Most fission products show better decontamination with lower
acidity, though some elements with higher acidity. The acid
deficient feed solutions gives much higher decontamination
factors as explained in Chap. 3.3. However, in order to obtain

still higher D.F., split scrub streams (0.01 $\underline{M}$ HNO_3 and 5 $\underline{M}$ HNO_3) have been adopted in ORNL[10] instead of a single 1.0 $\underline{M}$ HNO_3 scrub stream. But split scrub streams can cause greater column instability than a single scrub stream relating to flow variations[33].

9.3   Co-stripping and partitioning process

In the presence of thorium, uranium is not reextracted. After reextraction of thorium (< 0.01 $\underline{M}$), uranium is stripped at an acidity of 0.01 $\underline{M}$. The HETS values are similar as those of thorium. In the strip section, the uranium concentration increases first with the distance from the organic feed point while the thorium concentration decreases.

In the partitioning column, a uranium concentration of 0.084 $\underline{M}$ (about 7.3 times higher than that of organic feed) was obtained at the column height of 4 m. This fact must be observed, because the uranium in actual reprocessing is mainly the U-233. The concentration must be limited in view of criticality.

10.   Conclusions

The conclusions of the experiments are:

1. The capacity depends critically on A/O ratio.

2. At the same cartridge conditions (free area of
    23 %), the organic continuous column has a
    capacity about 1.5 times larger than that of the
    aqueous continuous column at A/O = 0.33. On the
    other hand, at A/O = 1.0, the aqueous continuous
    column has a 12 % larger throughput.

3. Holdup can be estimated as a function of flow
    rate devided by flooding flow rate, independent
    of pulse frequency for both modes of operation.
    At least for the column used, the holdup tends
    to increase with distance from the dispersed phase

inlet, contrary to a former report[27].

4. Analysing the results of extraction and reextraction
   runs, it is concluded that there is not much
   difference between K_x values for operation in the
   organic continuous mode and for operation in the
   aqueous continuous mode. However, on account of the
   difference of holdup distribution, the solute is
   transfered differently along the column height.

5. The droplet diameters and the coalescence
   characteristics are changed by the presence
   of thorium in comparison to the pure aqueous
   phase. The droplet diameter increases and the
   coalescence time becomes shorter as the thorium
   concentration increases. In this study, the aqueous
   continuous column gives shorter HTU and shorter
   HETS than the organic continuous column in thorium
   extraction. However, comparing the contact time, it
   must be noticed that the aqueous continuous operation
   gives a contact time 1.37 times longer than that of
   the organic continuous operation. On the other hand,
   the organic continuous operation gives shorter HTU
   than the aqueous continuous operation in thorium re-
   extraction, though the diffference is smaller.

6. Uranium and thorium were co-extracted, co-stripped,
   and partitioned in this study. They were extracted
   in the organic continuous column and co-stripped and
   partitioned in the aqueous continuous column. Both
   acid feed solution and acid deficient feed solution
   were investigated in the extraction column. The
   obtained HETS values in the extraction section are
   $\approx$ 54 cm for thorium and $\approx$ 56 cm for uranium. In the
   scrub section the HETS for thorium is 160 ~ 170 cm,
   whereas no decrease of the uranium concentration has
   been observed. As for HETS values, no great differences
   exist between the acid feed solution and the acid
   deficient feed solutions. However, in the extraction
   section, a much lower HNO_3 concentration has been

observed with acid deficient feed solution, which
might give higher D.F. for this process.

In the co-stripping column a HETS of ≈ 100 cm has
been obtained for thorium and of ≈ 130 cm for uranium.
In the lower part of the stripping column uranium is
not reextracted because thorium is present.

In the partitioning process the HETS for thorium is
≈ 76 cm in the stripping section. In the uranium scrub
section, both uranium and thorium are pinched out. The
analysis of uranium using McCABE-THIELE diagrams is
very hard in the presence of thorium. The agreement of
the experimental results with the diagram is poor for
uranium. If the equilibrium data of uranium in the
presence of thorium were available, a better agreement
might be observed.

11. Appendixes

11.1 Analytical procedures

Acetic acid determination

The acetic acid concentration was measured by direct titration with standard 0.1 N NaOH. Some ethylalcohol was added in the case of the organic phase analysis. Phenolphtalein was used as an indicator.

Nitric acid determination

The nitric acid concentration was measured by potentiometric titration. In order to remove the interference of thorium, potassium oxalate ($K_2C_2O_4$) was added, which formes oxalato-complexes with thorium.

Thorium determination

The thorium concentration was determined by titration with EDTA in 0.05 N NaOH in the pH range of 2.6 to 2.8 (Buffer system)[34]. Alizarin S was used for the indicator.

Uranium determination

The uranium concentration was measured by titration with 0.01 N cerium (IV) sulfate solution. UO_2^{2+} was reduced first with titanium (III) chloride in the presence of amidosulfonic acid. The indicator was ferroin solution.

11.2 Flow sheets of uranium-thorium separation processes
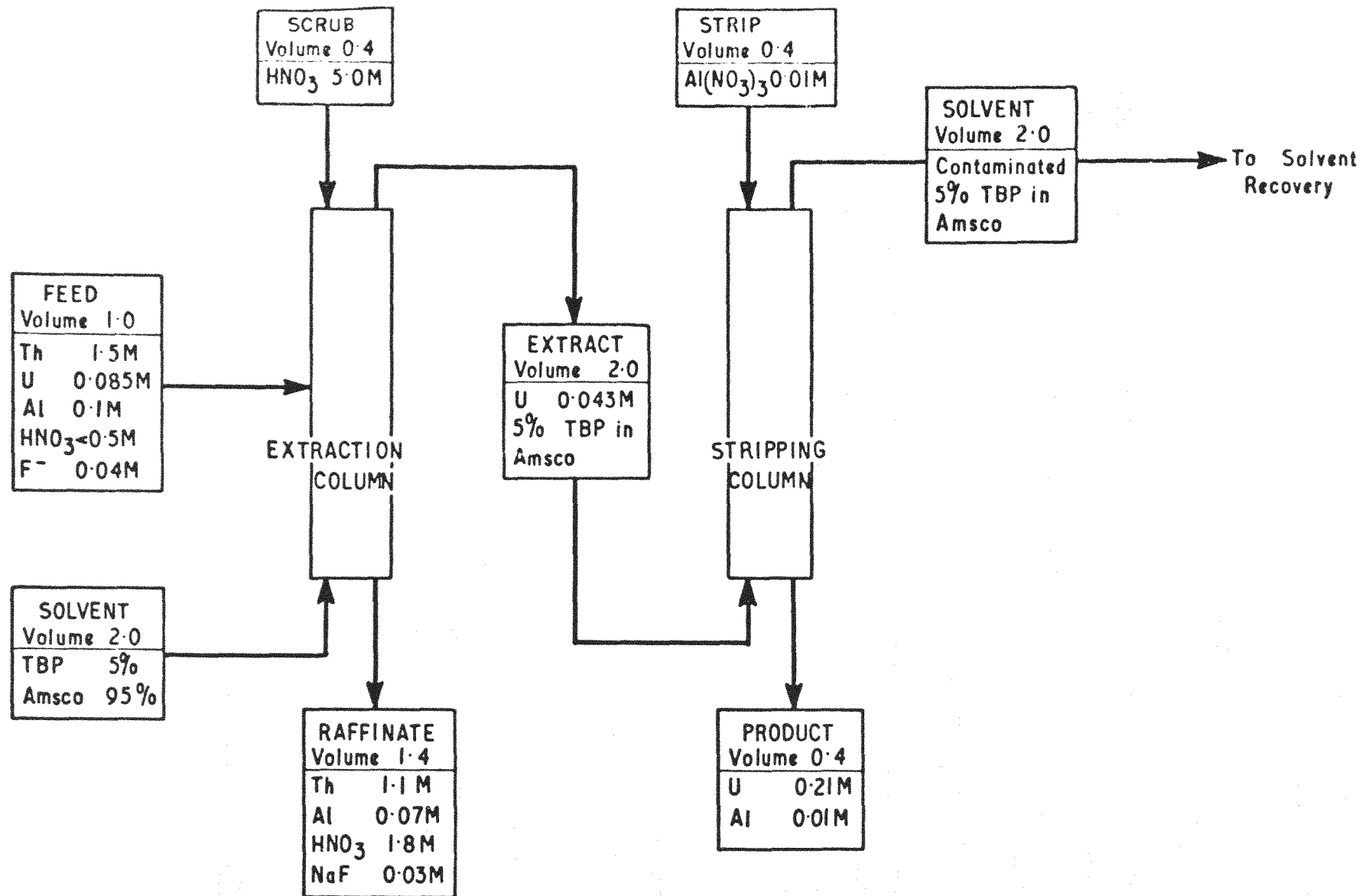
Fig. 11.1: Acid interim 23 process flowsheet[35]
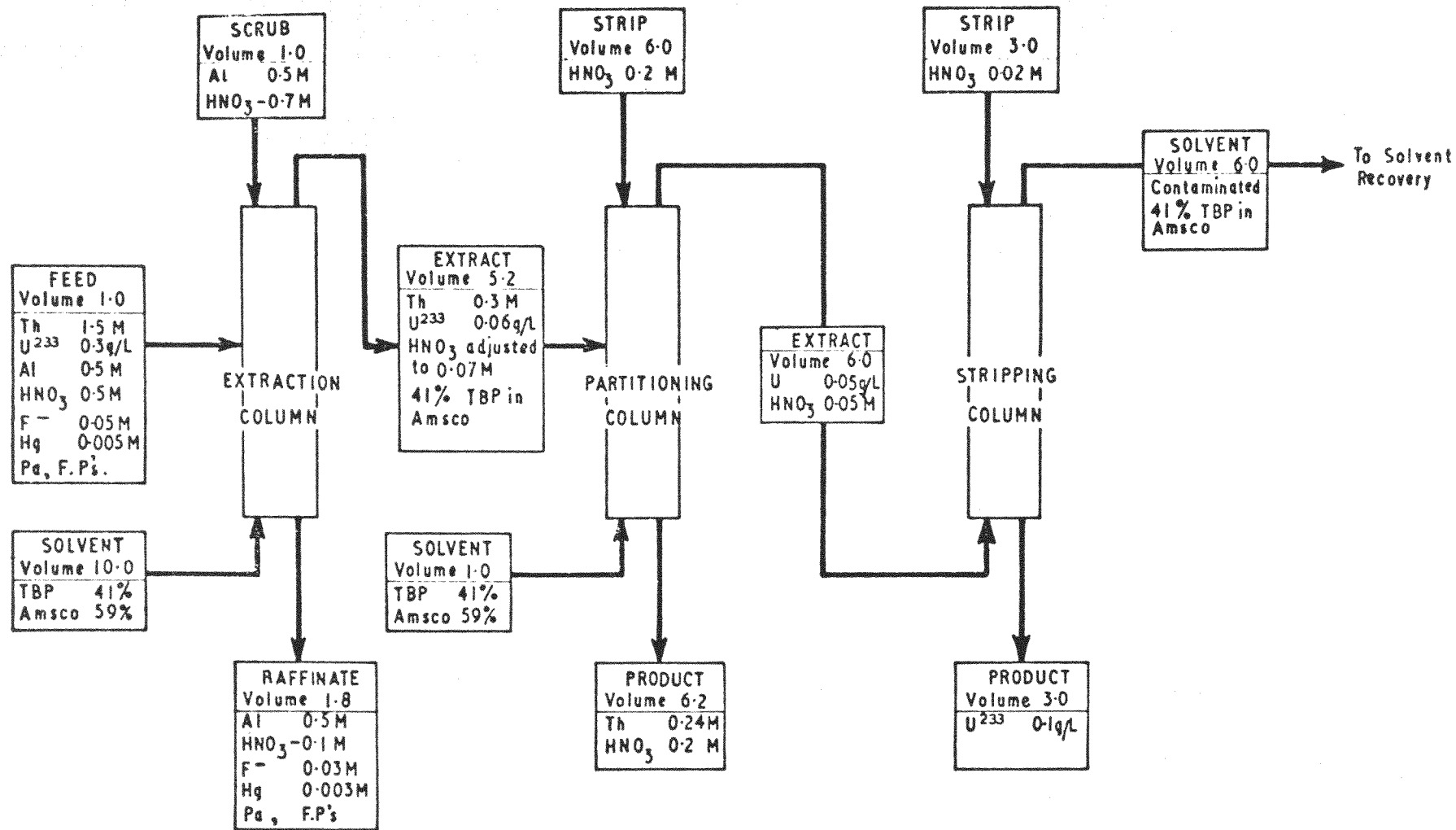
Fig. 11.2: Thorex process no. 2 flowsheet[8]
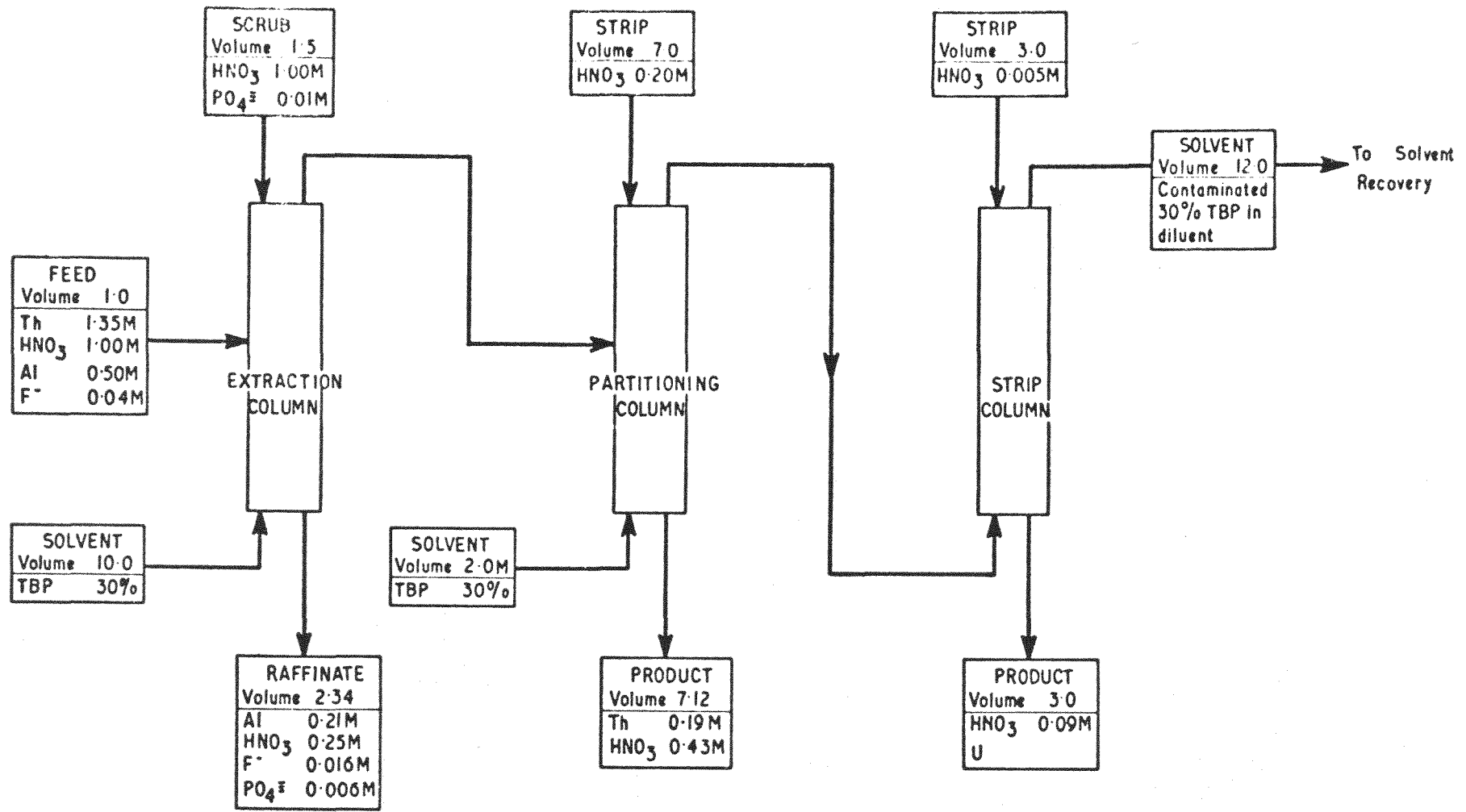
Fig. 11.3:   KAPL acid thorex process flowsheet[11]

SCRUB
Volume 0.8
H$_2$O
H$_3$PO$_4$ 0.003M
Fe(NH$_2$SO$_3$)$_2$ 0.01M

STRIP
Volume 4.2
Al(NO$_3$)$_3$ 0.008M

STRIP
Volume 1.7
Al(NO$_3$)$_3$ 0.008M

SOLVENT
Volume 8.4
Contaminated
30% TBP in
Amsco

To Solvent
Recovery

SCRUB
Volume 0.2
HNO$_3$ 5.0M

FEED
Volume 1.0
Th 265g/L
U 15g/L
Al 0.115M
HNO$_3$ 0.15M
F$^-$ 0.046M
NaHSO$_3$ 0.1M

SALTING ACID
Volume 0.3
HNO$_3$ 13M

SOLVENT
Volume 7.0
TBP 30%
Amsco 70%

EXTRACTION
COLUMN

EXTRACT
Volume 7.0
Th 38g/L
U 2.1g/L
HNO$_3$ 0.05M
30% TBP in
Amsco

PARTITIONING
COLUMN

EXTRACT
Volume 8.4
Th <0.3g/L
U 1.8g/L
HNO$_3$ <0.01M
30% TBP in
Amsco

STRIPPING
COLUMN

SOLVENT
Volume 1.4
TBP 30%
Amsco 70%

RAFFINATE
Volume 2.3
Th <0.22g/L
U <0.007g/L
Al 0.05M
HNO$_3$ 1.6M
F$^-$ 0.02M
PO$_4$$^≡$ 0.001M
Fe(NH$_2$SO$_3$)$_2$ 0.003M

PRODUCT
Volume 4.2
Th 63g/L
U <0.005g/L
HNO$_3$ 0.08M

PRODUCT
Volume 1.7
Th 1.5g/L
U 9.4g/L
HNO$_3$ <0.05M

Fig. 11.4: Acid Thorex flowsheet for Consolidated Edison fuel[36]

1AX 30 Vol % TBP dodecane 2.965 1/h

1AH 13 M HNO₃ 0.0686 1/h

1AF 1.15 M Th 0.046-0.23 M U 0.7-1.1 M HNO₃ F⁻ Al⁺³ 0.312 1/h

1AS 0.1 M HNO₃ 0.312 1/h

16 13 9 1

1A

1AW Abfall 1.1-1.3 M HNO₃ 0.693 1/h

1AP 0.121 M Th (5-19) 10⁻³ M U 0.12 M HNO₃ 2.965 1/h

1CX 0.01 M HNO₃ 2.495 1/h

16 1

1C

1CR 30 Vol % TBP dodecane 2.965 1/h

1CUT 0.144 M Th (6-29) 10⁻³ M U ~0.16 M HNO₃ 2.495 1/h

2. Speiselösungs- einstellung

2AX 30 Vol % TBP dodecane (2.50-2.65) 1/h

2AH 13 M HNO₃ 0.0935 1/h

2AF 1.15 Th 0.046-0.23 M U ~0.15 M HNO₃ 0.312 1/h

2AS 1 M HNO₃ 0.01 M H₃PO₄ 0.312 1/h

16 13 9 1

2A

2AW Abfall ~1.45 M HNO₃ 0.717 1/h

2BS 30 Vol % TBP dodecane (0.437-0.530) 1/h

2AP 0.14 M Th (5.6-28) 10⁻³ M U ~0.17 M HNO₃ (2.50-2.65) 1/h

2BX 0.01 M HNO₃ (1.31-1.60) 1/h

16 9 1

2B

2BT (0.24-0.27) M Th ~0.3 M HNO₃ (1.31-1.50) 1/h

2BU ~(4.8-24) 10⁻³ M U (2.94-3.18) 1/h

2CX 0.01 M HNO₃ (1.25-1.87) 1/h

16 1

2C

2CU (11-39) 10⁻³ M U ~0.01 M HNO₃ (1.25-1.87) 1/h

2CR 30 Vol % TBP dodecane (2.94-3.18) 1/h

Fig. 11.5: Two-cycle thorex process [14]
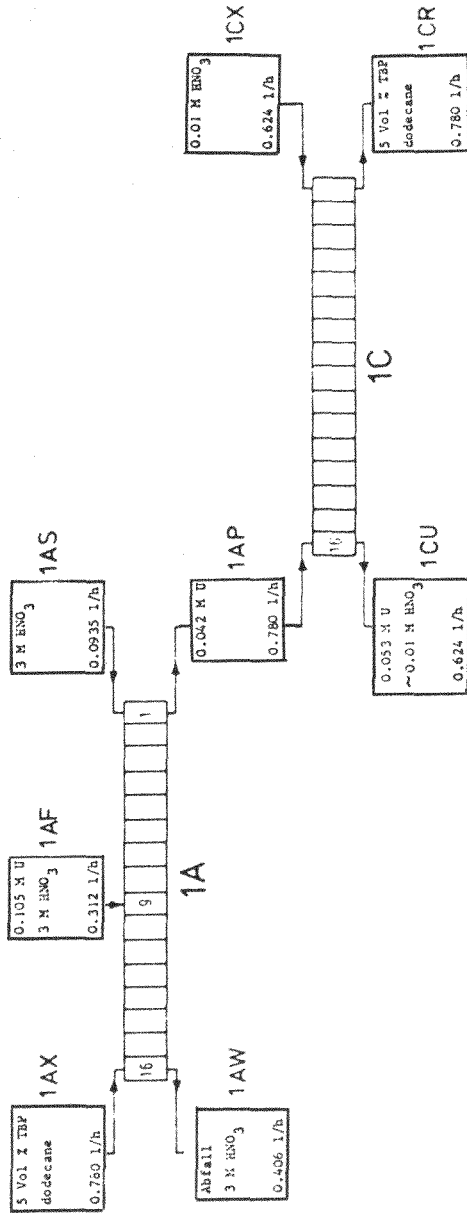
Fig. 11.6: Third uranium cycle (14)

11.3 Experimental data

Table 11.1

Flooding flow rate, $U_{aq}+U_{org}$ (l/h)

frequency (min^{-1})	(Aqueous continuous)		(Organic continuous)	
	A/O = 0.33	A/O = 1.0	A/O = 0.33	A/O = 1.0
17	22	20	32	28
24	–	–	40	30
32	28	34	42	32
48	28	36	42	30
63	26	34	32	26
77	22	28	21	18
91	18	24	18	16
106	14	20	–	12
120	–	16	–	–
133	–	12	–	–

Table 11.2

Thorium concentration profile along the
column height (Chap. 7.2)

	Extraction ($\underline{M}$ in Aq. phase)		Reextraction ($\underline{M}$ in Org. phase)	
Continuous phase	*organic	aqueous	organic	*aqueous
Frequency (min^{-1})	32	32	32	48
U_a (1/h)	8.1	6.1	14.2	15.3
U_o (1/h)	24.2	18.2	13.8	15.1
Column height h = 1 (m)	0.0043	0.0002	0.0022	0.0103
2	0.0113	0.0003	0.0007	0.0010
2.24		0.0003		0.0009
3	0.0275		0.0006	
3.24	0.0279	0.0036	0.0005	0.0004
4.24	0.0815	0.0395	0.0004	0.0003
Aqueous inlet ($\underline{M}$)	0.397	0.397	–	–
Organic inlet ($\underline{M}$)	–	–	0.116	0.0983
Aqueous outlet ($\underline{M}$)	0.0022	0.0003	0.110	0.0955
Organic outlet ($\underline{M}$)	0.131	0.129	0.0004	0.0003
Error of material Balance (%)	0.8	3.4	2.8	1.9
Thoriumloss (%)	0.5	0.08	0.3	0.3

*The concentrations are estimated by material balance

Table 11.3

Profiles of thorium, uranium, and nitric acid
concentration along the column height in the co-
extraction process with acid feed solution
(mol/l in organic phase)

		thorium	uranium	nitric acid
	$h = 1$	0.00245	0.00003	0.495
Extraction	2	0.0192	0.00004	0.405
Section	3	0.131	0.0088	0.234
Scrub	3.24	0.153	0.0115	0.188
Section	4.24	0.143	0.0115	0.125
Feed		0.800	0.0796	1.0
Scrub		—	—	0.1
Salting agent		—	—	13
Organic outlet		0.114	0.0114	0.084
Aqueous outlet		0.00035	0.00002	1.48
Error of material balance (%)		1.4	2.4	1.1
% loss		0.1	0.06	

Organic continuous operation, $f = 63$ $(\min^{-1})$, $U_f = 3.5$ (1/h),
$U_s = 3.55$ (1/h), $U_{sa} = 0.74$ (1/h), $U_o = 24.2$ (1/h)

Table 11.4

Profiles of thorium, uranium, and nitric
acid concentration along the column height
in the co-extraction process with acid
deficient feed solution (mol/l in organic
phase)

		thorium	uranium	nitric acid
	$h = 1$	0.0124	0.00004	0.505
Extraction	2	0.064	0.00016	0.218
Section	3	0.156	0.0173	0.083
Scrub	3.24	0.151	0.0116	0.083
Section	4.24	0.135	0.0116	0.11
Feed		0.805	0.0810	-0.143
Scrub		–	–	1.0
Salting agent		–	–	13
Organic outlet		0.114	0.0115	0.128
Aqueous outlet		0.0018	0.00003	1.70
Error of material balance (%)		2.4	2.6	2.6
% loss		0.5	0.1	–

Organic continuous operation, $f = 63$ (min^{-1}), $U_f = 3.5$ (1/h),
$U_s = 3.46$ (1/h), $U_{sa} = 1.02$ (1/h), $U_o = 24$ (1/h)

Table 11.5

Profiles of thorium, uranium, and nitric
acid concentration along the column height
in the co-stripping process (mol/l in
aqueous phase)

	thorium	uranium	nitric acid
h = 1 (m)	0.0124	0.0255	0.0135
2	0.0006	0.00387	0.011
2.24	0.0005	0.00305	0.011
3.24	0.0002	0.00050	0.011
4.24	0.0001	0.00010	0.011
Organic feed	0.113	0.0114	0.132
Strip	-	-	0.011
Organic outlet	0.00045	0.00004	0.003
Aqueous outlet	0.135	0.0137	0.163
Error of material balance (%)	2.5	2	0.9
% loss	0.4	0.3	-

Aqueous continuous operation, $f = 77$ (min^{-1}), $U_f = 13.1$ (1/h),
$U_{st} = 10.7$ (1/h)

Table 11.6

Profiles of thorium, uranium, and nitric acid concentration along the column height in the partitioning process (mol/l in aqueous phase)

		thorium	uranium	nitric acid
U-Scrub	h = 1	0.214	0.00096	0.183
Section	2	0.218	0.00264	0.18
Th strip	2.24	0.202	0.00438	0.148
Section	3.24	0.0202	0.00636	0.013
	4.24	0.0005	0.00836	0.01
Organic feed		0.111	0.0114	0.088
Th strip		-	-	0.01
Organic outlet		0.00008	0.0091	0.0009
Aqueous outlet		0.185	0.00051	0.163
Error of material balance (%)		0.05	1.1	1.3
% loss		0.08	2.7	-

Aqueous continuous operation, $f = 77$ (min^{-1}), $U_f = 13.2$ $(1/h)$, $U_{st} = 7.91$ $(1/h)$, $U_{sc} = 2.73$ $(1/h)$
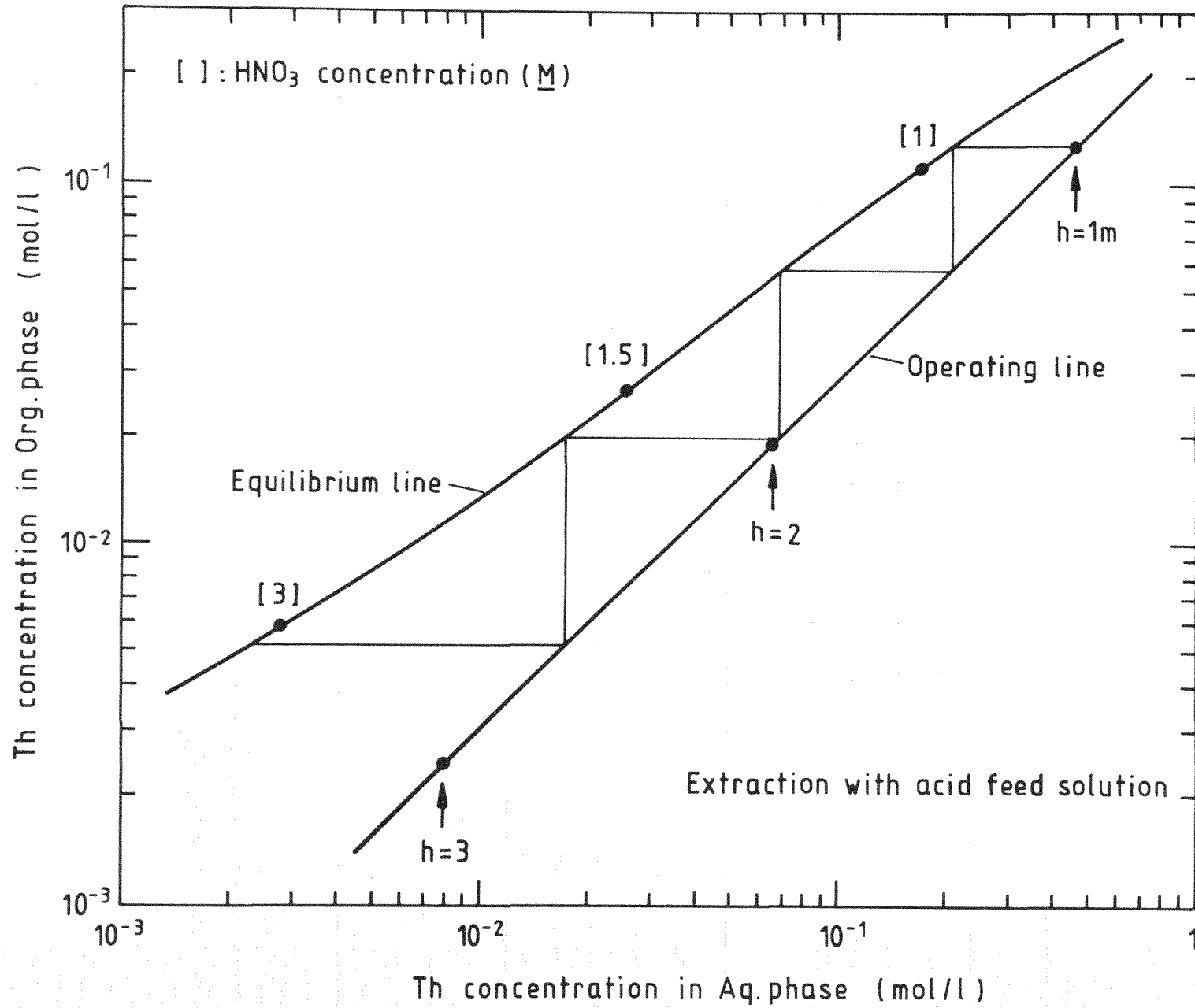
Fig. 11.7: McCABE-THIELE diagram for thorium in extraction (acid feed solution)
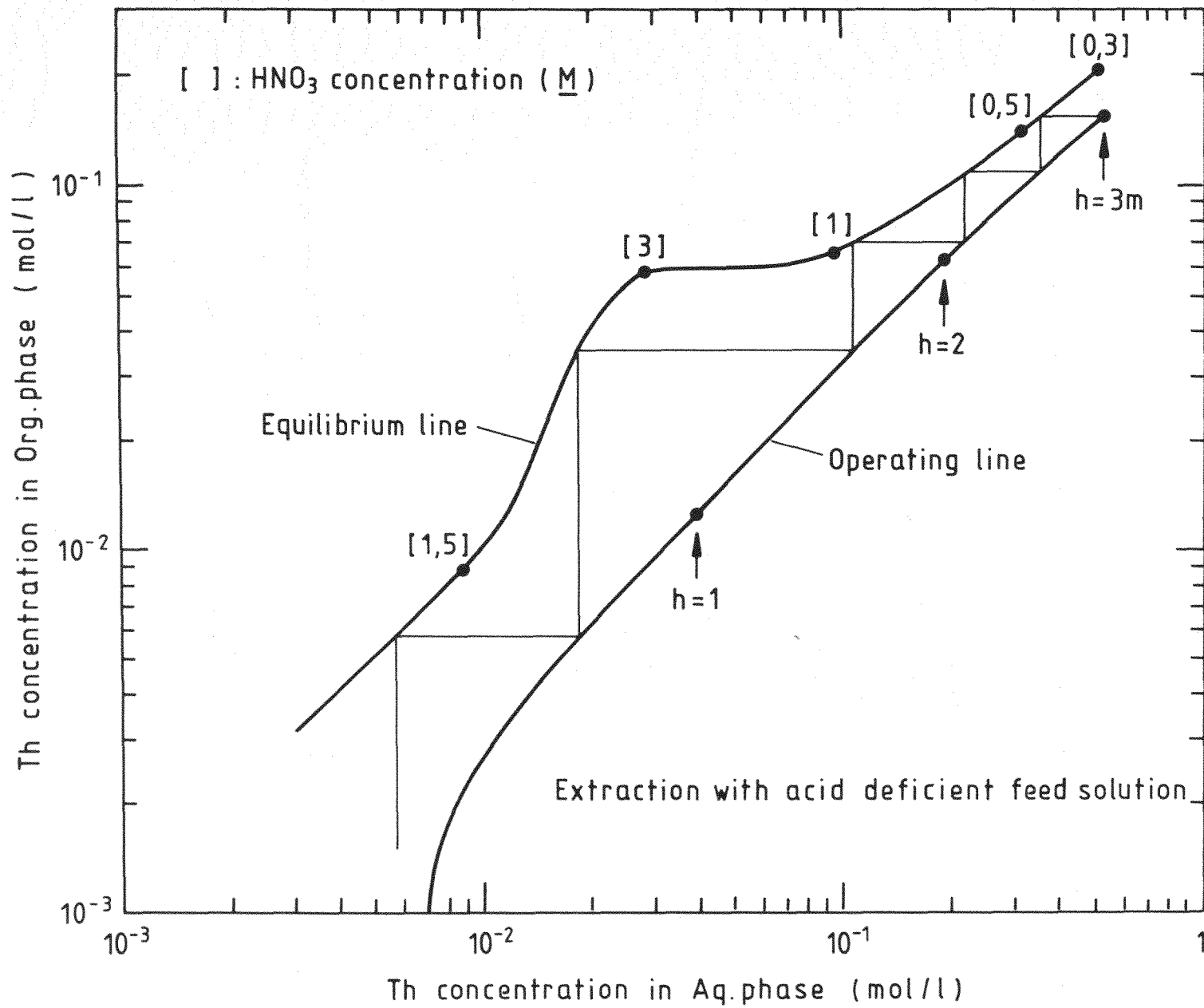
Fig. 11.8: McCABE-THIELE diagram for thorium in extraction (acid deficient feed solution)

Nomenclature

A: Specific contact surface area (cm^2/cm^3)

A/O: Aqueous to organic flow rate ratio

a: Pulse amplitude (cm)

C: Tracer concentration (mg/l)

$C(\theta)$:   Concentration at exit of a system at time θ (mg/l)

C_o: Orifice coefficient

D: Column diameter (m)

D_v: Diffusivity of solute in dispersed phase (m^3/h)

d: Hole diameter (m)

E: Longitudinal eddy diffusivity (m^2/h)

F: Constant

$F(\theta)$:   Fraction of material in outflow at time θ

f: Pulse frequency (cycle/min)

f_H: Transition frequency (cycles/min)

G: Constant

HETS: Height Equivalent Theoretical Stage (cm)

HTU: Height of a Transfer Unit (cm)

h: Column height (m)

K: Constant

K_x: Overall mass-transfer coefficient based on aqueous phase (m/h)

L: Length of the column (m)

l: Plate spacing (m)

NTU: Number of Transfer Units

R: Flow rate ratio to flooding flow rate

Q: Quantity of tracer material injected

T: $U\theta/V_m$

t: Plate thickness (m)

U: Volumetric flow rate (l/h)

V: Superficial flow velocity (m/h)

V_m: Volume of a continuous flow system

V_o: fa/ϵ (m/h)

x: Solute concentration in aqueous phase (mol/l)

y: Solute concentration in organic phase (mol/l)

γ: Interfacial tension (kg/hr^2)

ϵ: Free area

η: Holdup fraction of dispersed phase

θ: Time intervals

μ: Viscosity (kg/m·h)

$\Delta\rho$:   Phase density difference (kg/m^3)

Subscription

aq: aqueous phase

c: continuous phase

d: dispersed phase

e: equilibrium

f: feed

oc: overall based on the continuous phase

org: organic phase

sa: salting agent

sc: scrub

st: strip

Literature cited

(1)   E. Merz
        Wiederaufarbeitung von Kernbrenn- und Brutstoffen
        KFA-ICT-IB-418/77, S.12

(2)   R.C. Dahlberg, K. Asmussen, D. Lee, L. Brooks, and
        R.K. Lane
        Nuclear Engineering and Design, Vol. 26, 1974, pp. 58

(3)   T.D. Gulden, C.L. Smith, P.P. Harmon, and W.W. Hudritch
        Nuclear Technology, Vol. 16, 1972, pp. 101

(4)   M.J. Bradley and L.M. Ferris
        I&EC, Vol. 53, 1961, pp. 279

(5)   R. Böhnert, G. Kaiser, and E. Merz
        Advances in chemistry, ser. 133
        Chemical Reaction Engineering II. 1974, pp. 25

(6)   R.H. Rainey and J.G. Moore
        ORNL-3155, 1962

(7)   F.G. Bodewig
        Jahres-Tätigkeitsbericht für den Zeitraum vom
        1. Juli 1973 bis 30. Juni 1976, ICT, KFA Jülich,
        S. 42

(8)   A.T. Gresky, M.R. Bennett, S.S. Brandt, W.T. McDuffee,
        and J.E. Savolainen
        ORNL-1367 (rev), 1952

(9)   A.D. Ryon and R.S. Lowrie
        ORNL-3732, 1965

(10)   F.R. Bruce, E.M. Shank, R.E. Brooksbank, J.R. Parrott,
        and G.S. Sadowski
        Proceedings of the second United Nations International
        Conference on the Peaceful Uses of Atomic Energy 17,
        49, 1958

(11)   S.M. Stoller and R.B. Richards
        Reactor Handbook, vol. II Fuel Reprocessing, 1969, pp. 219

(12)   E. Zimmer and H. Ringel
        Chemie-Ing. Techn. 47 Jahrg. Nr. 17, 1975, S. 710

(13)   L. Küchler, L. Schäfer, and B. Wojtech
        Kerntechnik, 13, 1971, S. 225

(14)   L. Küchler, L. Schäfer, and B. Wojtech
        Kerntechnik, 13, 1971, S. 319

(15)   L.D. Smoot, B.W. Mar, and A.L. Babb
        I&EC, Vol. 51, 1959, pp. 1005

(16)   G.A. Schmel and A.L. Babb
        I&EC, PDD, Vol. 2, 1963, pp. 38

(17)   R.L. Bell and A.L. Babb
        I&EC, PDD, Vol. 8, 1969, pp. 392

(18)   B.W. Mar and A.L. Babb
        I&EC, Vol. 51, 1959, pp. 1011

(19)   L.D. Smoot and A.L. Babb
        I&EC Fundamentals, Vol. 1, 1962, pp. 93

(20)   J.D. Thornton
        British Chemical Engineering, May 1958, pp. 247

(21)   R.G. Geier and L.W. Brown
        BNWL-2186 Pt 1 UC-10, Jan. 1977

(22)   W. Johannisbauer
        Jül-1073-CT, KFA Jülich GmbH, 1974

(23)   A.T. Gresky
        ORNL-1367, 1952

(24)   J. Klitgaard
        ORNL-TM-1256, 1965

(25)   A.A. Kishbaugh
         DP-841, 1963

(26)   C. Bernard
         ISEC 71, 2:1282

(27)   R.L. Bell and A.L. Babb
         I&EC, PDD, Vol. 8, 1969, pp. 393

(28)   P.V. Danckwerts
         Chemical Engineering and Science
         Vol. 2, 1953, pp. 1

(29)   Octave Levenspiel and W.K. Smith
         Chemical Engineering Science, Vol. 2, 1953, 227

(30)   T.H. Siddall
         DP-181, 1956

(31)   A.D. Ryon
         ORNL-3045, 1961

(32)   J.W. Codding, W.O. Haas, Jr., and F.K. Heumann
         I&EC, Vol. 50, 1958, pp. 145

(33)   Thorium Utilization program
         GA-A 13593, UC-77, pp. 6-1, 1975

(34)   E. Merck AG Darmstadt
         Bestimmungsmethoden mit Titriplex

(35)   R.E. Blanco, L.M. Ferris, J.R. Flanary, F.G. Kitts,
         R.H. Rainey, and J.T. Roberts
         TID-7583, 1959

(36)   R.E. Blanco, L.M. Ferris, and D.E. Ferguson
         ORNL-3219, 1962